# Ultrastructural Localization of Embryonic Cholinesterase in the Chick Limb Bud and in the Genital Tract of the Mouse Embryo

Dissertation

zur Erlangung des Grades eines Doktors
der Naturwissenschaften

der Fakultät für Biologie
der Eberhard-Karls-Universität Tübingen

vorgelegt von

**Pramote Vanittanakom**
aus Nakhonsawan/Thailand

~~1984~~
1983

Digitized by the Internet Archive
in 2026

https://archive.org/details/IA41547613_0006

# Ultrastructural Localization of Embryonic Cholinesterase in the Chick Limb Bud and in the Genital Tract of the Mouse Embryo

Dissertation

zur Erlangung des Grades eines Doktors
der Naturwissenschaften

der Fakultät für Biologie
der Eberhard-Karls-Universität Tübingen

vorgelegt von

**Pramote Vanittanakom**
aus Nakhonsawan/Thailand

1984

Tag der mündlichen Prüfung: 30. September 1983

Dekan: Prof. Dr. K. P. Hadeler
(am Tag der mündlichen Prüfung)
1. Berichterstatter: Prof. Dr. U. Drews
2. Berichterstatter: Prof. Dr. W. Engels

Offsetdruck Spengler
Lessingstraße 4 · 7401 Neustetten 1
Telefon (0 74 72) 2 21 45

# Acknowledgements

I wish to express my gratitude to:

Prof. Dr. Ulrich Drews for his proposal of this work, experienced guidance, judgement and the introduction into the field of histochemistry and embryology.

Prof. Dr. Wolf Engels who promoted my doctoral study, for his generous advice and judgement in completion of this dissertation.

P.D. Dr. Klaus-Ulrich Thiedemann who introduced me to EM work with many useful suggestions and helpful assistance.

Prof. Dr. Georg W. Kreutzberg, Max Planck-Institute for Psychiatry, Munich, who gave me the opportunity to study the methods of ultrastructural histochemistry in his laboratory.

Mr. Peter Michael Weber for his photographic assistance.

Mr. Hermann Guckes for his assistance in EM techniques.

Mrs. Carmen Burgfeld for typing of this thesis.

The members of Prof. Dr. Drews Department, Institute of Anatomy, University of Tübingen, who, in one way or the other, helped me to complete this work.

The Faculty of Medicine, Chiang Mai University, Chiang Mai, Thailand and the China Medical Board of New York Fellowship Fund for the financial support.

And above all, to my parents and wife for their moral support.

CONTENTS


I. General Introduction 1

1. Embryonic Cholinesterase in developmental processes 1

2. Characterization of Cholinesterases 1

3. Distribution of Cholinesterases 2

4. Purpose of this study 3

II. Materials and Methods 5

1.0. Preparation of Tissues 5

1.1. Chick embryo limb bud 5

1.2. Urogenital tract of mouse embryo 5

2.0. Histochemical reaction 6

3.0. Histochemical controls 7

4.0. Embedding, sectioning and staining for electron microscopy 7

4.1. Postfixation 7

4.2. Dehydration 7

4.3. Embedding and polymerization 7

4.4. Sectioning and staining 8

III. Ultrastructural localization of embryonic cholinesterase in the chick embryo limb bud 9

1.0. Introduction 9

1.1. General development of the limb 9

1.2. Chick embryo limb bud 9

1.3. The apical ectodermal ridge 9

1.4. The role of ectoderm and mesoderm in limb differentiation 10

1.5. Differentiation of mesoderm in limb bud 11

1.6. Chondrogenesis and pattern formation in limb bud 12

1.7. Myogenesis in limb bud 13

1.8. Cholinesterase activity in chick limb bud 14

2.0. Results 16

2.1. Limb bud stage 23 and 24 16

2.2. Limb bud stage 25 21

2.3. Limb bud stage 26 23

2.4. Limb bud stage 27 25

3.0. Summary 28

IV. Ultrastructural localization of embryonic cholinesterase in the genital tract of mouse embryo 31

1.0. Introduction 31

1.1. Development of the genital tract 31

1.2. The indifferent genital tract 31

1.3. The differentiated genital tract 32

1.4. Morphogenesis of male genital tract 33

1.5. Morphogenesis of female genital tract 34

1.6. Histochemical studies in genital tract 35

2.0. Results 37

2.1. Indifferent stage at day 15 and 16 p.c. 37

2.2. Male embryo at day 17 p.c. 41

2.3. Male embryo at day 18 p.c. 42

2.4. Female embryo at day 17 p.c. 44

2.5. Female embryo at day 17.5 p.c. 45

2.6. Female embryo at day 18 p.c. 45

3.0. Summary 47

V. Ultrastructural localization of embryonic cholinesterase during myogenesis of the urethral muscle of mouse embryo 50

1.0. Introduction 50

2.0. Results 55

2.1. Morphology of myoblasts 55

2.2. Cholinesterase activity of myoblasts 57

2.3. Morphology of myotube development 57

2.4. Cholinesterase activity of myotubes 58

3.0. Summary 59

VI. General discussion 60

1. Ultrastructural localization of embryonic cholinesterase 60

2. Relation of ChE activity to differentiation 61

3. Specificity of embryonic ChE 62

4. Possible functions of embryonic ChE 63

VII. General summary 70

VIII. References 72

Figures and explanation of figures

Curriculum Vitae

Academic teachers

# I. General Introduction

## 1. Embryonic Cholinesterase in Developmental Processes

Cholinesterase (ChE) activity during early development of the sea urchin, the amphibian, the chick and the rat embryo was studied histochemically by Drews and his coworkers (for review see Drews 1975). They found that ChE appears in the early stage of embryonic blastemata independent from innervation. It disappears from the embryonic cells after they have assembled into definite organ structures. Thus, ChE plays a role in embryonic development which is different from its known function in the adult. Therefore, ChE activity present in differentiating cells during a limited phase of development, is termed "Embryonic Cholinesterase". This embryonic ChE is expressed in all organs of various species. It is correlated to morphogenetic movements and disappears when the respective organ structure has formed. The ultrastructural localization of embryonic ChE has not yet been described.

## 2. Characterization of Cholinesterases

Cholinesterases constitute a specific group of esterases (Augustinsson and Nachmansohn, 1949; Augustinsson, 1950; Pearse, 1972). They are characterized by their ability to hydrolyze choline esters. Cholinesterases are divided into two types: true or specific-cholinesterase (or acetylcholinesterase, acetylcholine acetylhydrolase, E.C. 3.1.1.7) and non-specific cholinesterase (pseudo-cholinesterase or butyryl-cholinesterase, E.C. 3.1.1.8). Both enzymes are capable of hydrolyzing simple choline esters. They can be differentiated from non-specific esterases by their capacity only to hydrolyze choline esters and by the action of the specific inhibitor eserine ($10^{-5}$M). Non specific esterases are not inhibited by eserine.

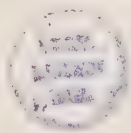

The differences between acetylcholinesterase and non-specific cholinesterase are the following (Barka and Anderson, 1963):

(a) Acetylcholinesterase has an affinity for its physiological substrate, acetylcholine, while non-specific cholinesterase hydrolyzes also other choline esters.

(b) Acetylcholinesterase hydrolyzes acetylthiocholine more rapidly than acetylcholine; hydrolysis of butyrylcholine and butyrylthiocholine are very slow.

(c) Non-specific cholinesterase hydrolyzes acetylcholine as well as butyrylcholine and butyrylthiocholine at a rapid rate.

The application of specific substrates and inhibitors to the histochemical reactions have permitted a more accurate identification of both enzymes. Inhibitors recommended for histochemical use include eserine (physostigmine), neostigmine (prostigmine), diisopropylfluorophosphate (DFP), tetraisopropylpyrophosphoramide (iso-OMPA), ethopropazine and 62 C - 47 1,5 - bis (4-trimethylammoniumphenyl) pentan - 3 - one di-iodide (Augustinsson, 1950; Pearse, 1972). Eserine inhibits both acetylcholinesterase and non-specific cholinesterase in the concentrations of $10^{-6}$M to $10^{-5}$M. Neostigmine and DFP are strong inhibitors of both enzymes. Iso-OMPA and ethopropazine are selective inhibitors for non-specific cholinesterase, and 62 C - 47 and BW 284C51 for acetylcholinesterase. Iso-OMPA acts irreversibly at a concentration of $10^{-5}$M of non-specific cholinesterases without affecting acetylcholinesterase. Inhibition of non-specific cholinesterase by ethopropazine is equally effective as Iso-OMPA but is reversible. The effective concentration is $3 \times 10^{-5}$M.

## 3. Distribution of Cholinesterase

Acetylcholinesterase has been found in all vertebrates, in most of invertebrates, in plants, in Pseudomonas and in snake venom C (Dixon and Webb, 1979). Non-specific cholinesterase

has been reported in the blood serum, pancreas, liver, salivary glands, brown fat, testis and ovary. Acetylcholinesterase occurs as the predominant enzyme in nervous tissue, muscular tissue and in erythrocytes. Erythrocyte acetylcholinesterase varies in different species, being highest in man and in the guinea-pig (Burstone 1962, Pearse 1972).

In general, non-specific cholinesterase and acetylcholinesterase are widely distributed in excitable membranes of nerve and muscle. They play a role in acetylcholine mediated neural transmission. After release of the transmitter acetylcholine at the myoneural or interneural junction, these enzymes stop excitation by splitting acetylcholine into its inactive components (Katz 1966; Nachmansohn, 1970).

However, both enzymes are also widespread in many tissues and cells independent from innervation where a function is not known. Particularly, specific and unspecific cholinesterase activities are expressed in embryonic tissues independent from the nervous system (Drews 1975).

## 4. Purpose of this study

Cholinesterase activity in undifferentiated embryonic cells is independent from innervation. Since it disappears with differentiation, it cannot be explained in terms of development of the adult enzyme pattern. Up to now, embryonic cholinesterase has only been studied by light microscopic histochemistry. The purpose of my study is to describe the ultrastructural localization of embryonic ChE and to correlate the phase of ChE activity with intracellular organization in the curve of differentiation.

In my study two embryonic tissues are selected in which some knowledge about embryonic ChE already exists. In the chick limb bud ChE was described histochemically (Drews and Drews 1971), and biochemically (Schröder 1980). In addition in the chick limb bud a muscarinic acetylcholine receptor has been described (Schmidt, 1981) and activity of choline acetyltransferase has been demonstrated (Reich and Drews, 1983). In the development of the mouse genital tract Schweers (1979) described the histochemical localization of embryonic ChE in cryostat serial sections and Bok and Drews (1983) studied the morphogenetic processes during male versus female development in organ culture.

Aims in this work are to study and describe embryonic cholinesterase in the following tissues and locations by means of ultrastructural level:

1) In the developing chick limb bud from stage 23 to stage 27, four areas of the limb bud are studied (a) the apical ectodermal ridge (b) the mesenchyme in the subridge area (c) the central cartilage forming area and (d) the dorsal and ventral muscle forming areas.

2) In the genital tract of the mouse embryo at day 15, 16, 17 and 18 p.c., three levels are studies (a) cross sections at the junctional area of the genital ducts and the urogenital sinus (b) cross sections cranial to the junctional area and (c) cross sections caudal to the junctional area.

3) During myogenesis of the urethral muscle of the mouse embryo, the muscular layer of urethra is studied at day 15, 16, 17, and 18 p.c.

## II. Materials and Methods

### 1.0. Preparation of Tissues

### 1.1. Chick Embryo Limb Bud

Limb buds of chick embryos stages 23 - 27 according to Hamburger and Hamilton (1951) were cut off and fixed in a mixture of 2% glutaraldehyde and 4% paraformaldehyde dissolved in 0.05 M cacodylate buffer (pH 7.2) for 6 hours at 4 °C. The limb buds were washed overnight in an isotonic buffer (pH 7) consisting of 25 ml 0.2 M sodium cacodylate and 1 ml 0.2 M calcium acetate made up to 100 ml with isotonic sodium sulfate solution. The isolated limb buds from each stage were cut with a razor blade into longitudinal sections in the dorso-ventral plane or into cross sections in proximo-distal direction (Fig. 1). Of the longitudinal sections, only intact central sections about 200 µ thick were used. Cross sections were taken from three areas of each limb bud designed from distal to proximal as block I (the tip of the limb bud), block II (the middle part of the limb bud), and block III (the proximal part of the limb bud).

### 1.2. Urogenital Tract of Mouse Embryo

Female NMRI mice obtained from a local commercial breeder were mated to NMRI males. Embryos were collected on days 15, 16, 17 and 18, the day of plug detection being day 1. The sex of the embryos was determined by inspection of the gonads. The urogenital tracts were excised under a dissection microscope and fixed and washed as outlined above. They were trimmed by cutting off the lower part of the urogenital tract and the bladder. Then each specimen

was cut into 2 - 4 cross sections ranging from the level of the symphysis to the neck of the bladder (Fig. 36, Fig. 47, Fig. 60)

## 2.0 Histochemical Reaction

The tissue blocks were incubated for demonstration of cholinesterase activity after the method of Lewis and Shute (1969). The incubation media were made up as follows: 100 mg acetylthiocholine iodide was dissolved in 4.0 ml distilled water and added drop by drop to 7.0 ml of 0.1 M copper sulphate; the solution was centrifuged and to 4 ml of the supernatant were added 25 mg glycine, 4 ml isotonic sodium sulphate, 1 ml water or 1 ml ethopropazine hydrochloride solution (containing 3.5 mg dissolved in 5 ml distilled water), and 0.5 ml of 0.5 M succinic acid; the solution was then slowly adjusted by 1.0 N NaOH to final pH of 5.3. Two media were used: (1) acetylthiocholine plus water to demonstrate the non-specific cholinesterase, and (2) acetylthiocholine plus ethopropazine $2 \times 10^{-4}$ M to demonstrate the specific cholinesterase. The tissue blocks were incubated in the media for 2 hours at 4° C.

After incubation, specimens were washed 1 hour in two changes of isotonic buffer consisting of 10 ml 0.5 M succinic acid, 1 ml 0.2 M calcium acetate, 60 ml isotonic sodium sulphate, adjusted to pH 5.3 with 1N sodium hydroxide and made up to 100 ml with distilled water. They were then transferred to the developing solution for 30 minutes. The developing solution was made up from a fresh filtered sodium sulfide solution consisting of 10 ml 0.5 M succinic acid, 1 ml 0.2 M calcium acetate, 60 ml isotonic, 1 ml sodium sulfate, adjusted to pH 5.3 with a 4% solution of sodium sulfide. Tissue blocks were washed again 1 hour in two changes of the latter isotonic buffer.

## 3.0. Histochemical Controls

The following histochemical controls were performed:
(1) incubation in a medium containing 2 x $10^{-4}$M ethopropazine hydrochloride or $10^{-5}$M iso-OMPA (tetra-isopropylpyrophosphoramide), an inhibitor for non-specific cholinesterase.
(2) incubation in a medium containing $10^{-5}$M eserine, an inhibitor for specific cholinesterase and non-specific cholinesterase.
(3) incubation in substrate-free medium.

## 4.0 Embedding, Sectioning and Staining for electron microscopy

### 4.1. Postfixation

The tissue blocks were postfixed in Dalton's solution (1955) for 1 hour at 4° C. This fixative contained 1 part of 4% potassium dichromate brought to pH 7.2 with KOH, 1 part of 3.4% NaCl and 2 parts of 2% Osmium tetroxide solution.

### 4.2. Dehydration

Specimens were dehydrated in 30%, 50%, 70%, 80%, 90% acetone and in two changes of anhydrous acetone (by using copper II sulfate, anhydrous), each step 30 minutes.

### 4.3. Embedding and Polymerization

Samples were embedded in Durcupan ACM (Fluka) and polymerized at 60° C for 48 hours.

4.4. Sectioning and Staining

The ultracut microtome (Reichert Jung) was used. Semithin sections 0.5 to 1 µm thick were cut with glass knives and used for light and phase contrast microscopy. Semithin sections stained with Azure II were examined by light microscopy for orientation and unstained-semithin sections were used for evaluation of the reaction product by phase contrast.

Ultrathin sections of silver and gold interference color were cut on a diamond knife (Diatome) and picked up on 200-mesh uncoated copper grids. The grids were stained with uranyl acetate and lead citrate (Reynolds 1963; Venable and Coggeshall 1965) and examined with a Zeiss 9S-2 or Philips EM 300 electron microscope at 60 kV.

## III. Ultrastructural localization of embryonic cholinesterase in the chick limb bud

### 1.0. Introduction

#### 1.1. General Development of the Limb

The development of paired limbs in vertebrates starts in the lateral plate mesoderm on each side of the embryo. The upper edge of the somatic layer of the lateral plate mesoderm thickens. The cells of this thickening lose their association with the mesodermal epithelium and migrate laterally beneath the overlying ectoderm. These mesenchymal cells proliferate locally and consequently produce two pairs of disc like masses, the limb discs, at sites representing the future pectoral and pelvic appendages. In the amniote embryo, the mesenchymal cells accumulate beneath the ectoderm as a distinct horizontal ridge, the Wolffian ridge. Enlargement of each ridge in the pectoral and pelvic positions, coupled with the gradual disappearance of the intermediate portion of the Wolffian ridge, results in the formation of the definitive limb buds. The pectoral and pelvic limb buds develop progressively and give rise to the forelimbs and hindlimbs (Saunders 1948; Ampino 1965; Zwilling 1968, 1972).

#### 1.2. Chick Embryo Limb Bud

In the chick embryo, the limb buds appear as thickening of the somatopleure that are lifted off the embryo by the inturning of the lateral body folds. The wing bud first appears at stage 16 and the leg bud at stage 17 (Hamburger and Hamilton, 1951).

#### 1.3. The Apical Ectodermal Ridge

The ectoderm of the lateral body wall in the chick embryo consists of two layers of cells, an outer layer of flattened cells called the periderm and an inner layer of cuboidal cells resting

on the basement membrane that covers the mesoderm. Correlated with the thickening of the somatopleural mesoderm beneath the ectoderm (Searls and Janners, 1971), the cuboidal layer of the distal and ventral sides of the future limb becomes slightly thickened and bulges outwards (Milaire 1965; Saunders 1977). As the limb bud grows and increases its proximo-distal dimension, the thickened zone of ectoderm becomes a well defined ridge, which follows the rim of the bud in the antero-posterior plane. This well-defined ridge changes its form from a single cuboidal to a pseudostratified columnar epithelium called the Apical Ectodermal Ridge (AER) (Saunders 1948; Saunders and Reuss 1974).

## 1.4. The Roles of Ectoderm and Mesoderm in Limb Differentiation

The apical ectodermal ridge (AER) is required for mesodermal outgrowth (Saunders 1948; Zwilling 1949) while limb mesoderm is required for the maintenance of the apical ectodermal ridge (Zwilling and Hansborough 1956; Saunders and Gasseling 1968).

According to the Saunders-Zwilling hypothesis of ectodermal-mesodermal interaction (Zwilling 1961; Saunders 1969), the apical ectodermal ridge induces outgrowth in the underlying mesoderm. In recent years the hypothesis has been modified by the addition of a further element, the zone of polarizing activity and its control of antero-posterior differentiation (Tickle et al. 1976; Fallon and Crosby 1977; Saunders 1977).

In the latest, the main feature of the Saunders-Zwilling hypothesis are as the following (reviewed by Hinchliffe 1977):

1. Initially the apical ectodermal ridge is induced in the ectoderm by the underlying prospective limb mesoderm

2. The apical ectodermal ridge induces the outgrowth of the underlying mesoderm, which forms progressively more distal structures

3. The apical ectodermal ridge is not autonomous, but is itself maintained by a mesodermal factor. This factor is transmitted in a proximo-distal direction and is thought to be more concentrated in the postaxial mesoderm than preaxially.

4. The limb type, wing or leg, is controlled by the mesoderm.

5. The posterior margin of the limb or zone of polarizing activity when transplanted to the preaxial margin, acts as the source of a morphogenetic gradient imposing a secondary antero-posterior axis of differentiation.

The apical ectodermal ridge induction hypothesis was challenged by Amprino. His hypothesis of a dio-mesenchymal role for the ectoderm has questioned the view that the apical ectodermal ridge has an inductive role in limb outgrowth (Amprino 1965, 1974, 1977). In his opinion, the apical ectodermal ridge consists of ectodermal cells which have "piled up" distally during growth. The distal movement of the ectoderm is greater than that of the mesoderm. This ectodermal sliding provides a distal space which is constantly filled by mesoderm. Limb outgrowth is thus controlled not by the special ectodermal ridge, but by the topography of the whole ectodermal cap, which shapes the enclosed mesoderm. The outgrowth and differentiation of the mesoderm are an expression of the [illegible] properties of this tissue. The morphogenetic control is exerted by the more proximal regions on the more distal, and does not depend on the inductive influence of the ridge.

## 1.5. Differentiation of Mesoderm in Limb Bud

The mesoderm is the major component of the limb bud. In early stages the mesoderm consists of a loosely packed primary mesen-

chyme. The mesenchymal cells show irregular shape, each cell having many fine filopodial cytoplasmic extensions which make contact with neighbouring cells. In the case of cells close to the ectoderm, they make contact to the basal lamina of the ectoderm (Kapyris 1977). During the course of development, the initial uniformity of the mesodermal cells is differentiated and begins to produce the distinctive histological structure associated with the skeleton, the musculature and the blood vessels.

One characteristic feature of development in the mesoderm is the occurence of highly localized areas of cell death. Cell death occurs along the anterior and posterior edges of the limb bud. These anterior and posterior necrotic zones play a role in contour formation. Later, there are the interdigital necrotic zones which appear between the digits. The massive destruction of cells in the interdigital zones brings about the separation of the individual limb digits (Saunders et al. 1962).

In conclusion, the mesenchymal cells produce the changes of form and pattern in limb development. These include proliferation by mitosis, cell death, cell movement, cell orientation and differentiation to give rise to various tissues in the limb bud.

## 1.6. Chondrogenesis and Pattern Formation in Limb Bud.

Concurrently with changes in the external appearance, differentiation occurs in the interior of the limb rudiments. The mesenchymal cells which are closely packed in young limb buds become segregated into loose peripheral and dense central areas. The latter are the rudiments of the skeletal parts of the limb. The mesenchymal condensations appear proximally earlier than distally. This distinct condensation represents the proximal limb skeleton. The development of the limb skeleton proceeds in a proximodistal direction (Summerbell et al. 1973). The skeletal element is initially blocked out in mesoderm as mesenchymal mass and subsequently becomes converted into precartilage.

and then differentiates into cartilage by further deposition of intercellular matrix (Searls et al. 1972).

Pattern formation in the pentadactyl limb is a sequence of sets of elements along the proximo-distal axis with an increasing number of elements in each set: a single one (humerus in the fore-limb, femur in the hind-limb) in the first set forming the stylopod; two in the next (radius and ulna, tibia and fibula) - forming part of the zeugopod; a complicate set of carpals and tarsals next - completing the zeugopod; five in the next set (metacarpals, metatarsals) - forming part of the autopod; and five again in the last set (phalanges) - completing the autopod. In the chick the number of the digits is secondarily reduced to 4 in the wing and leg (Saunders 1948; Ede 1971; Summerbell and Lewis 1975).

## 1.7. Myogenesis in Limb Bud

The mesenchyme of the early limb bud does not contain all the mesodermal cells used for the development of a limb. After the limb bud is formed it receives an additional supply of mesodermal cells from the lower edges of the myotomes. These cells produce the muscles of the limb (Christ et al. 1977; Chevallier et al. 1977, 1978; Jacob et al. 1978).

The general pattern of muscular development is similar wherever it has been studied. Premuscle blastemata develop into muscles by an orderly sequence of changes.

The limb musculature develops from proximally to distally (Wortham 1948). Dorsal muscle masses differentiate ahead of ventral ones (Wortham 1948), although the reverse situation has also been described (Schellswell and Wolpert 1977).
In the stage 22 chick limb bud, proximal condensations can be distinguished. By stage 24, the myogenic condensations are

more marked. At stage 26, the myogenic blastemata have subdivided proximally to form the complex musculature of the limb (Hilfer 1973).

## 1.8. Cholinesterase Activity in Chick Limb Bud

In the chick limb bud, cholinesterase activity was demonstrated and described by Drews and Drews (1972). They found that at stage 16 cholinesterase appears in the ectodermal epithelium and in the apical ectodermal ridge. At stage 20 the single cholinesterase active cells are distributed throughout the mesenchyme of the limb bud. This cholinesterase activity accumulates in a central core constituting the chondrogenic blastema by stage 24. At stage 25, in addition, solitary myoblasts begin to express cholinesterase activity. By now they begin to differentiate and to form muscle anlagen. After fusion of myoblasts, cholinesterase activity in the myotube enhances. From stage 29 onwards, the cartilaginous anlagen of the large bones lose their cholinesterase activity. The tip of the limb bud still exhibits histochemical features similar to those of the whole limb bud at stage 24. From tissue culture experiments (Drews and Drews 1973) concluded that the cholinesterase active phase of chondroblasts is correlated with aggregation and formation of the chondrogenic blastema. At the end of the morphogenetic process embryonic cholinesterase disappears from the chondroblasts.

Embryonic cholinesterase in the chick limb bud has been characterised by colorimetry and disk gel electrophoresis (Schröder 1980). He found that acetylcholinesterase and non-specific cholinesterase are present in the early limb bud. Acetylcholinesterase activity increases slowly between stage 23 to stage 25 and then enhances more rapidly from stage 25 onwards.

Presence of a muscarinic acetylcholine receptor in the chick limb bud was demonstrated by Schmidt (1981). He exmained the receptor by binding studies which were done with the specific muscarinic ligand quinuclidinyl benzilate in a tritium labeled

form ($^3$H-QNB). The homogenate of limb buds at stage 24 shows specific binding of $^3$H-QNB reflecting a muscarinic receptor. This specific muscarinic acetylcholine receptor is part of the cholinergic system whose presence is indicated by cholinesterase activity in the chondrogenic core of the limb bud during morphogenesis.

## 2.0. Results

Since wing buds and legs principally showed the same distribution of ChE activity, for the sake of clarity, the following description concentrates on the wing bud. The description is based on three types of sections:

1) Semithin sections stained with AzureII used for orientation;
2) Unstained semithin sections for examination of enzyme reaction by phase contrast;
3) Ultrathin sections prepared for ultrastructural localization of ChE activity.

In the blocks of the chick limb bud described here the reaction medium always contained 2 x $10^{-5}$ M ethopropazine, a blocker of unspecific cholinesterase activity. Therefore, the cholinesterase activity (ChE) described in the limb bud, by this definition is specific cholinesterase (AChE). At stage 24, one experiment was carried out without ethopropazine. Localization and intensity of the reaction was the same as with the blocker.

### 2.1. Stage 23 and 24

Light microscopy: In the wing bud stage 23 - 24 the ectodermal epithelium is two cell layers thick, consisting of inner basal cells and outer flat peridermal cells. The ectodermal epithelium changes distally from cuboidal to columnar. The columnar cells form the apical ectodermal ridge (AER) at the tip of the limb bud. The AER shows a fan shaped structure. The subridge mesenchymal cells have random orientation. In stage 23 the mesenchymal cells are already condensed in a small central and proximal area (Fig. 2a). This condensed cell mass is presumptive cartilage. Beneath the epithelium a condensed area of basophilic cells arranged in palisades can be distinguished on the central and dorsal side of the limb bud (Fig. 2b). The ventral and dorsal muscle masses later on will differentiate within this palisade mesenchyme.

Phase contrast microscopy: Some ChE active cells are found in the AER, lateral epithelium, subridge area, presumptive proximal cartilage forming area and ventral and dorsal muscle forming areas. However, in contrast to the ultrastructural observation, most of the cells appear negative. The single positive cells show coarse granules in the perinuclear area and diffusely in the cytoplasm (see Fig. 16, 17, 18 from stage 25). It is obvious that when compared with ultrastructural distribution of reaction product, in the phase contrast only the heavy precipitate is visible but not the homogeneous end product visible with the electron microscope.

Electron microscopy: In lower magnification the apical ectodermal ridge appears as pseudostratified columnar epithelium covered with an outer layer of flat peridermal cells (Fig. 3). Some peridermal cells show necrotic changes with autophagic vacuoles. The columnar cells possess all the characters of an epithelium with intercellular junctions (junctional complex, desmosomes) and rest on a basal lamina. The nuclei show homogeneous chromatin with one or two nucleoli. The nuclear envelope usually appears as double membrane with pores. The cytoplasm contains many free ribosomes and polysomes, endoplasmic reticulum, mitochondria, Golgi complex and lysosomes.

All the columnar cells show ChE activity. The peridermal cells display no ChE activity (Fig. 3). The enzyme activity in the positive cells is localized in the cisterna of the nuclear envelope, the endoplasmic reticulum and in the Golgi apparatus (Fig. 3). The reaction product in the nuclear envelope is not homogeneous. Areas with strong reaction interchange with areas without reaction or weak reaction (Fig. 4,5). The reaction product in the perinuclear cisterna is located between the two membranes. In the tangential section of some cells,

nuclear pores are often visible as unstained circular areas. The perinuclear cisterna is directly connected to the ChE active profiles of endoplasmic reticulum (E.R.) (Fig. 4). The Golgi zone is located around or in the vicinity of the nucleus. The ChE activity of the Golgi complex is localized inside the cisternae. Numerous mitochondria situate deeper in the basal part of the columnar cells. The mitochondria are often very elongated which presumably indicates that these cells are metabolically very active (Fig. 3,4). The mitochondria contain round homogeneous electron dense granules not related to the enzyme reaction.

The lateral epithelium exhibits an inner cuboidal cell layer and an outer flat peridermal cell layer. The cuboidal cells show ChE activity whereas the flat peridermal cells are negative. Intercellular distribution is the same as in the AER. The activity, however, is weaker than in the ridge area. Towards proximal negative epithelial cells are also encountered in the inner cuboidal layer.

In the subridge area, the mesenchymal cells are randomly oriented. The interspace between the basal ectodermal cells and mesenchymal cells is relatively wide. This subridge interspace contains extracellular fibrils (Fig. 3). The mesenchymal cells are interconnected by cytoplasmic processes forming small contacts with each other (Fig. 6-7). The mesenchymal cell processes that spread beneath the basal lamina make contact with it. Between the mesenchymal cells, there are also wide intercellular spaces containing some fibrillar and granular material.

Most of the undifferentiated mesenchymal cells in the subridge area possess relatively large and rounded nuclei with well developed nucleolus (Fig. 6). The perinuclear cisterna always

contains ChE activity. The reaction product may be spotty or may involve the entire nuclear envelope. Nuclear pores have no enzyme activity. In the cytoplasm the ER is present as short profiles, and shows ChE activity. The reaction product is distributed inhomogeneously in the cisternae of ER. Within particular areas profiles with strong and weak rection alternate. ER cisternae showing a positive reaction and such devoid of reaction are always observed within the same cell (Fig. 7). In some cells continuity between the ChE active cisternae of the ER and of the nuclear envelope can be seen.

Some profiles of the ER showing positive reaction extend into close proximity of the plasma membrane (Fig. 8,9). Occasionally, such ER cisternae course parallel to the plasma membrane for some distance, leaving a gap of approximately 10 - 15 nm between the outer face of the ER membrane and the inner face of the plasma membrane. The space between the membranes sometimes contains small amounts of a moderately electron dense material (Fig. 9).

The Golgi complex consists of stacks of lamellae and small vesicles, which show ChE activity (Fig. 7,10). Some vesicles of Golgi complexes may also be negative (Fig. 9). The mitochondria have the usual organization of cristae. Some mitochondria contain round homogeneous electron dense granules (Fig. 9). There are many free ribosomes and some polysomes. The centriole displays no enzyme activity (Fig. 10).

In the cartilage forming area (proximal central mesenchyme) of stage 23 - 24, cells appear randomly arranged (Fig. 12). The cell bodies are irregular in shape and have an increased number of filopodia. The filopodia form contacts to neighbouring

cells. Extracellular spaces are large and filled with flocculent and fibrillar materials. The nuclei appear to be slightly smaller and have centrally located nucleoli. The cells contain ER and mitochondria in random distribution and a small Golgi complex near the nucleus. Most of the cells display ChE activity in the perinuclear cisterna and the ER (Fig. 12). Strong reactive areas alternate with weak or non-reactive areas. Nuclear pores are devoid of enzyme activity. Often connections between profiles of the ER are visible. Most of the Golgi complexes are now negative. Only occasionally, some Golgi complexes are positive.

In the muscle forming areas (ventral and dorsal mesenchyme) of stage 24, cells align in clusters (Fig. 13). Within the clusters, the cells are closely packed and form broad contacts with each other. In the contact zones, cell membranes are closely apposed. The gap between the membranes is about 35 nm (Fig. 14). At the junction the cytoplasmic face of the membrane is covered with electron dense material. The cell bodies appear to be bigger and have more cytoplasm than the cells in the cartilage forming area. Mitochondria are increased in number. Cells have elongated nuclei with homogeneous euchromatin and dense nucleoli. The nuclear envelopes show weak ChE activity in the cisternae. In the cytoplasm, there are small profiles of ER. Some profiles display enzyme activity and some of them have no activity. Ribosomes are increased in number. The distribution of free ribosomes in cytoplasm causes an increased density of the cytoplasm. In general, cells show weaker ChE activity than the cells in subridge and cartilage forming areas. Intracellular localization of the enzyme activity is similar to the cells from other areas, although less intense.

Mitosis: In the subridge area as well as in the cartilage and muscle forming areas mitotic cells are frequently observed. The mitotic cells show ChE activity in the segments of ER and remnants of the nuclear envelope which are dispersed in cytoplasm (Fig 15).

In summary, in stage 23 and 24, all columnar cells of the AER, the undifferentiated mesenchymal cells of the subridge area, the presumptive chondroblasts, and some cells in the muscle forming area show ChE activity. The reaction product is localized in the perinuclear cisterna, the profiles of ER and the Golgi complex. The enzyme reaction is blocked by addition of eserine to the incubation medium (Fig. 11).

## 2.2. Stage 25

Light microscopy: In the limb bud stage 25 (Fig. 1c), AER and subridge area are similar to stage 24. The marginal sinus and other blood vessels can be clearly distinguished. In the central area of the proximal part, the mesenchymal cells are more condensed and form the prechondrogenic mass. The premuscle masses consisting of basophilic cells are located at the dorsal and ventral side of the prechondrogenic mass.

Phase contrast microscopy: In the AER, ChE active cells could not be seen although in the EM all columnar cells exhibit homogeneous reaction product. Obviously this is not visible in phase contrast. In the subridge area some single positive cells with coarse dark granules of reaction product are found (Fig. 16). Most cells in the proximal cartilage forming area show ChE activity in the cytoplasm (Fig. 17). In the muscle forming area cells display strong ChE activity also in the cytoplasm (Fig. 18). The strongly reactive cells seem to contain more than one nucleus.

Electron microscopy: Cells in the AER (apical ectodermal ridge) and in the subridge area show ChE activity in the perinuclear cisternae and the profiles of ER similar to the previous stages (Fig. 19). In the subridge area, necrotic cells are often found, probably related to physiological necrosis in interdigital areas. The necrotic cells have no ChE activity.

In the cartilage forming area, the cells have an increased number of filopodia. They are separated by large interspaces which contain more floccular and fibrillar material than in stage 24. The cells appear stellate in shape. The nuclei show homogeneous euchromatin. The cells of the cartilage forming area show enzyme activity. The enzyme reaction is localized in the perinuclear cisterna and in the ER as observed in the previous stages (Fig. 20). In some cells the Golgi apparatus exhibits a positive reaction. In most chondroblasts enlarged vesicles are found in the Golgi region. Some contain amorphous material (Fig. 20). The enlarged vesicles in the Golgi area are ChE-negative.

In the muscle forming area, the cells start to organize into cords and lie parallel to the long axis of the limb bud. Most of the cells are elongated and have rectangular shape. They contain many mitochondria and a lot of ER (Fig. 21). All of the cells within the cords are closely apposed and make broad contacts with each other. Only in some of these cells the ER and the nuclear cisterna exhibit a strongly positive ChE reaction. The ChE-positive myocytes with strong reaction are surrounded by myoblasts with weak reaction and by ChE-negative mesenchymal cells (Fig. 21). Some negative myoblasts characteristic for the following stages are already present.

In the distal part of the muscle forming area, the cells are still aligned in the palisade like structure. The palisade structure disintegrates and randomly orientated clusters of cells appear. Some clusters appear to lie perpendicular to the lateral epithelium. The cells of the clusters show ChE activity in the perinuclear cisterna, the profiles of the ER and in some Golgi complexes (Fig. 13).

## 2.3. Stage 26

Light microscopy: In the wing bud of this stage, differentiation of cartilage and muscle anlagen is more advanced (Fig. 1d). The AER is still a distinctive structure with nipple like shape. In the mesenchyme of the subridge area, the marginal sinus and some capillaries are clearly visible. The central chondrogenic core and the dorsal and ventral muscle masses are well defined and separated from each other by a network of capillaries. The cartilaginous area consists of nests of dense cartilage cells and light areas filled with cartilage matrix. The dense ventral and dorsal muscle masses contain proximally more fused cells and nerve fibers.

Phase contrast microscopy: As in stage 25, it is difficult to see the reaction product in mesenchymal and epithelial cells. The coarse reaction product is still visible in the central chondrogenic core and in the muscle cells. Some muscle cells show strong ChE reaction. A close look shows that strongly reactive cells have already fused and are multinucleated. In sections without ChE reaction these cells cannot be distinguished.

Electron microscopy: The ultrastructure and the intracellular enzyme localization of the cells in the AER and the subridge area are still similar to stage 23.

In the cartilage forming area, the changes characteristic for cartilage differentiation are found. Most of the cells are elongated and have oval nuclei (Fig. 22). The cytoplasm contains more elongated mitochondria. The profiles of extended rough endoplasmic reticulum appear as described in detail in

stage 27. ChE activity of chondroblasts is localized in the perinuclear cisterna and in an elaborate system of small profiles of ER (Fig. 22). The extracellular spaces contain numerous fine fibrils 12 to 25 nm in a diameter.

In the muscle forming area, distally cells are still arranged in palisade. In the undifferentiated cells of the palisade the ChE reaction is rather weak. The enzyme is localized in the perinuclear area and in slender strands of ER. In the proximal part of the muscle forming area, fusion of myoblasts is in progress whereas most of the cells are still unfused. In the fused cells (Fig. 23), there is no evidence of an intervening plasmalemma between adjacent nuclei. The cytoplasmic organelles are located in a common cytoplasm. The fused cells contain a lot of thick and thin myofilaments which in some locations are loosely arranged into myofibrils (Fig. 24). There are diffuse Z-disc like bands crossing the myofibrils even if Z-discs are not yet well organized.

In addition to the increased formation of myofilaments, several intracellular changes occur, such as an increase in the number of polysomes, profiles of ER and mitochondria. The aggregation of ribosomes in the fused cells causes the cytoplasm to appear less dense. In contrast with unfused myoblasts, more ribosomes are present in the cytoplasm, giving rise to a more dense appearance of the cells. The fused cells show an increase in ChE activity. The enzyme is localized in the entire perinuclear cisterna and in the endoplasmic reticulum. The ChE active profiles of ER differentiate to sarcoplasmic reticulum by running parallel to myofibrils. The fused cells with strong ChE reaction are surrounded by myoblasts with no or weak reaction and by ChE-negative mesenchymal cells.

## 2.4. Stage 27

Light microscopy: The distal part of the limb anlage shows the same arrangement of AER and subridge mesenchyme. The obvious cartilage corresponds to the metacarpus (Fig. 1e). In the whole limb anlage the hand or foot plate with indication of digits is visible. The cartilageneous stylopod and zeugopod with metachromatic matrix are well delineated by capillaries and loose mesenchyme in the area of the prospective elbow. As well the broad dorsal and ventral muscle masses with nerve fiber invasion are seen.

Phase contrast microscopy: In the AER, ChE positive cells can not be seen although all columnar cells show enzyme activity in the EM. In the subridge and cartilage forming areas, some cells exhibit ChE activity. Numerous strongly ChE positive multinucleated muscle cells are found in the muscle forming area.

Electron microscopy: The columnar cells of the AER show ChE activity as in earlier stages (Fig. 25). Many necrotic cells are present in the peridermal layer. No ChE activity can be detected in intact flat peridermal cells.

The subridge area still is composed of undifferentiated mesenchymal cells with ChE activity.

In the chondrogenic area a gradual change occurs from undifferentiated cells in the tip to more differentiated chondroblasts in the proximal part of the limb bud. During this transformation the intracellular localization of ChE does not change.
In the distal part the chondroblasts have a stellate shape and an increased number of filopodia (Fig. 26). The cells are connected to each other by cytoplasmic processes. The extracellular

spaces are extended and contain floccular and fibrillar material. The chondroblasts display ChE activity in the narrow strands of ER. Some of the chondroblasts show less or no enzyme activity. The disappearance of ChE active ER goes along with appearance of extended ChE negative rough endoplasmic reticulum. The ChE negative Golgi zone tends to have more extended vesicles and contains homogeneous amorphous material (Fig. 26).

More proximally, the chondroblasts form parallel aligned stacks of cells. The cartilageneous areas are surrounded by flat perichondrial cells. The perichondrial cells show a stronger ChE activity than the central chondroblasts. In the center of the chondrogenic core cell to cell contacts are reduced in number and restricted to small areas of the cell membrane. The extracellular spaces contain fine fibrils and amorphous material. The chondroblasts are embedded in this amorphous matrix. Some of the amorphous material and fine fibrils lie close to the cell surface (Fig. 27). Relatively undifferentiated chondroblasts still show strong ChE activity. More differentiated cells become negative. The advanced state of differentiation of these cells is indicated by the presence of extended cisternae of rER and numerous vesicles, both filled with homogeneous amorphous material. The differentiated chondrocytes exhibit no ChE activity (Fig. 28). Only few differentiated cells containing extended cisternae show a positive reaction in the narrow strands of ER. The proportion of differentiated ChE negative chondrocytes is increased in this area because of the transition from ChE active chondroblasts to ChE negative chondrocytes.

In the muscle areas, at a distal part only a few differentiating myocytes are found. Fused myocytes increase in number from the middle towards the proximal part of the muscle forming area. In these areas many multinucleated cells or tubes are observed (Fig. 29). They contain euchromatic nuclei which are

aligned in chains. Myofilaments are arranged into myofibrils which now are wider and more compact than in younger stages. The Z-discs are well organized (Fig. 30, 31). Vesicles and tubular profiles as well as mitochondria are located between the myofibrils. The ChE active profiles of ER run parallel to the myofibrils. They represent the developing sarcoplasmic reticulum. The ribosomes form aggregates so that clear spaces are present in the cytoplasm. The multinucleated cells show ChE activity in the entire perinuclear cisterna and in the sarcoplasmic reticulum. At this stage of myogenesis, ChE negative myoblasts and mesenchymal cells are still present at the periphery of the differentiating myocytes or the multinucleated myotubes.

Soft tissue: By light microscopy the soft tissue between the lateral epithelium and the muscle forming area is ChE negative in this stage. Also in the electron microscopy, the cells of the lateral epithelium and the subepithelial tissue have no enzyme activity (Fig. 32). The soft tissue contains mainly fibroblasts. They are elongated and contain abundant rough endoplasmic reticulum as well as vesicles partly filled with an amorphous material. These vesicles are not observed in younger stages (Fig. 33). No reaction product can be found in these fibroblasts. A high amount of fibrils is present in the extracellular space of the soft tissue.

## 3.0. Summary "ChE in chick limb bud"

### 1. Intracellular localization of embryonic cholinesterase

The ChE positive epithelial and mesenchymal cells of the limb bud show the same intracellular localization of the enzyme. The reaction is localized in the perinuclear cisterna, the profiles of endoplasmic reticulum (ER) and the Golgi complex. The reaction product is not homogeneous in the nuclear cisterna and the ER. Areas with strong reaction interchange with areas of weak or no reaction (Fig. 7).

The ChE positive profiles of the ER are connected to the nuclear envelope. Between ChE positive ER and the plasma membrane specialized contact zones are observed. The ER is apposed to the plasma membrane or runs parallel close to it for some distance, leaving a gap of approximately 10 - 15 nm between the outer face of the ER membrane and the inner face of the plasma membrane (Fig. 9). In chick limb bud cells show similarly strong ChE activity with and without ethopropazine. This indicates that they contain only acetylcholinesterase (AChE) activity.

### 2. Apical ectodermal ridge and lateral ectoderm

The ectodermal epithelium of chick limb bud is two cell layers thick, consisting of inner cuboidal cells and outer flat peridermal cells. The inner layer changes distally from cuboidal to columnar forming the apical ectodermal ridge (AER) at the tip of the limb bud. The columnar cells of the AER and the cuboidal cells of the lateral epithelium now show ChE activity whereas the flat peridermal cells are negative. The enzyme activity in the columnar cells is stronger than in the cuboidal cells. Towards proximal more and more negative cuboidal cells are found, whereas the AER remains positive throughout all stages studied (stage 23 - 27).

3. Subridge mesenchyme

The subridge mesenchyme is composed of undifferentiated cells. Cells are randomly oriented and interconnected by cytoplasmic processes forming small contacts with each other (Fig. 6, 7). They exhibit AChE activity from stage 23 - 27.

4. Chondrogenesis

In the central area of the limb bud, the mesenchymal cells condense and form the chondrogenic core. The cells are irregular in shape and have many filopodia. These chondroblasts show strong AChE activity in the cisterna of the nuclear envelope and the ER (Fig. 12).

The AChE positive chondroblasts gradually change to more differentiated chondroblasts with weak AChE activity and later on become AChE negative differentiated chondrocytes in the older stages (compare Fig. 22, 27, 28). The advanced state of differentiation is indicated by ChE negative Golgi zone and appearance of extended AChE negative rough ER instead of AChE positive narrow strands of ER. Both extended rER and Golgi vesicles contain homogeneous amorphous material. This transformation into AChE negative chondrocytes starts proximally at stage 26 and proceeds distally.

5. Myogenesis

At stage 24, the first myoblasts appear in the dorsal and ventral palisade mesenchyme of the limb bud. The myoblasts align in clusters (Fig. 13). The palisade mesenchyme and the myoblasts show weaker AChE activity than the cells in the subridge and cartilage forming areas. Intracellular localization is the same as in other areas (Fig. 14).

In stage 25 (Fig. 21), differentiated myocytes appear. The myoblasts are closely attached to the myocytes and show no AChE activity. The myocytes (after fusion) contain strong AChE in the entire perinuclear cisterna and the developing sarcoplasmic reticulum (SR).

From stage 26 onward, the myotubes contain thick and thin myofilaments. The thick and thin myofilaments are loosely arranged into myofibrils. Within the myofibrils, there are developing Z-discs (Fig. 24). Later on, the myofibrils become wider and more compact. The Z-disc are now well organized (Fig. 31). The myotubes show strong AChE activity in the nuclear envelope and in the SR. The AChE active profiles of SR run commonly parallel to the myofibrils. The myotubes with strong AChE reaction are surrounded by myoblasts with weak or no reaction and by AChE negative mesenchymal cells (Fig. 30).

## IV. Ultrastructural localization of embryonic cholinesterase in the genital tract of mouse embryo

### 1.0. Introduction

### 1.1. Development of the genital tract

In mammals, the embryonic genital tract consists of two pairs of gonadal ducts, Wolffian ducts (mesonephric ducts) and Müllerian ducts (paramesonephric ducts) (Felix 1912; Müller 1830). Depending on the sex of the embryo, one pair of ducts develops while the other one regresses. This sexual differentiation of the genital tract is determined by the sex chromosomes and controlled by fetal testicular hormones (Jost 1947).

Differentiation of the genital tract proceeds in two steps

1) In the indifferent stage Wolffian and Müllerian ducts develop similarly in both sexes.
2) In the following stages the Wolffian ducts differentiate into the male and the Müllerian ducts into the female genital tract.

### 1.2. The indifferent genital tract

Although the genetic sex of an embryo is established at fertilization, the genital tract develops similarly in both sexes during early embryonic life (Price et al. 1975).

The Wolffian ducts originate dorsolaterally to the segmented pronephric blastema and laterally to the somites. Lateron, they extend from the gonads caudally and reach the urogenital ridge. The duct opens into the coelomic cavity with a funnel like structure cranially. It runs caudally parallel to the Wolffian duct and then crosses the latter ventrally. Here it comes in close contact with the Müllerian duct from the opposite side in the median line. The two ducts fuse later and

project into the dorsal wall of the urogenital sinus. The tip of the fused ducts causes an elevation of the dorsal wall called the Müllerian tubercle. The Müllerian tubercle consists of sinusal tissue. Müllerian ducts do not open into the urogenital sinus until later, when canalization of the vagina occurs. In contrast, the Wolffian ducts have a lumen and enter the urogenital sinus on each side of the Müllerian tubercle.

The urogenital sinus is formed by the transverse urorectal septum which divides the cloaca into the rectum dorsally and the urogenital sinus ventrally. The Müllerian tubercle demarcates the cranial vesico-urethral canal from the caudal urogenital sinus (Jirásek 1971; Wilson 1978).

### 1.3. The differentiated genital tract and the role of the fetal testis

The role of the testis in the control of differentiation of the genital tract was established by Raynaud (1937, 1938) and Jost (1947). Male sex differentiation of the genital trac is controlled by testosterone and antimüllerian hormone which are produced by the fetal testis. In contrast female differentiation of the genital tract requires no stimulation (Jost et al. 1973).

In the male embryo, the fetal testis produces androgen which is required for masculine morphogenesis of mesonephric tubules, the Wolffian ducts, urogenital sinus, external genitalia and mammary glands (Price et al. 1971; Jost et al. 1977). The mesonephric tubules will maintain and differentiate into efferent ducts. The Wolffian ducts which are the potentially male ducts, differentiate into epididymis, ductus deferens, seminal vesicles and ejaculatory ducts.

From the urogenital sinus, the prostate glands, bulbourethral glands and urethra develop. The Müllerian ducts regress by action of the anti-Müllerian hormone which is also produced by the fetal testis in the male fetus (Picon 1971;Josso et al 197 Donohoe et al. 1977; Picard et al. 1978).

In the female embryo, the urogenital tract develops in the absence of these testicular hormone (Price and Ortiz 1965; Jost 1965; Jost et al. 1977). The Müllerian ducts differentiate while the Wolffian ducts regress. The Müllerian ducts are the potentially female ducts that differentiate into uterine tubes, uterus and a portion of vagina.

## 1.4. Morphogenesis of the male genital tract

In the male embryo, after regression of the mesonephros, the cranial mesonephric tubules which connect the rete testis to the mesonephric ducts persist and become the efferent ductules (ductuli efferentes or vasa efferentia) of the testis. These ductules open into the Wolffian duct. The cranial end of the Wolffian duct forms the appendix of the epididymis (appendix epididymis). The Wolffian duct develops into a convoluted epididymis (ductus epididymis). The portion of the Wolffian duct caudal to the epididymis becomes covered by smooth muscle layer and differentiates into the vas deferens (ductus deferens). The terminal portion of the vas deferens will dilate and gives rise to the seminal vesicle (vesicular gland). Those portions of the mesonephric system not involved in genital organogenesis degenerate.

The Müllerian duct in the male embryo degenerates entirely except for a small portion at the cranial tip which becomes the appendix testis, and the caudal end which becomes the prostatic utricle (utriculus prostaticus). Regression of the Müllerian duct proceeds in a cranio-caudal direction due to the action of anti-Müllerian factor (Jirásek 1971; Josso 1977).

The urogenital sinus in male embryo is characterized by the development of the prostate glands and the prostatic utricle. Prostatic rudiments appear as epithelial buds at the site of the Müllerian tubercle. This epithelial buds grow laterally from the side walls of the urogenital sinus. The buds develop and are transformed into prostate glands (Glenister 1962). Bud development is induced by mesenchymal differentiation and mesenchymo-epithelial interaction (Kellokumpu-Lehtinen et al. 1979).

## 1.5. Morphogenesis of female genital tract

In the female embryo, the Wolffian ducts degenerate and contribute mesenchymal tissue to the formation of the uterine wall (Witschi 1970).

The Müllerian ducts develop into the main genital tract of the female. The cranial unfused portions of the Müllerian ducts develop into the uterine tubes. The middle portion or the Müllerian ducts fuse and give rise to the unpaired body of the uterus (O'Rahilly 1977; Josso 1981).

The development of the vagina is still controversial with respect to its derivation. It may develop from the Müllerian ducts, from the Wolffian ducts, from the urogenital sinus, or from a combination of these structures (Müller 1830; Valentin 1835; Hart 1901; Mijsberg 1924; Bulmer 1957; Forsberg 1963, 1965, 1973; Witschi 1970; Jost 1971; O'Rahilly 1977). According to Koff (1933) the vagina is formed by the caudal tip of the fused Müllerian ducts (Müllerian vagina), by two dorsolateral evagination of the dorsal sinus wall (Sino-vaginal bulbs) and by medial outgrowth of the dorsal sinusal wall at the site of the Müllerian tubercle. These structures fuse to form the vaginal plate which occludes the lumen of the caudal portion of the utero-vaginal canal. Later the vaginal lumen is formed by necrosis of the central cells.

Bok and Drews (1983) have studied the role of the Wolffian ducts in the formation of the sinus vagina by organ culture. They found that the sinus protrusions or sinovaginal bulbs observed during development of the vagina, are the caudal segments of the Wolffian ducts. They serve as a link between Müllerian ducts and urogenital sinus.

## 1.6. Histochemical studies in the embryonic genital tract

In general, only few histochemical studies were conducted in embryonic tissues the reason being mainly technical difficulties. Forsberg and Olivecrona (1964) studied the activity of succinic dehydrogenase, malate dehydrogenase, lactate dehydrogenase and 6-phosphogluconate dehydrogenase in the vaginal plate, the sinus epithelium, the Müllerian epithelium and the Wolffian epithelium from human female fetuses. The aim of this study was to clarify the epithelial derivation of the vagina. They found that the vaginal plate has a very low activity of succinic dehydrogenase compared with that in other epithelia. In case of the other enzyme, no differences in activity could be found between the epithelia studied.

Forsberg (1967) reported on the histochemical localization of succinic dehydrogenase, $\alpha$- naphtyl acetate esterase, thiamine pyrophophatase and aminopeptidase in the sinus and Müllerian epithelium of the vaginal anlage in newborn and young aged mice. He found changes in activity of these enzymes during lumen formation in the originally solid sinus vagina. During this developmental process, the activity of succinic dehydrogenase, esterase and aminopeptidase increases and becomes quantitatively the same as in the sinus and the Müllerian epithelium. In case of thiamine pyrophosphatase there is a transitory activity in the sinus vagina during the lumen formation.

In his medical dissertation, Schweers (1979) studied cholinesterase activity during development of male accessory glands and vagina of normal and testicular feminized (Tfm) mouse

embryos. He described location of the enzyme activity in cryostat serial sections submitted to the histochemical reaction after Karnovsky and Roots (1964). He found that in the indifferent stage, the mesenchyme caudal to the junction of the genital ducts (Wolffian and Müllerian ducts) showed a wedge shaped ChE activity ("Zwickelaktivität"). In the male embryo, the ChE active mesenchyme was located at the apical part of the seminal vesicles and prostate glands. In female and Tfm embryos, the ChE active mesenchyme moved caudally with the downgrowth of the vaginal anlage.

The aim of this work is to study ultrastructural localization of the ChE activity described by Schweers (1979) in the developing genital tract of the mouse embryo. In this study, the cryostat serial sections of Schweers were reexamined for light microscopic localization of ChE activity and some photographs were taken for orientation.

## 2.0. Results

Cholinesterase activity is studied in the indifferent genital tract of day 15 and 16 mouse embryos and in male and female embryos of day 17 and 18. In particular, the junctional zone between genital ducts and urogenital sinus is described. In this area, the urogenital tract develops alternatively into urethra with prostate glands and entering deferent ducts with vesicular glands or into urethra and vagina.

The following description is based on three types of sections:

1) Cryostat sections submitted to the histochemical reaction for cholinesterase were used for a survey of ChE activity in the urogenital tract of mouse embryos by light microscopy.
2) Semithin sections stained with Azure II were prepared for morphological orientation and for selection of appropriated areas for ultramicrotomy.
3) Ultrathin sections were performed for subcellular localization of enzyme activity at electron microscopical level.

The ChE reaction was performed with and without ethopropazine, a blocker of unspecific ChE activity. In general, localization of reaction product was the same in both cases. However, intensity of the reaction was stronger when ethopropazine was omitted.

## 2.1. Indifferent stage at day 15 and 16 p.c.

In the mouse embryos at day 15 and 16 p.c., the caudal part of the genital ducts (Wolffian and Müllerian ducts) is still in the indifferent stage whereas in the cranial part differentiation or involution of genital ducts is already visible. In sagittal cryostat sections (Fig. 34) submitted to the histochemical reaction for cholinesterase (ChE), the mesenchyme

caudal to the junction of the genital ducts and the urogenital sinus exhibits a wedge or triangular shaped enzyme activity. In cross section (Fig. 35) the ChE active mesenchymatous condensation is located at the dorsal side of the urogenital sinus beneath the entering of the genital ducts.

In the following, cross sections of the urogenital tract at three levels are described as shown in Fig. 36A:

1) Sections at the junctional area of the genital ducts and the urogenital sinus.
2) Sections cranial to the junctional area.
3) Sections caudal to the junctional area.

In the drawings of Fig. 36B the intensity of enzyme reaction is indicated as one plus to four plus to the positive reaction and none for negative reaction.

On semithin cross sections beneath the entering of the ducts where ChE reaction is strong (Fig. 37), the urogenital sinus is lined by stratified cuboidal epithelium. The epithelium is surrounded by mesenchymal tissue which can be subdivided into three layers. The inner layer consists of densely packed cells and is only one to two cell layers thick. The cells are circularly arranged. In the middle layer mesenchymal cells are loosely arranged at the ventral and lateral sides of the urogenital sinus. At the dorsal side, cells are densely packed into a whorl like mesenchymatous condensation which corresponds to the ChE active zone seen in the cryostat sections. The outer circular layer is myogenic tissue. The morphology and enzyme reaction of this muscular layer will be described in a separate chapter.

By electron microscopy, the epithelium of the dorsal sinus wall shows stronger ChE activity than the ventral sinus epi-

thelium (Fig. 38). The enzyme reaction is localized mainly in the apical part of the epithelium. Some glycogen is also present in the basal part of epithelium. The lateral epithelium has no ChE activity. The enzyme reaction is localized in the cisternae of the nuclear envelope and the ER. The distribution of the reaction product is not homogeneous throughout the cisternae. Areas with strong reaction alternate with areas of weak or non reaction (Fig. 38).

In the inner mesenchymal layer, the densely packed cells are small and irregular in shape and are aligned parallel to the basal lamina of the sinus epithelium (Fig. 39). They show a patchy ChE reaction in the perinuclear cisternae and in the profiles of the ER. The inner mesenchymal layer displays a strong activity at the dorsal side, moderate activity at the ventral side and weak activity at the lateral side.

The mesenchymatous condensation at the dorsal side of the urogenital sinus is composed of closely packed cells forming a whorl like structure (Fig. 37, 40). In the center of the whorl, cells are irregular in shape and are arranged longitudinally in cranio-caudal direction. Cells show small cytoplasmic contacts between neighbouring cells. The nuclei are polymorphic and contain one or two nuclei. The cytoplasm of these cells possesses some mitochondria and ER and a lot of free ribosomes and polysomes. The narrow extracellular spaces contain procollagen microfibrils (Fig. 41). Cells of mesenchymatous condensation exhibit ChE activity. Reaction is again localized in the perinuclear cisternae and in the profiles of ER. Throughout the cisternae areas of strong enzyme reaction alternate with areas of weak or non reaction (Fig. 41). The outer cells of the whorl are elongated and are arranged circularly. The cells have elongated nuclei and display weak ChE activity. The cells in the center of the mesenchymatous condensation exhibit stronger enzyme activity than the surrounding cells.

At the ventral and lateral sides of the urogenital sinus, the cells of the inner mesenchymal layer are densely arranged and possess weak ChE activity. In the middle layer of the mesenchyme (Fig. 42), cells are loosely arranged. The cells have long cytoplasmic processes which form small contacts between neighbouring cells. These cells contain a lot of rough ER, abundant mitochondria and Golgi complexes. The extracellular spaces are wide and contain bundles of microfibrils. Some cells are ChE active.

The ganglia which are located close to the outer myogenic cell layer at the dorso-lateral side of the urogenital sinus show a very strong ChE activity in neuronal cells (Fig. 43). The neurons possess abundant profiles of ER and mitochondria. Large amounts of reaction product are localized in the cisternae of nuclear envelope and the ER and sometimes in the interspaces between closely apposed membranes (Fig. 44). The satellite cells encapsulating the nerve cells are devoid of reaction product (Fig. 43). In those parts of the ganglia which are composed of unmyelineated nerve fibres, reaction product is also present in the interspaces between closely apposed axons. The axoplasm contains no reaction product (Fig. 45).

Cranial to the junction, the epithelium of the unfused Müllerian ducts and the Wolffian ducts shows no enzyme activity. The mesenchymal cells surrounding both ducts and the mesenchyme at the dorsal side of the ducts similarly show no ChE reaction.

Similarly caudally to the junction, no enzyme reaction is found in the epithelium of the urogenital sinus or in the surrounding mesenchymal cells.

2.2. Male embryo at day 17 p.c.

In sagittal cryostat sections, the ChE active mesenchyme is located caudally to the junction of the genital ducts with the urogenital sinus and in the mesenchyme directly above the outgrowth of the seminal vesicles (Fig. 46). The intensity of enzyme reaction is summarized as shown in the drawings of Fig. 47.

In semithin cross sections of the urogenital tract at the area where the Wolffian ducts are fused with the urogenital sinus, the lumen of the latter is U-shaped. The two lateral shanks point to the dorsal side. At the dorsal side, the urethral epithelium is considerably thicker than on the ventral side. The mesenchymal cells which are located between and dorsal to these epithelial protrusions are densely packed. Towards the lateral and ventral side, arrangement of the mesenchymal cells becomes more loose.

In the electron microscope, some ChE activity is observed in the epithelium of the urogenital sinus. The reaction is stronger on the dorsal than on the ventral side. The mesenchymal cells surrounding the sinus epithelium are also ChE positive. At the dorsal side, the cells have strong enzyme activity especially in the area of the mesenchymatous condensation (Fig. 48). Enzyme reaction is less intense on the lateral side, while the cells of the loose mesenchyme at the ventral side display very weak or no ChE activity. Intracellular localization is in the cisternae of the nuclear envelope and the ER. The extracellular spaces contain more procollagen microfibrils when compared to the younger stages.

The epithelium of both Wolffian ducts exhibit weak ChE activity in the basal cell layer. The mesenchymal cells at the dorsal side of the Wolffian ducts show strong reaction. The

subcellular localization of the enzyme reaction in the epithelial and mesenchymal cells is the same as described above for earlier stages.

Cranial to the junction, the fused Müllerian ducts and the Wolffian ducts show some ChE activity in the basal cell layer of the epithelium. The mesenchymal cells surrounding the fused Müllerian ducts and the Wolffian ducts display strong ChE activity in the cisternae of the nuclear envelope and the ER. The profiles of the ER are commonly located close to mitochondria and are continuous with the nuclear envelope (Fig. 49). In mitotic cells reaction product is in the ER and in the remnants of the nuclear envelope. The mesenchymal cells at the dorsal and lateral sides show stronger enzyme activity than those at the ventral side (Fig. 50).

Caudal to the junction, enzyme reaction is still found in the epithelium of the urogenital sinus and the surrounding mesenchymal cells. However, the cells in the mesenchymatous condensation exhibit less activity than in the junctional area (Fig. 51 compare to Fig. 48). Most of the cells in the loose mesenchymal layer at the ventral side have a weak or non reaction (Fig. 52). The negative cells in general are in an advanced stage of differentiation when compared to positive cells. ChE active narrow cisternae are replaced by extended cisternae of rough ER.

## 2.3. Male embryo at day 18 p.c.

In semithin cross sections of the junctional area, the urogenital sinus is still U-shaped. The buds of the vesicular glands are at the dorsal side. At the ventral and dorsal sides now prostrate buds appear.

By electron microscopy, the epithelium of the urogenital sinus and the seminal vesicle have very little ChE activity.

The surrounding mesenchymal cells show positive reaction (Fig. 53). The cells of the mesenchymatous condensation display strong reaction (Fig. 54). In the narrow extracellular spaces, they contain numerous collagen microfibrils.

At the ventral side of the urogenital sinus, the buds of the prostate glands show positive reaction in the surrounding mesenchymal cells while the reaction in the epithelium of the glands is very weak (Fig. 55).

In sections incubated for the AChE reaction, the mesenchymal cells surrounding the epithelium and the cells of the mesenchymatous condensation at the dorsal side of the urogenital sinus are as strongly positive as in the ChE sections (Fig. 56, 57 compare to Fig. 53, 54). A similar reaction of mesenchymal cells is present at the junction of the Wolffian ducts with the urogenital sinus and in the mesenchyme surrounding the buds of the vesicular glands. The enzyme reaction in the mesenchymal layer of the prostate buds is of similar intensity. Interestingly the centrioles have no reaction (Fig. 58).

In sections located more cranially, the epithelium of the Wolffian ducts and of the vesicular glands exhibits slightly positive reaction in the basal cells. The mesenchymal cells surrounding the ducts and the glands display strong ChE activity.

In sections through the caudal part of the urethra, the epithelial cells show slight ChE activity whereas the surrounding mesenchymal cells in the middle layer at the dorsal, ventral and lateral sides have no reaction.

2.4. The female embryo at day 17 p.c.

In sagittal cryostat sections, the ChE reaction is particularly strong in the mesenchyme located dorsally of the junction of the genital ducts with the urogenital sinus. The ChE active mesenchyme shifts caudally with the downgrowth of the vaginal anlage (Fig. 59). The intensity of enzyme reaction is shown in the drawings (Fig. 60).

By electron microscopy cells of the dorsal mesenchymatous condensation (Fig. 61) in the junctional area show strong ChE activity. In the loose mesenchyme at the dorsal side, cells exhibit only moderate ChE activity. In the ventral loose mesenchyme of the urogenital sinus, cells display a very weak activity. The enzyme reaction is localized in the perinuclear cisternae and in the profiles of the endoplasmic reticulum.

In the mesenchymatous condensation, cells are arranged irregularly and possess many pseudopodia. The cells are connected with gap junction between the neighbouring cells. Collagen fibres are found in the extracellular spaces. In the cytoplasm of the mesenchymal cells extended rough ER are present. In positive cells the reaction product is found in the small stretched ER in the continuity of the rough ER. The active strands are narrow when compared to the negative strands (Fig. 61).

In sections located more cranially, the fused Müllerian ducts and the Wolffian ducts are surrounded by loose mesenchyme. This surrounding mesenchymal cells exhibit very weak reaction in some areas of the perinuclear cisternae and the endoplasmic reticulum. Interestingly in this region the Wolffian duct is surrounded by some necrotic mesenchymal cells showing no ChE activity.

In sections located caudally to the junctional area as in the male, a whorl of densely packed mesenchymal cells is present at the dorsal side of the urogenital sinus (Fig. 51 from male embryo). The circular cell layer surrounding the mesenchymatous condensation shows no activity. In the female embryos the mesenchymatous condensation is smaller and shows only slight ChE activity.

2.5. The female embryo at day 17.5 p.c.

By electron microscopy, in the sections below the junctional area all of the cells surrounding the urogenital sinus are ChE negative or show very weak activity. The epithelial cells contain an increased amount of glycogen (Fig. 62).

In sections above the junctional area, the sinus and the vagina have common mesenchyme. In this tissue, the cells of the dense mesenchymal layer next to the epithelium of the vagina show very strong ChE activity (Fig. 63, 64). Some of the ChE active cisternae of the endoplasmic reticulum surround mitochondria and run parallel close to the plasma membrane (Fig. 65).

Towards the outside of the mesenchymal layer, cells are loosely arranged. Some of these cells exhibit positive reaction (Fig. 66). There is a lot of collagen fiber in the extracellular spaces.

2.6. The female embryo at day 18 p.c.

In the most cranial sections the sinus and the vagina have separate mesenchymal layers. The mesenchymal cells surrounding the urethra and the vagina show no enzyme reaction. As in the male the nerve cells have very strong activity in the vesico-urethral ganglion.

Cranial to the junction, the epithelium of the unfused Müllerian ducts and the Wolffian ducts shows no enzyme activity. The mesenchymal cells surrounding both ducts and the mesenchyme at the dorsal side of the ducts similarly have no ChE reaction.

Caudal to the junction, enzyme reaction can not be found in the epithelium of the urogenital sinus and in the surrounding mesenchymal cells.

## 3.0. Summary "Genital Tract"

1. In the indifferent stage at day 15 and 16 p.c. (Fig. 36) the caudal part of the genital ducts (Wolffian and Müllerian ducts) is still in the indifferent stage whereas in the cranial part differentiation or involution of genital ducts is already visible.

In sagittal cryostat sections submitted to the histochemical reaction for cholinesterase, the mesenchyme caudal to the junction of the genital ducts and the urogenital sinus exhibits a wedge or triangular shaped enzyme activity (Fig. 34). In cryostat cross section, this ChE active mesenchymatous condensation is located at the dorsal side of the urogenital sinus beneath the entering of the genital ducts (Fig. 35).

By electron microscopy, the following locations are described:
a) In cross sections at the junctional area of the genital ducts and the urogenital sinus, the epithelium of the dorsal sinus wall shows stronger ChE activity than the ventral sinus epithelium. The lateral epithelium has no ChE activity (Fig. 38).

The mesenchymal cells surrounding the urogenital sinus display a strong ChE activity at the dorsal side, moderate activity at the ventral side and weak activity at the lateral side (Fig. 39).

At the dorsal side of the urogenital sinus, a mesenchymatous condensation is found. It is composed of closely packed cells forming a whorl like structure. Cells of the mesenchymatous condensation show an undifferentiated character. They are irregular in shape. These cells exhibit ChE activity (Fig. 40).

The ganglia which are located close to the outer myogenic cell layer at the dorso-lateral side of the urogenital sinus show a very strong ChE activity in neuronal cells (Fig. 43). Large amounts of reaction product are localized in the cisternae of ER and nuclear envelope and sometimes in the interspaces between closely apposed membranes (Fig. 44). The satellite cells have no enzyme activity. In unmyelinated nerve fibres, reaction product is present in the interspaces between closely apposed axons (Fig. 45).

Cranial and caudal to the junction, there is no enzyme reaction in the epithelium and in the surrounding mesenchymal cells.

2. In male embryos at day 17 and 18 p.c., the prostate buds and the vesicular glands develop. ChE activity increases.

In sagittal cryostat sections, the ChE active mesenchyme is located caudally to the junction of the genital ducts with the urogenital sinus and in the mesenchyme directly above the outgrowth of the seminal vesicles (Fig. 46).

By electron microscopy, cells of the mesenchymatous condensation are more advanced in differentiation. They contain many long active cisternae of ER and exhibit stronger ChE activity than in younger stages (Fig. 48, 54).

Buds of the vesicular glands at the dorsal and prostate buds at the ventral sides appear. The epithelium of the seminal vesicle and the prostate gland show weak ChE activity. The surrounding mesenchymal cells exhibit strong positive reaction (Fig. 43, 55).

3. In female embryos at day 17 and 18 p.c., a vaginal plate forms by fusion of Wolffian and Müllerian ducts. Strong ChE activity is localized in the mesenchyme located dorsally of

the junction of the genital ducts with the urogenital sinus. The ChE active mesenchyme shifts caudally with the downgrowth of the vaginal anlage (Fig. 59).

By electron microscopy, the surrounding mesenchymal cells of this area exhibit strong ChE activity (Fig. 61, 64, 66).

In sections located more cranially, the urethra and the vagina have separate mesenchymal layers. The mesenchymal cells surrounding the urethra and the vagina show no enzyme reactions.

4. In general, the localization of enzyme reaction in mesenchymal cells is in the profiles of ER and in the perinuclear cisternae. Some of the ChE active cisternae of ER are continuous with the nuclear envelope. Commonly the positive ER is located close to mitochondria or run parallel close to the plasma membrane (Fig. 41, 49, 58, 61, 65, 66).

5. The intensity of ChE reaction is stronger than AChE reaction. The reaction product of both enzymes is similarly localized (Fig. 53, 54 compare to Fig. 56, 57).

## V. Ultrastructural localization of embryonic cholinesterase during myogenesis of the urethral muscle in mouse embryo

### 1.0. Introduction

Ultrastructural localization of acetylcholinesterase during myogenesis in the chick embryo limb bud has been described above ( page 16). In this chapter, the ultrastructural localization of cholinesterase and acetylcholinesterase during myogenesis of the urethral muscle in the mouse embryo is studied. The development of the urethral muscle has not yet been investigated by other authors. Only some light and electron microscopical observation have been reported by Thiedemann (1982). Therefore, not only the ultrastructural localization of cholinesterase during myogenesis of the urethral muscle is described in this chapter but also its ultrastructural development.

Cholinesterase activity in association with myogenesis in several species has been reported histochemically by many authors as shown in Table 1. In chick embryo, ChE activity during myogenesis of thigh and pectoral muscle at day 4 - 19 has been studied in vitro or in vivo. In general, myoblasts and fused myocytes contain non-specific and specific cholinesterase. Acetylcholinesterase activity increases considerably during fusion of myoblasts. The myoblasts exhibit enzyme activity first within the nuclear envelope, the endoplasmic reticulum and in some Golgi complexes. In the fused myocytes or myotubes, the enzyme activity is localized in the nuclear envelope, the perinuclear sarcoplasm, the sarcoplasmic reticulum, some elements of Golgi complex, the surface vesicles and the outer cell membrane.

In the developing muscle anlagen of the mouse and rabbit embryo (see Table 1) the myoblasts and myotubes show similar enzyme localization as in the chick embryo. Differentiation between non-specific cholinesterase and specific cholinesterase was performed by specific substrates and blockers as stated in

Table 1. In the chick embryo, myoblasts have non-specific and specific cholinesterase activity. The myoblasts in the rabbit embryo contain specific cholinesterase. In the mouse embryo (Holt 1975), blockers were not applied. Therefore the species specificity in the mouse remains open. From my observations, in the mouse embryo the myoblast have non-specific cholinesterase.

Only one paper (Miki and Mizoguti, 1982a) describes developing myogenic cells of the myotome in association with acetylcholinesterase activity. In my study of chick limb bud and urethral muscle also the development of early myogenic cells is described, so that only the latter paper (Miki and Mizoguti, 1982a) is directly comparable to my observation.

Table 1: Reports on ChE* and AChE activity in developing muscle

| Author | Tissue | Method** | Findings |
|---|---|---|---|
| Engel, 1961; Mummenthaler and Engel, 1961 | Chick embryo, 4-21 days<br>Thigh muscle<br>in vivo and in vitro | L.M. (Koelle)<br>AcThCh, BuThCh<br>DFP | Myoblast: ChE in cytoplasm<br>Myocyte: AChE along Z-lines |
| Wilson et al., 1973 | Chick embryo, 11 days<br>Pectoral muscle<br>in vitro | L.M. (Koelle; Karnovsky and Roots)<br>AcThCh, BuThCh<br>DFP, BW284C51, iso-OMPA<br>Biochemical assay | Myoblast: AChE<br>Myocyte: AChE activity increases after fusion, and secretion of AChE into medium |
| Fluck and Strohmann, 1973 | Chick embryo, 12 days<br>Skeletal muscle<br>in vitro | L.M. (Karnovsky and Roots)<br>AcThCh, BuThCh<br>iso-OMPA, BW284C51<br>Biochemical assay | Myoblast: ChE and AChE<br>Myocyte: ChE and AChE<br>AChE activity increases during fusion |
| Sawyer et al., 1976 | Chick embryo, 11 days<br>Pectoral muscle<br>in vitro | E.M. (Karnovsky and Roots; Tsuji)<br>AcThCh, BuThCh<br>iso-OMPA<br>Biochemical assay | Myoblast: ChE<br>Myocyte: AChE<br>in nuclear envelope, perinuclear sarcoplasm, SR, surface vesicles and outer cell membrane |

| Author | Tissue | Method | Findings |
|---|---|---|---|
| Wake, 1976 | Chick embryo, 9 - 17 days<br>Thigh muscle<br>in vitro | L.M. (Karnovsky and Roots)<br>E.M. (Lewis and Shute)<br>AcThCh<br>BW 284C51, iso-OMPA | Myocyte: AChE<br>in nuclear envelope, SR surrounding the myofibrils, Golgi complex and large granules |
| Golder et al., 1977, 1978 | Chick embryo, 10 days<br>Pectoralis muscle<br>in vitro | E.M. (Tsuji; Koelle and Friedenwald)<br>AcThCh<br>DFP, iso-OMPA,<br>Biochemical assay | Myocyte: AChE<br>in nuclear envelope, perinuclear sarcoplasm, SR, surface vesicles and outer cell membrane |
| Silman et al., 1979 | Chick embryo, 19 days and after hatching<br>Pectoral muscle<br>normal, denervated and dystrophy | Biochemical assay<br>AcThCh<br>iso-OMPA | AChE decrease after denervation and in dystrophy |
| Rotundo and Fambrough, 1980 | Chick embryo, 11 days<br>Leg muscle<br>in vitro | Biochemical assay<br>$^{3}$H-DFP + $^{14}$C-acetylcholine<br>BW 284C51, iso-OMPA | Myocyte: AChE<br>1/3 of activity on cell surface<br>2/3 of activity in the cell |

| Author | Tissue | Method | Findings |
|---|---|---|---|
| Miki and Mizoguti, 1982 a | Chick embryo; stage 13-18<br>Myotome<br>in vivo | L.M. (Karnovsky and Roots)<br>E.M. (Lewis and Shute)<br>AcThCh<br>DFP, iso-OMPA | Myotome cell: AChE<br>in nuclear envelope,<br>profiles of ER and<br>Golgi complex |
| Hagopain et al., 1970 | Rabbit embryo, 9-18 days<br>Cardiac muscle<br>in vivo | E.M.(Koelle and Friedenwald)<br>iso-OMPA, BW 284C51 | Myoblasts: AChE<br>Myocytes: AChE<br>in nuclear envelope,rER,<br>Golgi complex, SR and<br>subsarcolemma cisterna |
| Tennyson et al., 1971, 1973 | Rabbit embryo, 9-26 days<br>Myotome and myotube<br>in vivo | L.M. and E.M. (Koelle and<br>Friedenwald) | Myoblasts: AChE<br>Myocytes and myotubes:<br>AChE<br>in nuclear envelope, ER,<br>Golgi complex, SR and sub-<br>surface reticulum |
| olt, 1975 | Mouse embryo, 12-21 days<br>Tongue musculature<br>in vivo | L.M. (Karnovsky and Roots)<br>E.M. (Lewis and Shute) | Myoblasts: AChE<br>Mycytes and myotubes:<br>AChE, in nuclear envelope<br>ER and SR |

* ChE in the table means non specific ChE

** for explanation see General Introduction: 2. Characterization of cholinesterase p. 1-2

## 2.0. Results

The morphology and the location of ChE and AChE activity of the muscular layer of the embryonic urethra are studied in mouse embryos of day 15 to 20 p.c.. Between day 15 and 17 p.c., the development of the muscular layer is the same in male and female embryos. From day 18 p.c. onward, the muscular layer of male embryos is thicker than in female embryos. In female embryos, the muscle is temporally ruptured by downgrowth of the vagina. The cellular differentiation and the localization of enzyme reaction product is the same in male and female urethral muscle. Therefore, both sexes are described together.

In the semithin sections of Fig. 1, development of the male urethral muscle is shown at day 15, 17 and 20 p.c.. At day 15 p.c. (Fig. 67 a), the outer circular mesenchymal layer consists of densely packed mononucleated cells. The cells are spindle-shaped and aligned in parallel. At day 17 p.c. (Fig. 67 b), most of the mononucleated cells have elongated nuclei and cell bodies. Some of the cells show a light cytoplasm and nuclei. These light cells are the first differentiating myotubes. Although in histological and ultrastructural single sections, often only one nucleus is visible, these cells are already fused multinucleated cells. In tissue culture studies, it has been shown that differentiation starts after fusion. At day 20 p.c. (Fig. 67 c), the myogenic layer is thicker than in the younger stages. It consists mainly of multinucleated cells. The multinucleated cells are clearly distinguished by their large size, the light cytoplasm and many nuclei. The mononucleated dark myoblasts are aligned in parallel to the multinucleated cells.

### 2.1. Morphology of myoblasts

By electron microscopy, the spindle shaped cells show the morphological criteria of myoblasts. The nucleus of the myo-

blast has an elongated form and contains one or two nucleoli. The nucleus is located in the central part of the cell body and is only surrounded by a small seam of cytoplasm (Fig. 68, 69). The cytoplasm of the myoblast is relatively electron dense. It contains many free ribosomes, polysomes and microtubules. The cytoplasmic organelles, such as mitochondria and small profiles of ER are mostly found in the perinuclear zones (Fig. 70). Rough ER is also observed in some cells. At day 15 p.c., only some of the myoblasts contain thin filaments (Fig. 71).

The myoblasts are arranged with their long axis in parallel and form broad contacts with each other. In these areas, the cell membranes of neighbouring cells are closely apposed and form small maculae adherentes in the contact zones (Fig. 72). The myoblasts taper into slim cytoplasmic processes which also form contacts with each other and with the bodies of neighbouring cells. The extracellular space between myoblasts contains small amounts of thin collagen fibrils occasionally mixed with procollagen microfibrils.

At day 16 p.c., the myoblasts contain large amounts of thin filaments. The bundles of thin filaments are located close to the plasma membrane and run parallel to the longitudinal axis of the cells. The diameter of the filaments is about 5 - 10 n.m. (Fig. 73). Between day 17 and 20 p.c., the myoblasts form long cytoplasmic processes. They contain numerous cisternae of ER and bundles of thin filaments (Fig. 75, 76). At the outside of the cell membrane, some areas are covered with flocculent material as precursor of a basal lamina.

In summary, between day 15 to 20 p.c. the mononucleated myoblasts show signs of differentiation. There is an elongation of the nuclei and cell bodies. The myoblasts form long cytoplasmic processes and develop bundles of thin filaments. On the exterior surface of each cell flocculent material appears

as precursor of a basal lamina.

## 2.2. Cholinesterase activity of myoblasts

The myoblasts through all stages exhibit strong ethopropazine sensitive ChE activity (Fig. 69, 70) and no ethopropazine resistant ChE (AChE) activity (Fig. 68). At day 15 and 16 p.c., the enzyme reaction is localized in the cisternae of the ER and the nuclear envelope. However, ChE negative myoblasts are also observed. In the ER, stretches of heavy activity alternate with areas of weak or no reaction (Fig. 73). From day 17 p.c. onward, in the differentiated myoblast with thick bundles of thin filaments the strong ChE cisternae of ER align around the mitochondria (Fig. 75, 78). Some of them also run parallel and close to the plasma membrane or extend directly to contact the plasma membrane. Thus, the myoblasts of the urethral muscle contain only ethopropazine sensitive ChE in tubules of the ER closely related to mitochondria.

## 2.3. Morphology of myotube development

The myoblasts start to arrange in clusters at day 16 p.c. (Fig. 74). Fusion of myoblasts begins in the outer muscular layer and gives rise to differentiating myotubes. The fused cells or differentiating myotubes contain bigger and more rounded nuclei than myoblasts. Their nuclei appear less electron dense. The cytoplasm of differentiating myotubes contains numerous ribosomes and polysomes, many mitochondria, lipid droplets and bundles of myofilaments. Within the bundles of myofilaments, thick myofilaments (18 - 24 nm in diameter) are mixed with thin myofilaments (5 - 7 nm in diameter). They run parallel to the length of the cell. In the bundles of myofilaments, small irregular electron dense lines are observed. They are considered to be precursors of Z-lines.

At day 17 p.c., the clusters of myogenic cells have increased in number and size. The differentiating myotubes are clearly seen in this stage. They contain more contractile material. Thick and thin myofilaments are aligned in order and arranged into myofibrils. The myofibrils show Z-line (Fig. 77, 79).

Between day 18 and 20 p.c. (Fig. 82 and Fig. 67c) the myogenic cell layer is thicker than in previous stages especially at the ventrolateral side. The myotubes are clustered in groups and are surrounded by or mixed with myoblasts. Mitotic cells are often found in the clusters. The myotubes show well arranged sarcomeres. They contain also nests of unordered thin and thick myofilaments. Between the myofilaments, there are numerous ribosomes, polysomes and tubules of SR (Fig. 81, 83, 84). No T-tubules, diads and triads can be seen in the myotubes up to day 20 p.c.. At the surface of the myotube, there is also flocculent material.

## 2.4. Cholinesterase activity of myotubes

The myotubes show similarly strong ChE activity with and without ethopropazine (compare Fig. 77, 79 and 80, 81). With respect to ethopropazine they contain only specific AChE activity. The enzyme reaction is sometimes localized in the small areas of the perinuclear cisternae. The tubules and the vesicles of developing sarcoplasmic reticulum (SR) exhibit strong enzyme activity. The active tubules of SR run commonly parallel to the myofibrils or the plasma membrane (Fig. 81, 84). Occasionally AChE positive terminal cisternae of the SR forming junctions with the plasma membrane are observed (Fig. 85).

## 3.0. Summary "Urethral muscle"

### Development of the myoblast

The outer circular layer of the urethral wall consists of myogenic cells (Fig. 67, 68). At day 15 p.c., only some of the myoblasts contain thin filaments (Fig. 7). From day 16 p.c. on, they contain large amounts of thin filaments and ER (Fig. 74). Between day 17 and 20 p.c., the myoblasts form long cytoplasmic processes and contain numerous cisternae of ER and bundles of thin filaments (Fig. 75).

The myoblasts show strong ethopropazine sensitive ChE activity (Fig. 69, 70) and no ethopropazine resistant (AChE) activity (Fig. 68). The enzyme reaction is localized in the cisternae of ER and nuclear envelope. The enzyme positive profiles of ER are usually located close to mitochondria. Some of them also run parallel to the plasma membrane or extend directly to contact the plasma membrane (Fig. 73, 78).

### Development of the myotube

The myoblasts start to arrange in clusters at day 16 p.c. (Fig. 74). The fusion of myoblasts begins in the outer muscular layer and gives rise to differentiating myotubes. The fused cells or the differentiating myotubes are clearly seen in day 17 p.c.. They contain bundles of thick and thin myofilaments. Thick and thin myofilaments are aligned in order and arranged in myofibrils. The myofibrils show Z-lines (Fig. 79). Between day 18 and 20 p.c., the myotubes develop well arranged sarcomeres (Fig. 83).

The myotubes show similarly strong ChE activity with and without ethopropazine (compare Fig. 79 and 80). The enzyme reaction is localized in the cisternae of nuclear envelope and in the tubules of the sarcoplasmic reticulum. The active tubules of SR run commonly parallel to the myofibrils or the plasma membrane (Fig. 81, 84).

## VI. General discussion

### 1. Ultrastructural localization of embryonic cholinesterase

My observations on the ultrastructural localization of cholinesterase reveal a rather uniform pattern in embryonic cells of different origin and different destination. Embryonic cholinesterase is localized in the cisterna of the nuclear envelope, narrow strands of mostly smooth endoplasmic reticulum and in vesicles and cisternae of the Golgi zone. This ChE localization is found in undifferentiated mesenchymal cells, early chondroblasts and early myoblasts of the chick embryo limb bud. The same localization is present in the mesenchymal cells of the developing genital tract of the mouse embryo.

In adult tissues (as shown in Table 2) AChE and non-specific ChE are found ultrastructurally in the synaptic clefts of the motor end plate (neuromuscular junction); the nuclear envelope, s ER and r ER of the neuron; the axolemma; the dendritic membrane; the plasma membrane of the glial and Schwann cells; the plasma membrane and diffuse activity in cytoplasm of the myotubes; the nuclear envelope, the SR and in the A-band of cardiac muscle cells; and in the nuclear membrane, the SR and the sarcolemma of the smooth muscle cells in all species so far.

A localization similar to my observations in undifferentiated embryonic tissues was described in myogenic cells (see Table 1, page 52), in the neural tube (Miki and Mizuguti, 1982 b) and in the neural crest cells (Miki et al., 1983). All the above authors explained this localization by synthesis of the enzyme in the endoplasmic reticulum. Kreutzberg et al. (1979) studied synthesis of acetylcholinesterase in the neuron, transport in the axon and dendrite, release from the neuronal or dendritic membrane (which they termed

"dendritic secretion") and absorption by endothelial cells of brain capillaries.

In the undifferentiated embryonic cells the localization of ChE in the ER seems not to be sufficiently explained by assuming synthesis in this location. As outlined below ChE might have a function in intracellular signal transmission. The ChE-active endoplasmic reticulum of embryonic cells then could be compared to the sarcoplasmic reticulum of muscle cells.

## 2. Relation of ChE activity to differentiation

In the chick embryo limb bud, the undifferentiated chondroblasts exhibit ChE activity in the short and narrow cisternae of the endoplasmic reticulum and in the nuclear envelope. These ChE positive undifferentiated chondroblasts develop gradually to more differentiated chondroblasts with weak ChE activity and finally to ChE negative differentiated chondrocytes. The disappearance of ChE activity corresponds to the advance in differentiation of the cells indicated by appearance of extended ChE negative cisternae of rough endoplasmic reticulum. The differentiated ChE negative chondrocytes finally contain an increased amount of rER and vesicles, both filled with homogeneous amorphous material.

In the mesenchyme of the mouse genital tract, the undifferentiated mesenchymal cells with ChE positive narrow strands of ER also seem to develop into differentiated cells with ChE negative extended profiles of the rER. These extended rER usually contains homogeneous amorphous material and microfibrillar collagen. This indicates that the decrease in ChE activity is substituted by synthesis of the amorphous matrix and collagen fibers. During development of both cell types chondroblasts in the chick limb bud and mesenchymal cells in the mouse genital tract, continuities between narrow ChE positive ER and broad ChE negative rER are observed. This indicates that during differentiation the narrow ChE active ER is transformed to rough extended ER being ChE negative.

During myogenesis in the chick limb bud and the urethral muscle a transformation of ChE positive endoplasmic reticulum of myoblasts and early myocytes into ChE positive sarcoplasmic reticulum seems to occur. The transformation goes along with an increase of ChE activity. In the urethral muscle the transformation is accompanied by a change of specificity of the ChE. According to my observations with ethopropazine the myoblast of the mouse embryo contains non-specific ChE, whereas the fused myocyte contains specific cholinesterase.

3. Specificity of embryonic ChE

In order to distinguish specific AChE and non-specific ChE, I used the inhibitor ethopropazine as described by Lewis and Shute (1969). Ethopropazine specifically blocks non-specific ChE-activity. In the chick limb bud, the ChE reaction was identical when studied with and without ethopropazine. This means that the activity of embryonic ChE demonstrated on the ultrastructural level in the undifferentiated cells, chondroblasts, and during myogenesis corresponds to AChE activity as defined by ethopropazine.

In the mouse embryo genital tract, I observed a difference between tissue blocks incubated with or without ethopropazine. In the mesenchyme, the ChE reaction was stronger when ethopropazine was omitted. This indicates that both specific and non-specific ChE are present in the mesenchyme. In the myoblasts of urethral muscle, the enzyme reaction was blocked by ethopropazine. On the other hand, activity in the fused cells were not inhibited by ethopropazine. My observations show that in the mouse in the undifferentiated mesenchymal cells both AChE and non-specific ChE are present. The myoblasts contain only non-specific, and the myocytes after fusion only AChE activity.

In the chick embryo (Drews 1975), specificity of embryonic ChE was tested histochemically by light microscopy using the inhibitors, iso-OMPA and BW 284C51. He found the presence of specific AChE. Biochemical studies with the same material revealed that embryonic ChE was composed of acetylcholinesterase and butyrylcholinesterase. Layer (1983) described the ChE activity during morphogenesis of the 8 - 10 day chick embryo brain by light microscopy. He used the substrates acetylthiocholine or butyrylthiocholine and the inhibitors, iso-OMPA or BW 284C51 for comparative localization of these enzyme activities. He found specific ChE in the mesenchymal tissue and in the epidermis.

In the mouse genital tract, the embryonic ChE was previously characterized by Schweers (1979) using the inhibitors, iso-OMPA and BW 284C51. He stated that in the mouse embryo embryonic ChE corresponds to non-specific ChE.

With respect to the specificity, it is important to note which substrates and inhibitors were used for characterization. In conclusion, it seems that embryonic ChE contains specific and non-specific cholinesterase. The proportion of both enzyme activities depends on the species studied. The non-specific ChE might be a precursor of specific AChE.

## 4. Possible functions of embryonic ChE

In myogenesis in the chick limb bud and in the urethral muscle I observed the development of ChE positive sarcoplasmic reticulum of the undifferentiated precursor cells. In the cross striated muscle cell the function of the sarcoplasmic reticulum in regulation of calcium movement resulting in associated muscular contraction is well known (Ebashi and Endo, 1968; Hasselbach et al., 1975; Malan et al., 1975). It might be that the ChE-positive endoplasmic reticulum of undifferentiated cells has a function during regulation of morphogenesis similar to the

sarcoplasmic reticulum of muscle cells. In favour of this assumption is my observation of special contact zones between ChE positive ER and the surface membrane (Figs. 9, 58). These contact points resemble primitive junctional complexes between ChE positive sarcoplasmic reticulum and the plasmalemma of young myocytes (Fig. 85).

Table 2: Reports on specific and non-specific ChE activity in adult tissues

| Author | Tissue | Method | Findings |
|---|---|---|---|
| Teräväinem, 1967 | Rat, 3-5 months | E.M. (Karnovsky, 1964)<br>AcThCh, BuThCh, iso-OMPA<br>BW 284C51<br>Eserine | Myoneural junction: AChE in the sarcoplasm at the postsynaptic membrane. Non-specific ChE in the primary and secondary synaptic clefts and between axon and teloglial cells |
| Davis et al., 1972 | Rat<br>Intercostal musculature: motor end plate | L.M. and E.M.<br>∝-acetylthiol-m-toluene-diazonium ion, ∝-acetoxy-5-indolediazonium ion<br>Eserine, iso-OMPA,<br>BW 284C51, Quinidine sulfate | Motor end plate: AChE and pseudocholinesterase on the inner surface of the synaptic cleft |
| Kreutzberg et al., 1975 | Cat, guinea pig and rat<br>Facial nucleus, Motor neurons | L.M. (Gomeri, 1952), E.M. (Lewis and Shute, 1969)<br>AcThCh, Ethopropazine | AChE in rER, Golgi complex, perinuclear cisterna and plasma membrane |

| Author | Tissue | Method | Findings |
|---|---|---|---|
| Schober and Thomas, 1978 | Albino rat<br>Muscle spindle from lumbricalis muscles of hind limb | E.M. (Lewis and Shute, 1969)<br>AcThCh, Ethopropazine | Motor nerve ending: AChE in the synaptic cleft. Muscle fiber: AChE in the nuclear envelope, SR and transverse tubular system<br>Intrafusal muscle fiber: AChE on the sarcolemma<br>Extrafusal and intrafusal myelinated nerve fiber: AChE on the axolemma |
| Tôth and Kreutzberg, 1979 | Rat<br>Cerebral cortex<br>Neurons | E.M. (Lewis and Shute, 1969)<br>Ethopropazine<br>BW 248C51 | AChE in rER, Golgi complex, perinuclear cisterna, subsurface cisternae and dendrite membrane |
| Girgis, 1980 | Rat, rabbit, monkey<br>Brain: amygdala | L.M. (Girgis, 1967)<br>E.M. (Tsuji, 1974) | Neuron: AChE in nuclear envelope and rER<br>Synaptic terminal: AChE on their limiting membrane |

| Author | Tissue | Method | Findings |
|---|---|---|---|
| Gautron, 1982 | Chick<br>Ciliary ganglion in vivo | L.M. and E.M. (Crevier and Belanger, 1955)<br>Acetyl sulfide,<br>AcThCh perchlorate<br>iso-OMPA, BW 284C51<br>Eserine | Neuron: AChE in nuclear envelope, rER of the Nissl bodies, plasma membrane |
| | Mouse embryo, 18 days<br>Diaphragm muscle in vivo | | Muscle: AChE in plasma membrane and diffuse activity in cytoplasm, synaptic cleft and post synaptic membrane. Schwann cell: AChE in plasma membrane |
| Davis and Koelle, 1978, 1981 | Cat<br>Super cervical ganglion | E.M. (Koelle, et al., 1974)<br>AcThCh, BuThCh, iso-OMPA | AChE in the plasma membrane of the preganglionic axons and their terminals, and in the dendritic and perikaryonal plasma membranes of the postsynaptic ganglion cells.<br>AChE in the postsynaptic neuronal plasma membranes |

| Author | Tissue | Method | Findings |
|---|---|---|---|
| Ide, 1982 | Mouse embryo, 14,17,20 days<br>Hind limb, Meissner corpuscle<br>Young mice, 1-20 days | L.M. and E.M. (Karnovsky and Roots, 1964)<br>AcThCh, Eserine, iso-OMPA | Schwann cell: ChE in nuclear envelope and rER.<br>Periaxonal area: ChE<br>Lamellar cells: intense ChE activitiy in nuclear envelope and rER<br>After birth: ChE activity decreases |
| Dubovy and Malinovsky, 1982 | Cat<br>Pacinian corpuscles of the mesentery | L.M. and E.M. (Karnovsky, 1964), AcThCh, BuThCh, iso-OMPA, BW 284C51<br>Eserine | Non-specific ChE on the surface of plasma membranes of the inner core lamelles, rER and vesicles of the Golgi complex |
| Karnovsky, 1964 | Rat<br>Heart | E.M. (Karnovsky)<br>AcThCh, BuThCh, DFP<br>Eserine | Cardiac muscle: non specific ChE in the nuclear envelope, SR, and in the A band |

| Author | Tissue | Method | Findings |
|---|---|---|---|
| Macjen and Brzin, 1979 | Guinea pig<br>Longitudinal muscle of the ileum | E.M. (Koelle and Friedenwald, 1949)<br>AcThCh, BuThCh,<br>iso-OMPA, BW 284C51<br>Eserine | Smooth muscle cell: AChE and BChE in the nuclear membrane, SR, and invaginations of the sarcolemma |

## VII. General summary

Undifferentiated embryonic cells exhibit cholinesterase (ChE) activity during phases of morphogenesis which is termed embryonic ChE. Here I describe the ultrastructural localization of the embryonic ChE activity in the chick embryo limb bud from stage 23 to 27, in the mouse embryo genital tract at day 15 to 18 of pregnancy, and during myogenesis of the mouse embryo urethral muscle at day 15 to 20 of pregnancy.

In the chick limb bud I describe ChE activity in the apical ectodermal ridge, in the mesenchyme of the subridge area and during chondrogenesis and myogenesis in the extremities. In the mouse embryo I describe ChE activity in the mesenchyme of the indifferent genital tract, the differentiating male and female genital tract and during myogenesis of the cross striated urethral muscle.

For determination of specificity of the ChE, I use ethopropazine, a blocker of unspecific ChE. In the chick limb bud ChE activity is not influenced by ethopropazine. In the mouse embryonic ChE activity is ethopropazine sensitive. ChE activity in fused myocytes of the urethral muscle is ethopropazine resistant.

In general, embryonic ChE is localized in the cisterna of the nuclear envelope, in narrow strands of mostly smooth endoplasmic reticulum and in vesicles and cisternae of the Golgi complex. This localization is found in undifferentiated mesenchymal cells, early chondroblasts and early myoblasts of the chick embryo limb bud. The same localization is present in the mesenchymal cells of the developing genital tract and in myoblasts of the urethral muscle of the mouse embryo.

Embryonic ChE activity in undifferentiated chondroblasts of the chick limb bud and in undifferentiated mesenchymal cells of the mouse genital tract decreases in intensity during the course of development. In both cell types, continuities between narrow ChE positive ER and extended ChE negative rER are observed. This indicates that during differentiation the narrow ChE active ER is transformed to extended ChE negative rough ER.

On the other hand, ChE activity increases after fusion of the myoblasts in the developing muscle fibres in the chick limb bud and the mouse urethral muscle. ChE positive endoplasmic reticulum of myoblasts is transformed into ChE positive sarcoplasmic reticulum.

Often the ChE positive ER of undifferentiated cells was located close to mitochondria. Occasionally I observed contact zones with the inner face of the plasma membrane. These contact zones were similar to primitive junctional complexes between ChE positive SR and the sarcolemma which I observed in young myocytes.

Ultrastructural localization of ChE activity in the nuclear envelope and the endoplasmic reticulum in nerve and muscle cells has been interpreted in terms of synthesis of ChE by other authors. My observation that embryonic ChE disappears with differentiation from chondroblasts and mesenchymal cells and the observation of contact zones between ER and the plasma membrane points to a function in intercellular or intracellular signal transmission during morphogenesis.

## VIII. References

AMPRINO, R.: Aspects of limb morphogenesis in the chicken. In: Organogenesis (eds. R.L. DeHaan & H. Ursprung), Holt, Rinehart & Winston , New York, p. 225 - 281, 1965.

AMPRINO, R.: Developmental ability of the apical mesoderm of the chick embryo limb bud in sectors deprived of the ectoderm ridge. Nova Acta Leopoldina, 217 : 235 - 270, 1974.

AMPRINO,R: Morphogenetic interrelationships between ectoderm and mesoderm in chick embryo limb development. In: Vertebrate limb and somite morphogenesis (eds. D.A. Ede, J.R. Hinchliffe and M. Balls), Cambridge, Cambridge University Press, p. 245 - 255, 1977.

AUGUSTINSSON, K.B. and NACHMANSSOHN, D.: Distinction between acetylcholinesterase and other choline ester splitting enzymes. Science 110 : 98, 1949.

AUGUSTINSSON, K.B.: Acetylcholine esterase and cholinesterase. In: The Enzymes, Chemistry and Mechanism of Action. (eds. J.B. Summer and K. Myrbäck), Academic Press, Inc. New York, Vol I, p. 443 - 472, 1950.

BARKA, T. and ANDERSON, P.J.: Histochemistry: Theory, Practice and Bibliography. Hoeber Medical Division, Harper & Row, Publishers Incorporated, New York, 1963.

BOK, G and DREWS, U.: The role of the Wolffian ducts in the formation of the sinus vagina: an organ culture study. J. Embryol. exp. Morph. 73 : 275 - 295, 1983.

BULMER, D.: The development of the human vagina. J. Anat. 91 : 490 - 509, 1957.

BURSTONE, M.S.: Enzyme Histochemistry and its Application in the Study of Neoplasms. Academic Press, London, 1962.

CHEVALLIER, A., KIENY, M. and MANGER, A.: Limb somite relationship: origin of the limb musculature. J. Embryol. exp. Morph. 41 : 245 - 258, 1977.

CHEVALLIER, A., KIENY, M. and MANGER, A.: Limb somite relationship: effect of removal of somite mesoderm on the wing musculature. J. Embryol. exp. Morph. 43 : 263 - 278, 1978.

CHRIST, B., JACOB, H.J. and JACOB, M.: Experimental analysis of the origin of the wing musculature in avian embryos. Anat. Embryol. 150 : 171 - 186, 1977.

DALTON, A.J.: A chrome-osmium fixative for electron microscopy. Anat. Rec. 121 : 181, 1955.

DAVIS, R. and KOELLE, G.B.: Electron microscope localization of acetylcholinesterase and butyrylcholinesterase in the superior cervical ganglion of the cat. J. Cell. Biol. 78 : 785 - 809, 1978.

DAVIS, R. and KOELLE, G.B.: Electron microscope localization of acetylcholinesterase and butyrylcholinesterase in the superior cervical ganglion of the cat. II. Preganglionically denervated ganglion. J. Cell Biol. 88 : 581 - 590, 1981.

DAVIS, D.A., WASSERKRUG, H.L., HEYMAN, I.A., PADMANABHAN, K.C., SELIGMAN, G.A., PLAPINGER, R.E. and SELIGMAN, A.M.: Comparison of ultrastructural cholinesterase demonstration in the motor end plate with α-acetylthiol-m-toluendiazonium ion and 3-acetoxy-5-indolediazonium ion. J. Histochem. Cytochem. 20 : 161 - 172, 1972.

DIXON, M. and WEBB, E.C.: Enzymes. 3rd edition, Longman Group Ltd., 1979.

DONOHOE, P.K., ITO, Y., PRICE, J.M. and HENDREN III, W.H.: Müllerian inhibiting substance activity in bovine fetal, newborn and prepubertal testis. Biol. Reprod. 16 : 238 - 243, 1977.

DREWS, U. and DREWS, U.: Cholinesterase in der Extremitätenentwicklung des Hühnchens: I. Phasen der Cholinesterase-Aktivität in der jungen Knospe und bei der Abgrenzung von Knorpel- und Muskelanlagen. Wilhelm Roux' Arch Entwicklungsmech.Org.169 : 70 - 86, 1972.

DREWS, U. and DREWS, U: Cholinesterase in der Extremitätenentwicklung des Hühnchens: II. Fermentaktivität und Bewegungsverhalten der präsumptiven Knorpelzellen in vitro. Wilhelm Roux' Arch Entwicklungsmech.Org.173 : 208 - 227, 1973.

DREWS, U.: Cholinesterase in embryonic development. Prog. Histochem. Cytochem., vol 7/3, Gustav Fischer, Stuttgart, 1975.

DUBOVY, P. and MALINOVSKY, L.: Electron microscopic localization of cholinesterase activity in Pacinian corpuscles of the cat mesentery. Z. mikrosk.-anat. Forsch., Leipzig 96 : 803 - 816, 1982.

EBASHI, S., ENDO, M.: Calcium ion and muscle contraction. Progr. Biophys. Mol. Biol. 18 : 123 - 183, 1968.

EDE, D.A.: Control of Form and Pattern in the Vertebrate Limb, Symposium, Soc. Exp. Biol. 28 : 235 - 254, 1971.

ENGEL, W.K.: Cytological localization of cholinesterase in cultured muscle cells. J. Histochem. Cytochem. 9 : 66 - 73, 1961.

FALLON, J.F. and CROSBY, G.M.: Polarizing zone activity in limb buds of amniotes. In: Vertebrate Limb and Somite Morphogenesis (eds. D.A. Ede, J.R. Hinchliffe and M. Balls), University Press, p. 55 - 69, 1977.

FELIX, W.: The development of the urogenital organs. In: Manual of Human Embryology (eds. Keibel and Mall), Lippincott, Philadelphia, Vol. 2, p. 752 - 879, 1912.

FLUCK, R.A. and STROHMANN, R.C.: Acetylcholinesterase activity in developing skeletal muscle cells in vitro. Dev. Biol. 33 : 417 - 428, 1973.

FORSBERG, J.G.: Derivation and differentiation of the vaginal epithelium. PhD Thesis. Lund: Ed Håkon Ohlssons Boktryckeri, 1963.

FORSBERG, J.G. and OLIVECRONA, H.: The dehydrogenase activity in the human vaginal anlage. Z. Anat. Entwicklungsgesch. 124 : 234 - 239, 1964.

FORSBERG, J.G.: An experimental approach to the problem of the derivation of the vaginal epithelium. J. Embryo. exp. Morph. 14 : 213 - 222, 1965.

FORSBERG, J.G.: Histochemical studies on the changing enzyme pattern at the lumen formation in the solid sinus vagina in the mouse. Z. Anat. Entwicklungsgesch. 126 : 117 - 126, 1967.

FORSBERG, J.G.: Cervicovaginal epithelium: its origin and development. Am. J. Obstet. Gynecol. 115 : 1025 - 1043, 1973.

GAUTRON, J.: Ultrastructural localization of acetylcholinesterase: A direct method for light and electron microscopy. Histochemistry 76 : 469 - 478, 1982.

GIRGIS, M: Acetylcholinesterase enzyme localization in the amygdala: A comparative histochemical and ultrastructural study. Acta. anat. 106 : 192 - 202, 1980.

GLENISTER, T.W.: The development of the utricle and of the so-called "middle" or "median" lobe of the human prostate. J. Anat. 96 : 443 - 455, 1962.

GOLDER, T.K., NIEBERG, P.S. and WILSON, B.W.: Ultrastructural localization of acetlycholinesterase in cultured cells. III. DFP treated embryo muscle. J. Histochem. Cytochem. 26 : 719 - 728, 1978.

HAGOPIAN, M., TENNYSON, V.M. and SPIRO, D.: Cytochemical localization of cholinesterase in rabbit cardiac muscle. J. Histochem. Cytochem. 18 : 38 - 43, 1970.

HAMBURGER, V. and HAMILTON, H.L.: A series of normal stages in the development of the chick embryo. J. Morph. 88 : 49 - 67, 1951.

HART, D.B.: A contribution to the morphology of the human urogenital tract. J. Anat. Physiol. (London) 35: 330 - 375, 1901.

HASSELBACH, W., SUKO, J. and STROMER M.H.: Mechanism of calcium transport in sarcoplasmic reticulum. Ann NY Acad. Sci. 264 : 335 - 349, 1975.

HILFER, S.R., SEARLS , R.L. and FONTE, V.G.: An ultrastructural study of early myogenesis in the chick wing bud. Del. Biol. 30 : 374 - 391, 1973.

HINCHLIFFE ,J.R. and JOHNSON, D.R.: The development of the vertebrate limb: An approach through experiment, genitics and evolution. Oxford University Press, 1980.

HOLT, T.M.: A morphological and histochemical study of the developing tongue musculature in the mouse: Its relationship to palatal closure. Am. J. Anat. 144 : 169 - 196, 1975.

IDE, C.: Histochemical study of lamellar cell development of Meissner corpuscles. Arch. histol. jap. 45 : 83 - 97, 1982.

JACOB, M., CHRIST,B.and JACOB, H.J.: On the migration of myogenic stem cells into the prospective wing region in chick embryos: A scanning and transmission electron microscope study. Anat. Embryol. 153 : 179 - 193, 1978.

JIRÁSEK, J.E.: Development of the genital system and male pseudohermaphroditism (eds. M.M. Cohen, JR), Baltimore, John Hopkins Press, 1971.

JOSSO, N., PICARD, J.P. and TRAM, D.: The anti-Müllerian hormone. In: Myogenesis and Malformation of the Genital System. (eds. R.J. Blandan and D. Bergsma), A.R. Liss, Inc. New York, p. 59 - 84, 1977.

JOSSO, N.: Differentiation of the genital tract. In: Mechanisms of sex differentiation in animals and man (eds. C.R. Austin and R.G. Edwards), London, New York, Academic Press, p. 165 - 203, 1981.

JOST, A.: Recherches sur la differenciation sexuelle de l'embryon de lapin. III. Rôle des gonades foetales dans la differenciation sexuelle somatique. Arch. Anat. micr. Morph. exp. 36 : 271 - 315, 1947.

JOST, A.: Gonadal hormones in the sex differentiation of the mammalian fetus. In: Organogenesis (eds. R.L. DeHaan and H. Ursprung), Holt, Rinehart and Winston, New York, p. 611 - 128, 1965.

JOST, A. PREPIN, J. and VIGIER, B.: Hormones in the morphogenesis of the genital system. In: Morphogenesis and Malformation of the genital system (eds. R.J. Blandan and D. Bergoma), A.R. Liss, Inc., New York, p. 85 - 98, 1977.

JOST, A., VIGIER, B., PRIPIN, J. and PERCHETTET, J.P.: Studies of sex differentiation in mammals. Recent. Prog. Horm. Res. 29 : 1 - 41, 1973.

KAPRIO, E.A.: Ectodermal-mesenchymal interspace during the formation of the chick leg bud: A scanning and transmission electron microscopic study. Wilhelm Roux's Archives 182: 213 - 225, 1977.

KARNOVSKY, M.J.: The localization of cholinesterase activity in rat cardiac muscle by electron microscopy. J. Cell. Biol. 23 : 217 - 232, 1964.

KARNOVSKY, M.J. and ROOTS, L.: A "Direct-coloring" thiocholine method for cholinesterase. J. Histochem. Cytochem. 12 : 219 - 221, 1964.

KATY, B.: Nerve, muscle and synapse. McGraw-Hill Co, New York, 1966.

KELLOKUMPU-LETHINEN, P., SANTTI, R. and PELLINIEMI, L.J.: Early cytodifferentiation of human prostatic urethra and Leydig cells. Anat. Rec. 194 : 429 - 444, 1979.

KOFF, A.K.: Development of the vagina in the human fetus. Contr. Embryol. No. 140, Carnegie Inst. 24 : 59 - 90, 1933.

KREUTZBERG, G.W., TÓTH, L. and KAIYA, H.: Acetylcholinesterase as a marker for dendritic transport and dendritic secretion. Advances in Neurology 12 : 269 - 281, 1975.

LAYER, G.L.: Comparative localization of acetylcholinesterase and pseudocholinesterase during morphogenesis of the chicken brain. Proc. Natl. Acad. Sci. 80 : 6413 - 6417, 1983.

LEWIS, P.R. and SHUTE, C.C.D.: An electron microscopic study of cholinesterase distribution in the rat adrenal medulla. J. Micros. 89 : 181 - 193, 1969.

MAJCEN, Z. and BRZIN, M.: Cholinesterase and choline acetyltransferase in the longitudinal muscle of the guinea pig ileum. Histochemistry 63 : 295 - 302, 1979.

MALAN, N.T., SABBADINI, R., SCALES, P. and INESI, G.: Functional and structural roles of sarcoplasmic reticulum protein components. FEBS Letters 60 : 122 - 125, 1975.

MIJSBERG, W.A.: Über die Entwicklung der Vagina, des Hymen und des Sinus urogenitalis beim Menschen. Z. Anat. Entw. Gesch. 74, 684 - 760, 1924.

MIKI, A. and MIZOGUTI, H.: Acetylcholinesterase activity in the myotome of the early chick embryo. Cell Tissue Res. 227 : 23 - 40, 1982 a.

MIKI, A. and MIZOGUTI, H.: Proliferating ability, morphological development and acetylcholinesterase activity of the neural tube cells in early chick embryos. An electron microscopic study. Histochemistry 76 : 303 - 314, 1982 b.

MIKI, A., FUJIMOTO, E. and MIZOGUTI, H.: Acetylcholinesterase activity in neural crest cells of the early chick embryo. Histochemistry 78 : 81 - 93, 1983.

MILAIRE, J.: Aspects of limb morphogenesis in mammals. In: Organogenesis (eds. R.L. DeHaan & H. Ursprung), New York, Holt, Rinehart & Winston, p. 283 - 300, 1965.

MÜLLER, J.: Bildungsgeschichte der Genitalien. Düsseldorf: Arnz, 1930.

MUMENTHALER, M. and ENGEL, W.K.: Cytological localization of cholinesterase in developing chick embryo skeletal muscle. Acta anat. 47 : 274 - 299, 1961.

NACHMANSOHN, D.: Proteins in excitable membranes. Science 168 : 1059, 1970.

O'RAHILLY, R.: The development of the vagina in the human. In: Morphogenesis and Malformation of the genital system (eds. R.J. Blandau and D. Bergsma) Birth defects: Original article series 13 (2), New York, p. 123 - 136, 1977.

PEARSE, A.G.E.: Histochemistry. Churchill, London, 3rd edition, 1972.

PICARD, J.Y., TRAN, D. and JOSSO, N.: Biosynthesis of labelled anti-müllerian hormone by fetal testis: evidence for the glycoprotein nature of the hormone and for its disulfide-bounded structure. Ml. Cell. Endocr. 12 : 17 - 30, 1978.

PICON, R.: Effect of the rat fetal testis on the regression of the Müllerian ducts in vitro. In: Hormones in development (eds. M. Hamburgh and E.J. Barrington), New York, Appleton-Century-Crofts, p. 645 - 650, 1971.

PRICE, D. and ORTY, E.: The role of the fetal androgens in sex differentiation in mammals. In: Organogenesis (eds. R.L. DeHaan and H. Ursprung), Holt, Rinehart & Winston, New York, p. 629 - 652, 1965.

PRICE, D., ORTY, E. and ZAAIJIER, J.J.P.: In vitro studies of the relation of fetal sex hormone to sex differentiation in the guinea pig. In: Hormone in Development. (eds. M. Hamburgh and E.J.W. Barrington), Appleton-Century-Crofts, New York, p. 631 - 644, 1971.

PRICE. D., ZAAIJIER, J.J.P., ORTY E. and BRINKMANN, A.O.: Current views on embryonic sex differentiation in reptiles, birds and mammals. Am. Zool. 15 (suppl. 1), 173 - 195, 1975.

REICH, A. and DREWS, U.: Choline Acetyltransferase in the Chick Limb Bud. Histochemistry 78 : 383 - 389, 1983.

RAYNAUD, A.: Intersexualité provoquée chez la souris femelle par injection d'hormone male âla mère en gestation. C.R. Soc. Biol. 126 : 866 - 868, 1937.

RAYNAUD, A.: Formation d'un urêtre mâle, d'un penis et absence de vagin chez les souris femelles intersexuées. C.R. Soc. Biol. 127 : 503 - 506, 1938.

REYNOLDS, E.S.: The use of lead citrate at high pH as an electron-opaque stain for electron microscopy. J.Cell Biol. 17 : 208 - 212, 1963.

ROTUNDO, R.L. and FAMBROUGH, D.M.: Secretion of acetylcholinesterase: Relation to acetylcholine receptor metabolism. Cell 22 : 595 - 602, 1980.

SAUNDERS, J.W. Jr.: The proximo-distal sequence of origin of the part of the chick wing and the role of the ectoderm. J. expt. Zoo. 108 : 363 - 403, 1948.

SAUNDERS, J.W. Jr.: The interplay of morphogenetic factors. In limb development and deformity (eds. C.A. Swinyard), Chas. C. Thomas, Illinois, p. 84 - 100, 1969.

SAUNDERS, J.W. Jr.: The experimental analysis of chick limb bud development. In: Vertebrate limb and somite morphogenesis (eds. D.A. Ede, J.R. Hinchliffe and M. Balls), Cambridge, Cambridge university press, p. 1 - 24, 1977.

SAUNDERS, J.W. Jr., GASSELING, M.T. and SAUNDERS, L.C.: Cellular death in morphogenesis of the avian wing. Dev. Biol. 5 : 147 - 178, 1962.

SAUNDERS, J.W. Jr. and GASSELING, M.T.:Ectodermal-mesenchymal interactions in the origin of limb symmetry. In: Epithelial Mesenchymal Interactions (eds. R. Fleischmajar & R.E. Billingham), Baltimore, Williams & Wilkins, p. 78 - 97, 1968.

SAUNDERS, J.W. Jr. and REUES, C.: Inductive and axial properties of prospective wing bud mesoderm in the chick embryo. Biol. Dev. 38 : 41 - 50, 1974.

SAWYER, H.R., GOLDER, T.K., NIEBERG, P.S. and WILSON, B.W.: Ultrastructural localization of acetylcholinesterase in cultured cells: I. Embryonic muscle. J. Histochem. Cytochem. 24 : 969 - 978, 1976.

SCHMIDT, H.: Muscarinic acetylcholine receptor in chick limb bud during morphogenesis. Histochemistry 71 : 89 - 98, 1981.

SCHOBER, R. and THOMAS, E.: The fine structural localization of acetylcholinesterase in the muscle spindle of the rat. Cell Tiss. Res. 186 : 39 - 52, 1978.

SCHRÖDER, C.: Characterization of embryonic cholinesterase in chick limb bud by colorimetry and disk electrophoresis. Histochemistry 69 : 243 - 253, 1980.

SCHWEERS, F.M.: Die Entwicklung der accessorischen Geschlechtsdrüsen und der Vagina bei der normalen und der testikulär feminisierten Maus dargestellt mit der Cholinesterase-Reaktion. Inaugural-Dissertation, Fakultät für Medizin, Münster, 1979.

SEARLS, R.L. and JANNERS, M.Y.: The imitation of limb bud outgrowth in the embryonic chick. Biol. Dev. 24 : 198 - 213, 1971.

SEARLS, R.L., HILFER, S.R. and MIROW, S.M.: An ultrastructural study of early chondrogenesis in the chick wing bud. Biol. Dev. 28 : 123 - 137, 1972.

SHELLSWERT, G.B., WOLPERT, L.: The pattern of muscle and tendon development in the chick wing. In: Vertebrate limb and somite morphogenesis (eds. D.A. Ede, J.R. Hinchliffe and M. Balls), Cambridge, Cambridge university press, p. 71 - 86, 1977.

SILMAN, I., GIAMBERARDINO, L., LYLES, J., COURAUD, J.Y. and BARNARD, E.A.: Parallel regulation of acetylcholinesterase and pseudocholinesterase in normal, denervated and dystrophic chicken skeletal muscle. Nature 280 : 160 - 162, 1979.

SUMMERBELL, D. and LEWIS, J.H.: Time, place and positional value in the chick limb bud. J. Embryol. exp. Morph. 33 : 621 - 643, 1975.

SUMMERBELL, D., LEWIS, J.H. and WOLPERT, L.: Positional information in chick limb morphogenesis. Nature 244 : 492 - 496, 1973.

TENNYSON, V.M., BRZIN, M. and KREMZNER, L.T.: Acetylcholinesterase activity in the myotome and muscle satellite cell of the fetal rabbit: An electron microscopic-cytochemical and biochemical study. J. Histochem. Cytochem. 21 : 634 - 652, 1973.

TENNYSON, V.M., BRZIN, M. and SLOTWINER, P.: The appearance of acetylcholinesterase in the myotome of the embryonic rabbit: An electron microscope cytochemical and biochemical study. J. Cell. Biol. 51 : 703 - 721, 1971.

TERÄVÄINEN, H.: Electron microscopic localization of cholinesterase in the rat myoneural junction. Histochemie 10 : 266 - 271, 1967.

THIEDEMANN, K.-U.: Der Urethralmuskel der Maus- Ein Modell zur Untersuchung der Wirkung von Androgen. Habilitationsschrift, Fakultät für Theoretische Medizin, Tübingen, 1982.

TICKLE, C., SHELLSWELL, G., CRAWLEY, A. and WOLPERT, L.: Positional signalling by mouse limb polarizing region in the chick wing bud. Nature 259 : 396 - 397, 1976.

TÓTH, L. and KREUTZBERG, G.W.: Acetylcholinesterase in neurons of the rat cerebral cortex. Acta anat. 103 : 125 - 129, 1979.

VALENTIN, G.: Handbuch der Entwicklungsgeschichte des Menschen mit vergleichender Rücksicht der Entwicklung der Säugetiere und Vögel. Berlin, Rücker, 1835.

VENABLE, J.H. and COGGESHALL, R.: A simplified lead citrate for use in electron microscopy. J. Cell. Biol. 25 : 407 - 408, 1965.

WAKE, K.: Formation of myoneural and myotendinous junctions in the chick embryo: Role of acetylcholinesterase-rich granules in the developing fibers. Cell Tiss. Res. 173 : 383 - 400, 1976.

WILSON, J.D.: Sexual differentiation. Ann. Rev. Physiol. 40 : 279 - 306, 1978.

WILSON, W., NIEBERG, P.S., WALKER, C.R., LINKHART, T.A. and FRY, D.M.: Production and release of acetylcholinesterase by cultured chick embryo muscle. Dev. Biol. 33 : 285 - 299, 1973.

WITSCHI, E.: Development and differentiation of the uterus. In: Prenatal life (ed. H.C. Mack), Detroit, Wayne State University Press, 11 - 35, 1970.

WORTHAM, R.A.: The development of the muscles and tendons in the lower leg and foot of chick embryos. J. Morph. 83 : 103 - 148, 1948.

ZWILLING, E.: The role of epithelial components in the developmental origin of the wingless syndrome of chick embryos. J. Expt. Zoo. 111 : 175 - 187, 1949.

ZWILLING, E.: Limb mophogenesis. Adv. Morphog. 1 : 301 - 330, 1961.

ZWILLING, E.: Morphogenetic phases in development. Dev. Biol. Suppl. 2 : 184 - 207, 1968.

ZWILLING, E.: Limb morphogenesis. Dev. Biol. 28 : 12 - 17, 1972.

ZWILLING, E. and HANSBOROUGH, L.: Interaction between limb-bud ectoderm and mesoderm in the chick embryo. III. Experiments with polydactylous lims. J. Expt. Zoo. 132 : 219 - 239, 1956.

Fig. 1: Schematic drawings which show the planes of sectioning of the wing bud after fixation before incubation in the Lewis and Shute medium for cholinesterase.

A = Longitudinal sectionings in the dorso-ventral plane
B = Cross section in the proximo-distal direction
I = Block I, the tip of the wing bud
II = Block II, the middle part of the wing bud
III = Block III, the proximal part of the wing bud

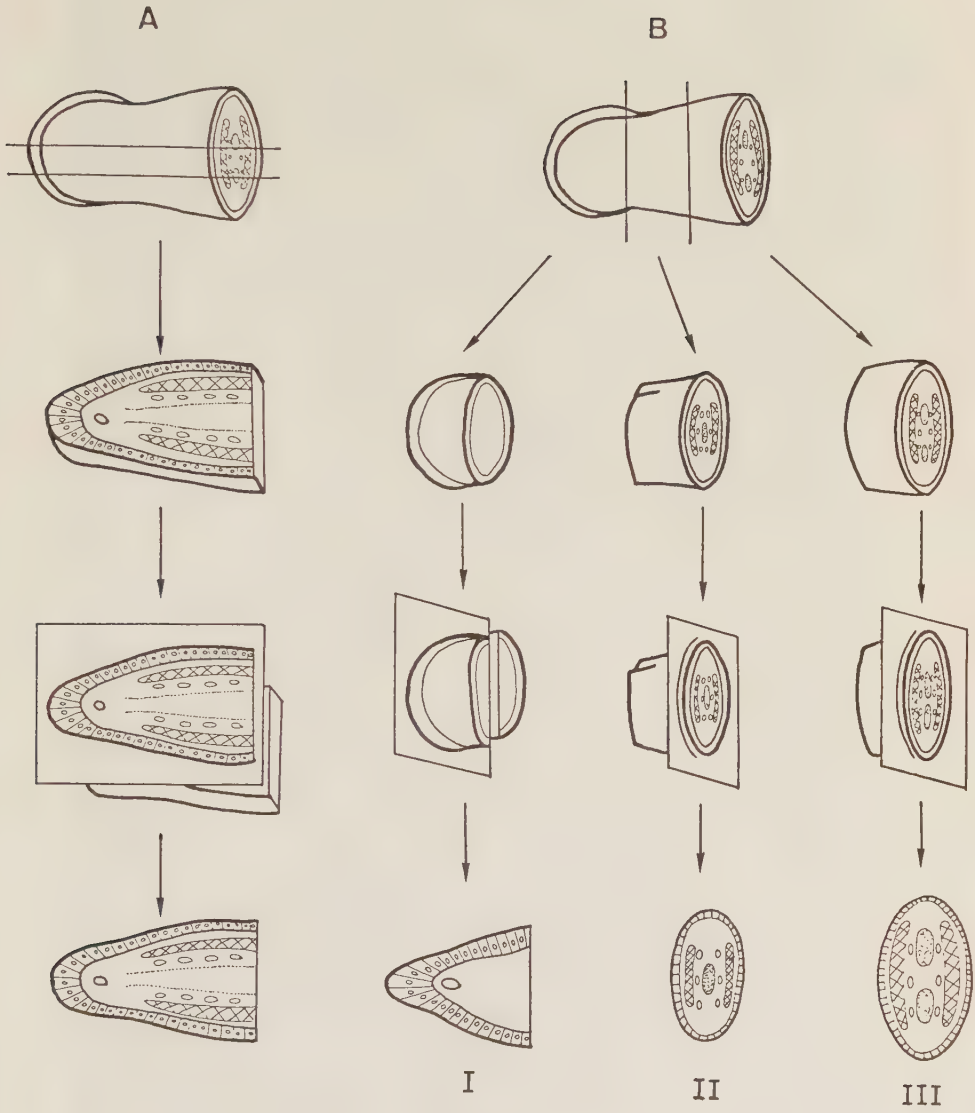


Fig.1

Fig. 2: Semithin longitudinal sections in the dorso-ventral plane of chick wing buds at stages 23 - 27 (stages after Hamburger and Hamilton, 1951). Staining Azure II.

A = apical ectodermal ridge
B = subridge area
C = proximal cartilage forming area
D = distal cartilage forming area
E = humeral cartilage condensation
F = condensation of radius
G = digits
H = dorsal muscle area
I = ventral muscle area
J = nerve fibers
K = marginal sinus
L = blood vessels

x 50

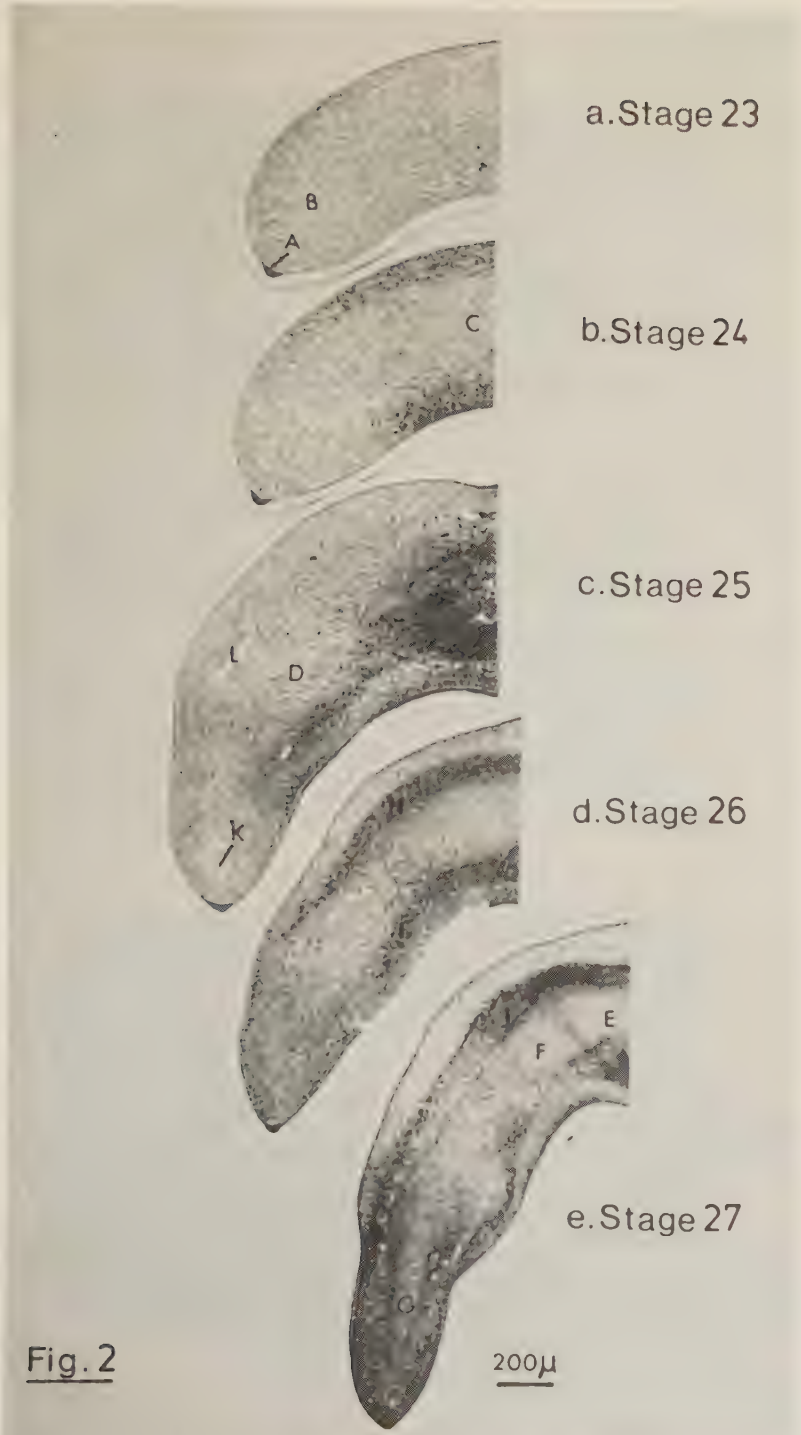
a.Stage 23
B
A
b.Stage 24
C
c.Stage 25
L
D
K
d.Stage 26
E
F
e.Stage 27
G
200μ

Fig. 2

Fig. 3: Apical ectodermal ridge (AER) and subridge area from chick wing bud stage 24. In the AER, the columnar cells show ChE activity in the cisternae of the nuclear envelope, the endoplasmic reticulum and in the Golgi complex. The peridermal cells have no ChE activity. The mesenchymal cells in the subridge area also exhibit ChE activity.

AER = apical ectodermal ridge
Cc = columnar cell
Pc = peridermal cell
Ms = mesenchymal cell

x 2325

Fig. 4: Higher magnification of the section in Fig. 3. The ChE activity in the columnar cells is localized in the cisterna of the nuclear envelope and the endoplasmic reticulum. The reaction product in the cisterna is not homogeneous. Areas with strong reaction interchange with areas with weak or no reaction.

N = nucleus
Ne = nuclear envelope
ER = endoplasmic reticulum
M = mitochondria

x 12303

Fig. 5: High magnification of the section in Fig. 3. The ChE positive perinuclear cisterna is connected to the ChE active profile of the ER. A nuclear pore is visible as unstained circular area (arrow).

N = nucleus
Ne = nuclear envelope
ER = endoplasmic reticulum
M = mitochondria

x 23940

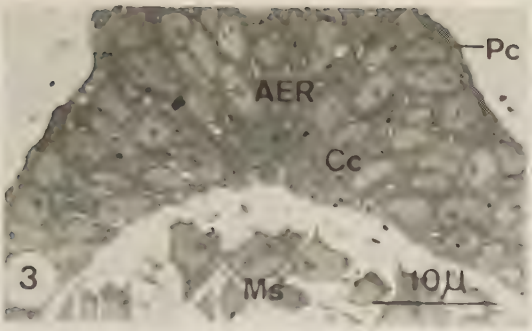
Pc
AER
Cc
3
Ms
10μ

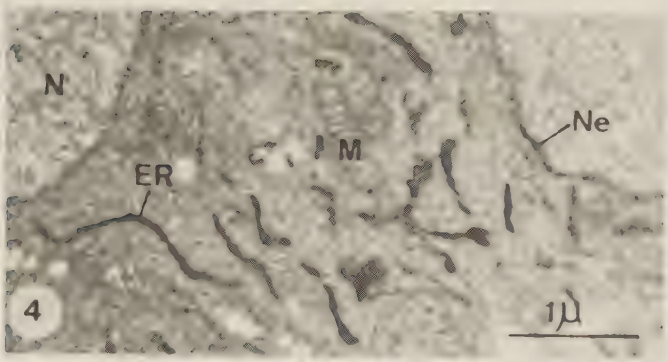
N
Ne
M
ER
4
1μ

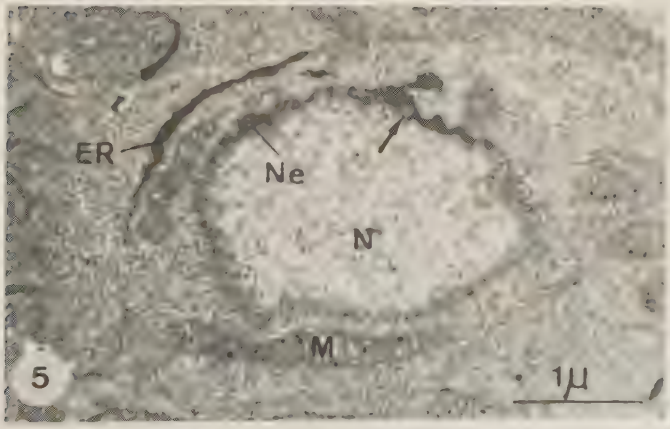
ER
Ne
N
M
5
1μ

Fig. 6: Mesenchymal cells in the subridge area of chick wing bud stage 24. The mesenchymal cells are interconnected by cytoplasmic processes forming small contacts with each other (arrow). They show ChE activity in the cisternae of the nuclear envelope and the endoplasmic reticulum.

N = nucleus
Nu = nucleolus
Ne = nuclear envelope
ER = endoplasmic reticulum
M = mitochondria

x 7524

Fig. 7: Mesenchymal cells in the subridge area of the section in Fig. 6. Cells show ChE activity in the cisternae of the nuclear envelope, the ER and Golgi complex. Note contact zone is also present (arrow).

N = nucleus
Nu = nucleolus
Ne = nuclear envelope
ER = endoplasmic reticulum
G = Golgi complex
M = mitochondria

x 12303

Fig. 8: Mesenchymal cells in the subridge area of the section in Fig. 6. ChE positive cisternae of the ER are located close to the nuclear envelope and the plasma membrane.

N = nucleus
Nu = nucleolus
Ne = nuclear envelope
ER = endoplasmic reticulum
M = mitochondria

x 22064

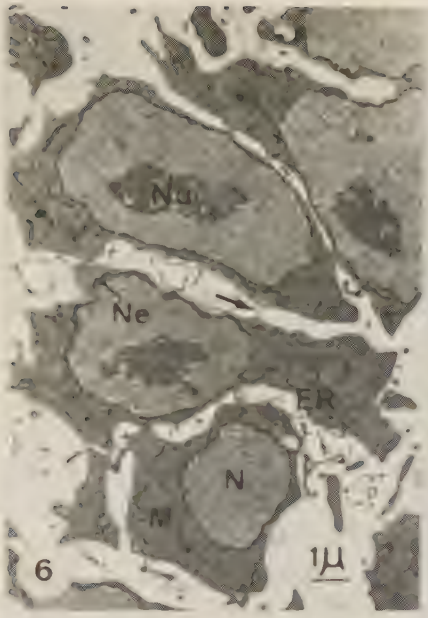
Nu
Ne
ER
N
M
1μ
6

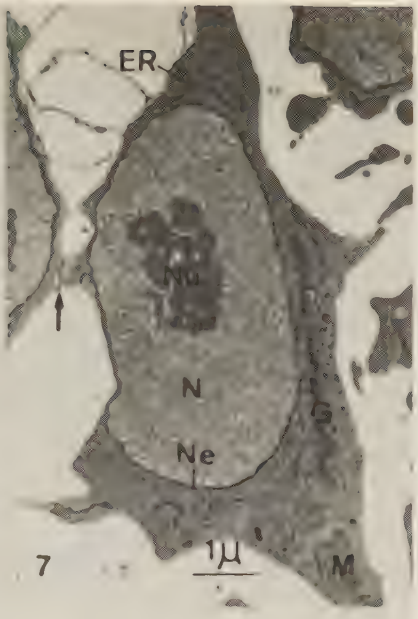
ER
Nu
N
Ne
G
1μ
M
7

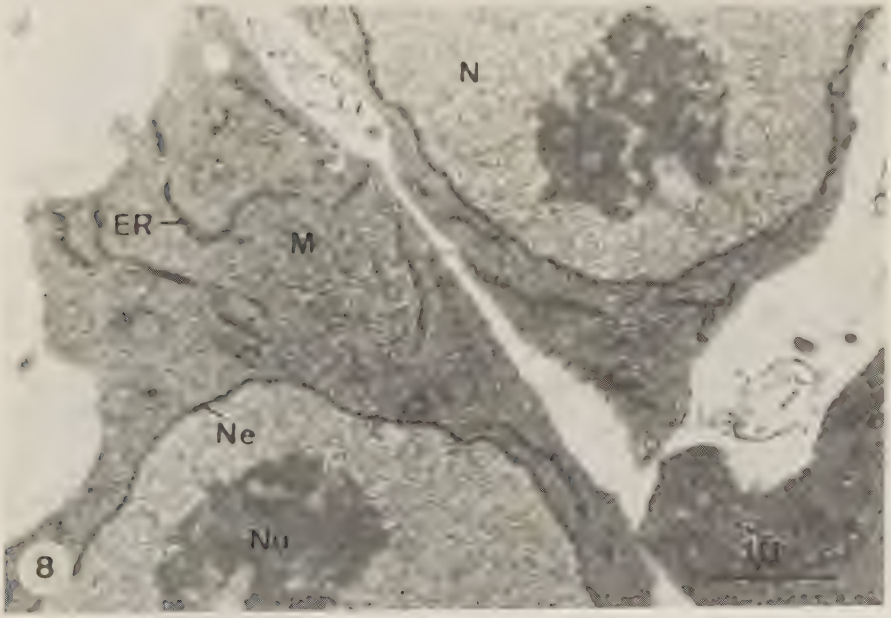
N
ER
M
Ne
Nu
1μ
8

Fig. 9: Mesenchymal cell in the subridge area of chick wing bud stage 24. ChE activity is present in the nuclear envelope and in the endoplamic reticulum. Some ChE positive profiles of the ER extend apposed to the plasma membrane (asterisks) or run parallel to the plasma membrane (arrow).

N = nucleus
Ne = nuclear envelope
ER = endoplasmic reticulum
G = Golgi complex
M = mitochondria

x 63840

Fig.10: Mesenchymal cells in the subridge area of chick wing bud stage 24. ChE activity is localized in the cisterna of the nuclear envelope, the ER and the Golgi complex. The centriole (arrow ) has no enzyme activity.

N = nucleus
Ne = nuclear envelope
ER = endoplasmic reticulum
G = Golgi complex
M = mitochondria

x 16548

Fig.11: Similar mesenchymal cell after incubation in medium containing the inhibitor, eserine ($10^{-5}$M). The enzyme activity is inhibited by eserine.

N = nucleus
Ne = nuclear envelope
ER = endoplasmic reticulum
G = Golgi complex
M = mitochondria

x 16548

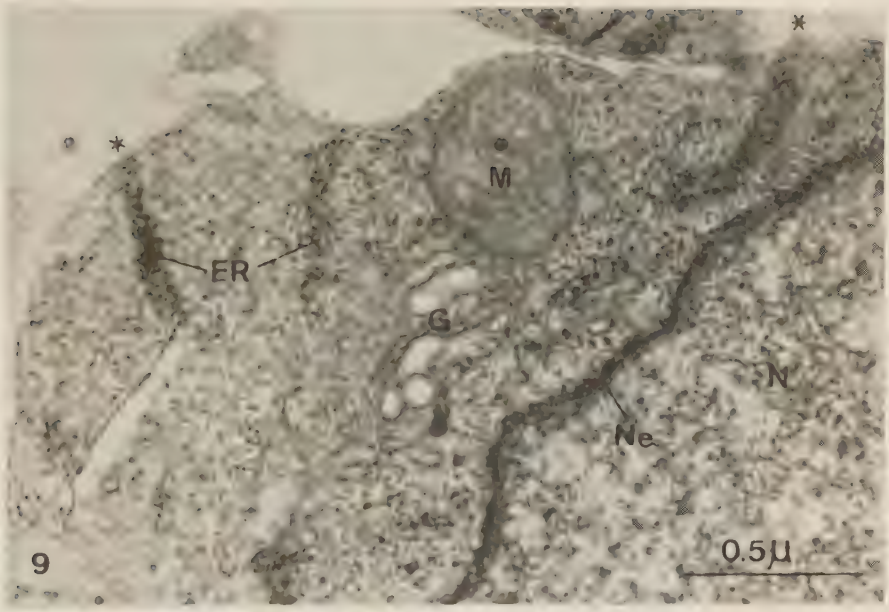
M
ER
G
N
Ne
0.5μ
9

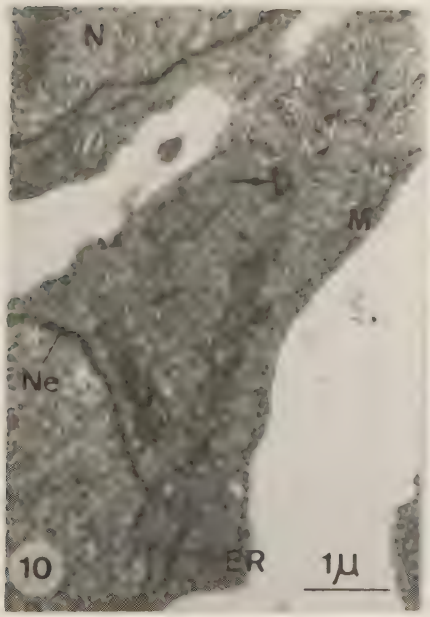
N
M
Ne
ER
1μ
10

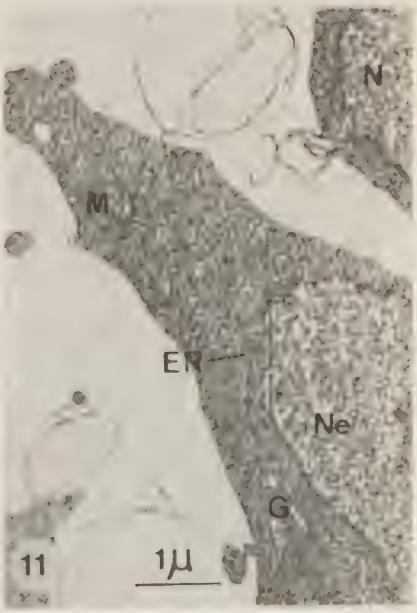
N
M
ER
Ne
G
1μ
11

Fig. 12: Mesenchymal cells in the central mesenchyme (cartilage forming area) of chick wing bud stage 24. Cells show ChE activity in perinuclear cisternae and ER. Nuclear pores (arrows) are devoid of enzyme activity. A connection between the ChE active perinuclear cisterna and the ChE active profiles of the ER is visible. Some ChE positive profiles of the ER run parallel close to the plasma membrane and/or extend to contact with the plasma membrane.

N = nucleus
Nu = nucleolus
Ne = nuclear envelope
ER = endoplasmic reticulum
M = mitochondria

x 7600

Fig. 13: Mesenchymal cells in the muscle forming area of the chick wing bud stage 24. Cells in the muscle forming area (MFA) align into clusters and lie parallel to the long axis of the limb bud. Whereas cells in the sublateral epithelium appear to lie perpendicular to the lateral epithelium.

MFA = cells in the muscle forming area
SLE = cells in the sublateral epithelium
MC = mitotic cell

x 1915

Fig. 14: Higher magnification of the section in Fig. 13. Cells in the muscle forming area are closely packed and form broad contacts with each other. They show weaker ChE activity than the cells in the subridge and cartilage forming area (compare to Fig. 6 and 12). Intracellular localization of the enzyme activity is similar to the cells from other areas. See abbreviations in Fig. 12.

x 6156

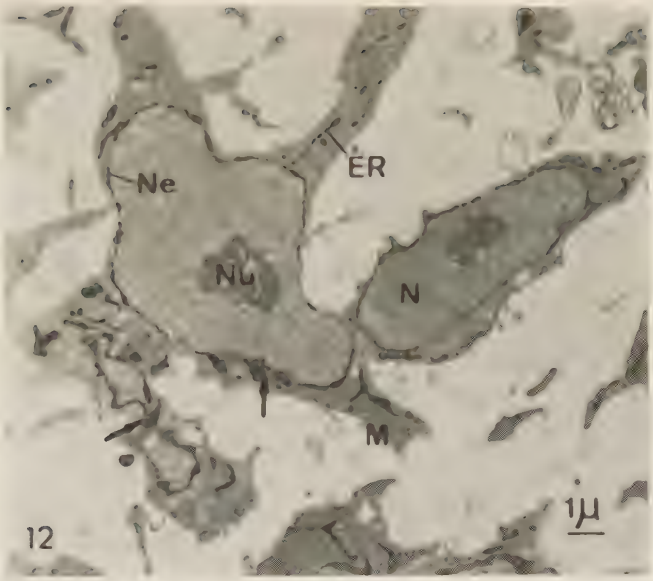
Ne
ER
Nu
N
M
1μ
12

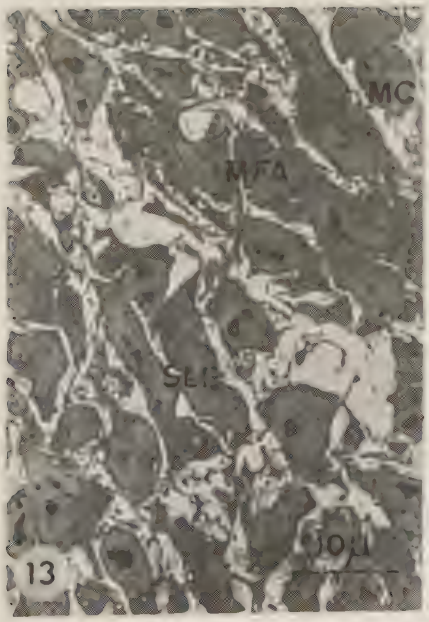
MC
MFA
SEI
10μ
13

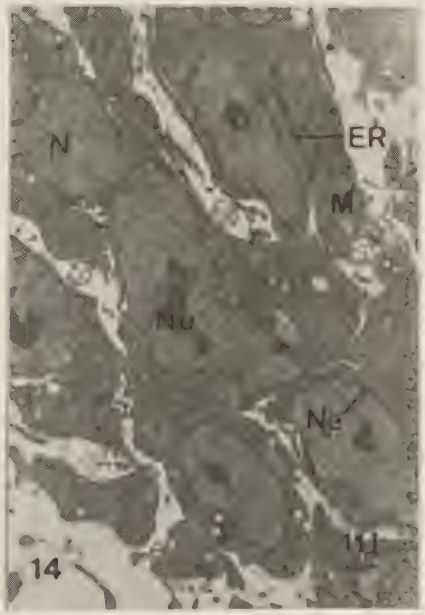
N
ER
M
Nu
Ne
1μ
14

Fig. 15: Mitotic cell in muscle forming area of the wing bud stage 24. The mitotic cells in ChE active areas show ChE activity in the segments of ER and remnants of the nuclear envelope.

N = nucleus
Nu = nucleolus
Ne = Nuclear envelope
ER = Endoplasmic reticulum
M = mitochondria
Ci = cilia

x 9200

Fig. 16: Unstained semithin section of the apical ectodermal ridge and subridge area in chick wing bud stage 25. Phase contrast microscopy. In the AER, ChE active cells cannot be seen althrough in the electron microscope all columnar cells show ChE activity. In the subridge area some single positive cells with coarse dark granules of reaction product are observed (arrows). With phase optics some of the black deposits of copper sulfide becomes also visible in the light microscope. However, only large deposits can be seen, whereas the homogeneous reaction evaluated by E.M. is still unvisible.

AER = apical ectodermal ridge
Mv = marginal venous sinus
Bv = blood vessel

x 250

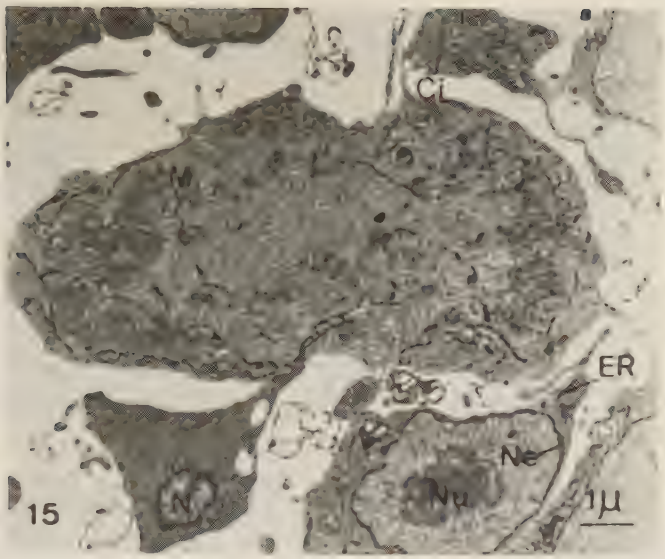
CL
ER
Ne
Nu
N
15
1μ

Bv
AER
Mv
16
100μ

Fig. 17: Phase micrograph of the cartilage forming area in chick wing bud stage 25. Most of the chondroblasts show ChE activity as dark granules in the cytoplasm (arrows). Compare EM Figure 20.

x 1330

Fig. 18: Phase micrograph of the muscle forming area in chick wing stage 25. Myotubes or multinucleated cells show ChE activity in the cytoplasm (arrows) whereas the surrounding mononucleated cells have no enzyme activity. Compare EM Figure 21.

x 800

Fig. 19: Epithelial cells of the apical ectodermal ridge. Chick wing bud stage 25. Cell shows ChE activity in the perinuclear cisterna and the profiles of endoplasmic reticulum.

N = nucleus
Ne = nuclear envelope
D = desmosome
ER = endoplasmic reticulum
L = lipid droplet
M = mitochondria
PM = plasma membrane

x 9576

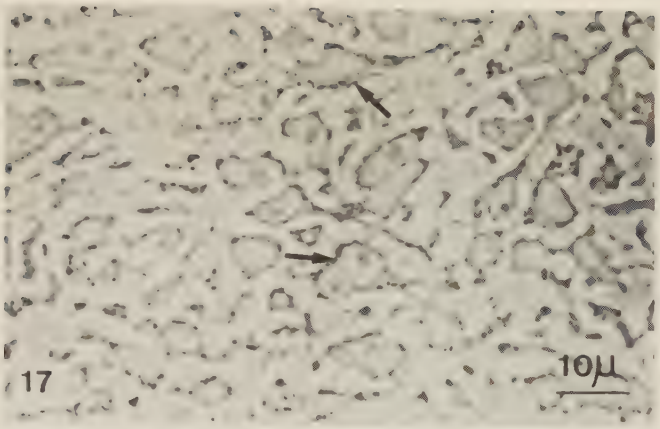
17
10μ

18
10μ

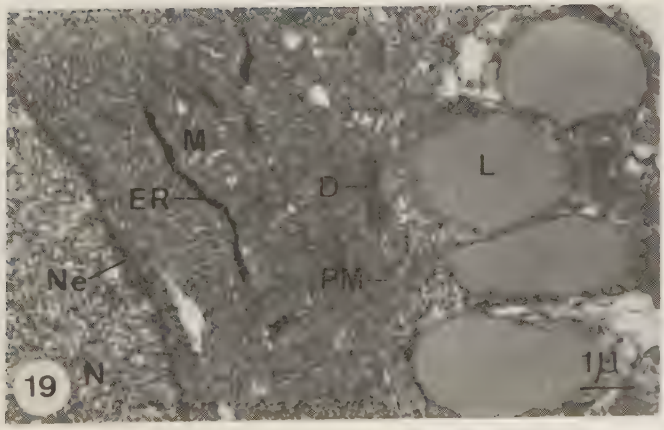
M
ER
Ne
N
D
PM
L
19
1μ

Fig. 20: Chondroblasts in chick wing bud stage 25. The cell shows stellate shape with homogeneous euchromatic nucleus and contains amorphous material in the enlarged vesicles of Golgi complex. Chondroblast exhibits ChE activity in the perinuclear cisterna and in the ER. Note the extracellular spaces filled with floccular and fibrillar material.

N = nucleus
Ne = nuclear envelope
Np = nuclear pore
ER = endoplasmic reticulum
G = Golgi complex
M = mitochondria
V = vesicle

x 14000

Fig. 21: a. Electron micrograph of the muscle forming area in chick wing bud stage 25. Cholinesterase staining without ethopropazine. ChE-positive myocytes with strong reaction are surrounded by ChE-negative myoblasts.

x 6165

b. Higher magnification of Fig. a. ChE-positive myocyte contains abundant ER, mitochondria and myofilament.

x 12303

Mb = myoblast
Mc = myocyte
Mf = myofilament
Ne = nuclear envelope
ER = endoplasmic reticulum

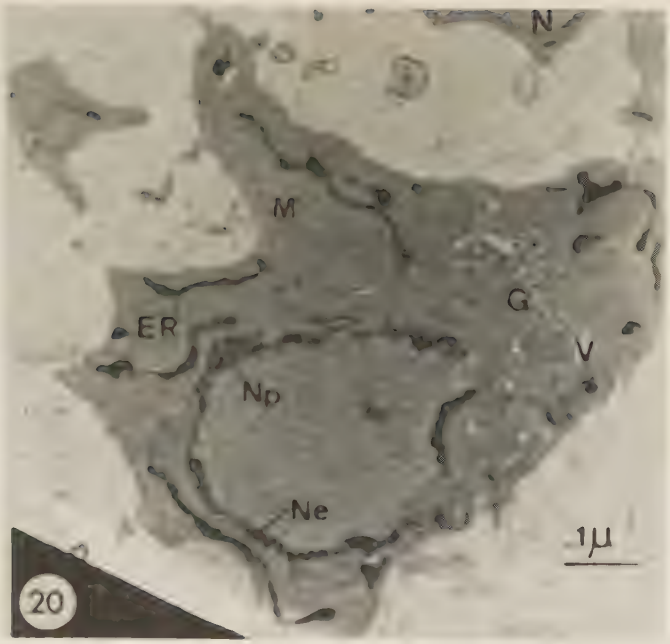
N
M
G
ER
V
Np
Ne
1μ
20

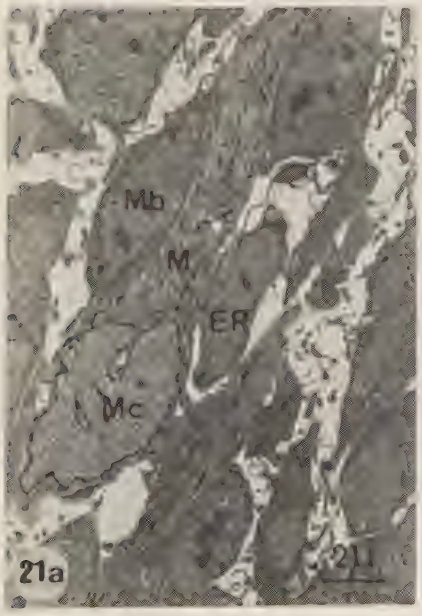
Mb
M
ER
Mc
21a

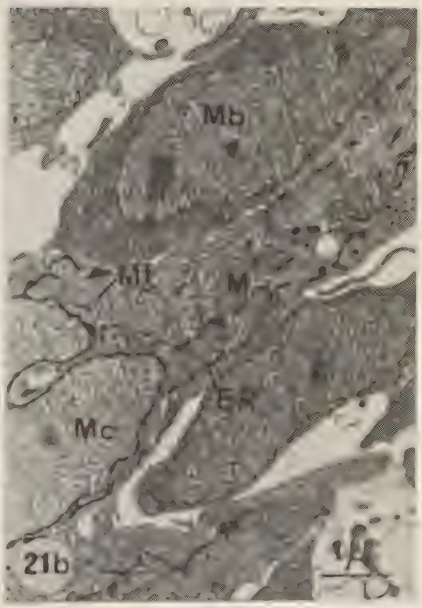
Mb
M
ER
Mc
21b

Fig. 22: Chondroblast at stage 26, showing elongated shape with oval nucleus. Its cytoplasm contains more elongated mitochondria and the extended rough endoplasmic reticulum. ChE activity is localized in the perinuclear cisterna and in the profiles of ER. The extracellular spaces contain numerous fine fibrils 12 - 25 nm in diameter (arrows).

N = nucleus
Nu = nucleolus
Ne = nuclear envelope
ER = endoplasmic reticulum
rER = rough endoplasmic reticulum
M = mitochondria

x 12768

Fig. 23: Myotube at stage 26. The myotube shows multinucleated nuclei and contains a lot of thick and thin myofilament. The profiles of ER and mitochondria are also increased in number. The myotube with strong Che reaction is surrounded by myoblasts with non or weak reaction.

Mb = myoblast
Mt = myotube
Ne = nuclear envelope
M = mitochondria
Mf = myofilament
SR = sarcoplasmic reticulum

x 14000

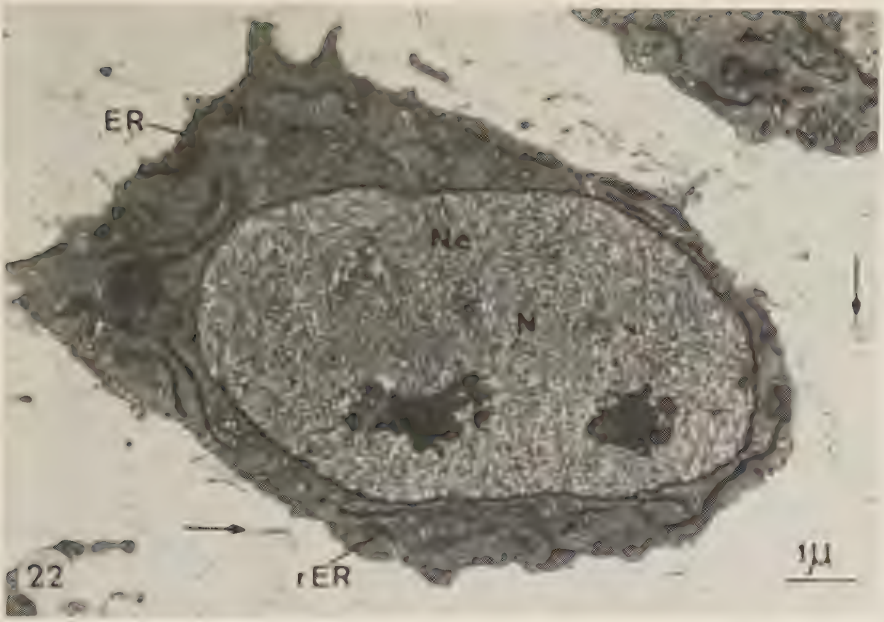
ER
Nc
N
22
rER
1μ

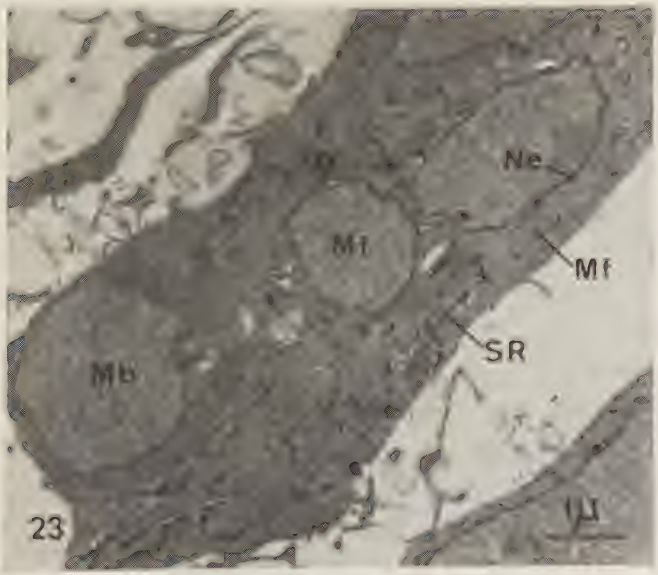
Nc
Mi
Mi
SR
Mb
23
1μ

Fig. 24: Myocyte at stage 26, showing myofilaments with developing Z-band. ChE activity is localized in the cisterna of the nuclear envelope and the developing sarcoplasmic reticulum.

N = nucleus
ER = endoplasmic reticulum
M = mitochondria
Mf = myofilament
Z = developing Z-band

x 31920

Fig. 25: The apical ectodermal ridge at stage 27. The columnar cells show ChE activity in the perinuclear cisternae and the ER as in earlier stages. Many necrotic peridermal cells are present.

N = nucleus
Ne = nuclear envelope
ER = endoplasmic reticulum
M = mitochondria
Pc = necrotic peridermal cell

x 3600

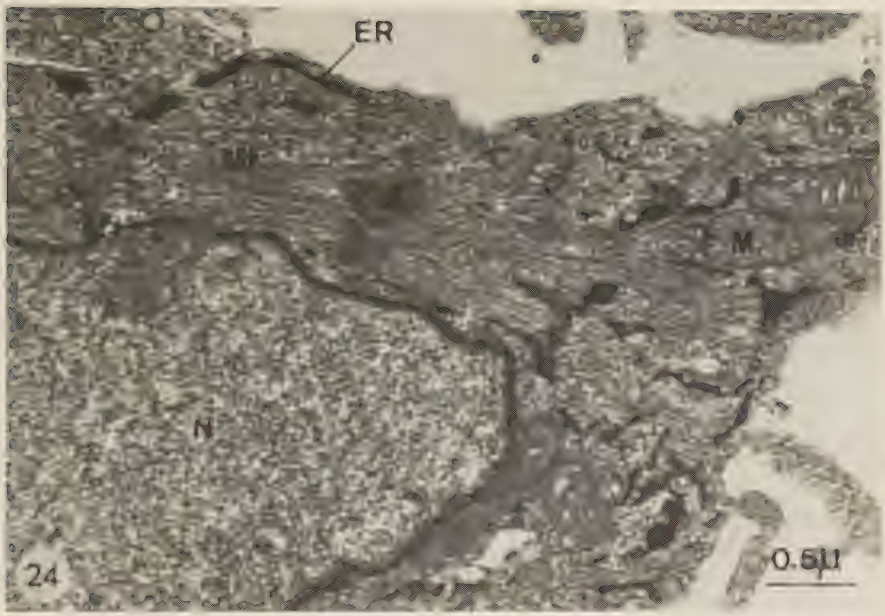
ER
M
M
N
24
0.5μ

Pc
N
Nc
25
5μ

Fig. 26: Chondroblast in the distal part of the chondrogenic area at stage 27. The cytoplasm contains more extended vesicles containing homogeneous amorphous material. ChE activity is localized in narrow strands of ER. The extended rough ER of the more differentiated chondroblast have no enzyme activity.

N = nucleus
Nu = nucleolus
Ne = nuclear envelope
ER = endoplasmic reticulum
rER = rough endoplasmic reticulum
M = mitochondria
V = vesicle
Fl = floccular material
Fi = fibrillar material

x 16404

Fig. 27: Chondroblast and chondrocyte in the proximal part of the cartilagineous area at stage 27. The ChE positive chondroblast is connected with the ChE negative chondrocyte by a primitive contact zone (arrow).

Cb = chondroblast
Cc = chondrocyte
Ne = nuclear envelope
ER = endoplasmic reticulum
rER = rough endoplasmic reticulum
M = mitochondria
V = vesicle

x 40000

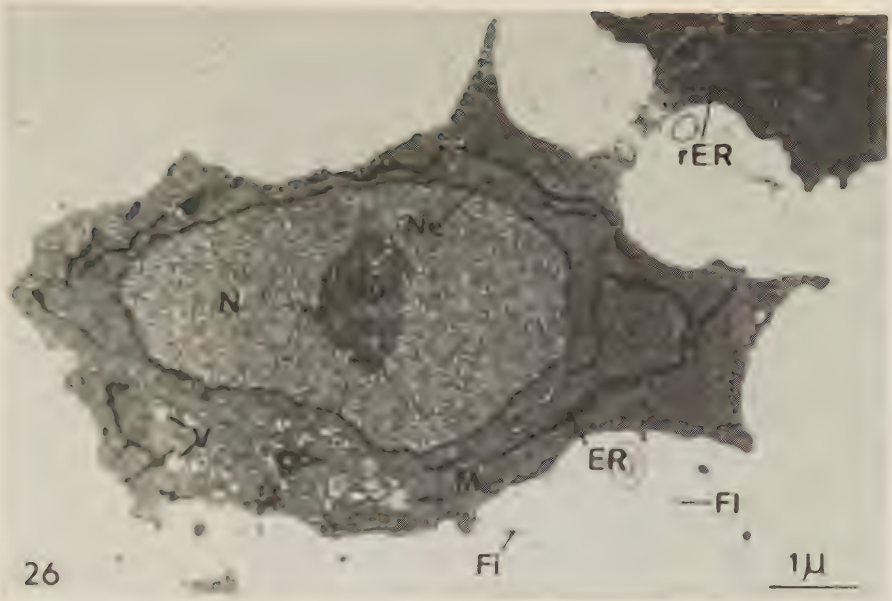
rER
Ne
N
V
M
ER
Fl
Fi
26
1μ

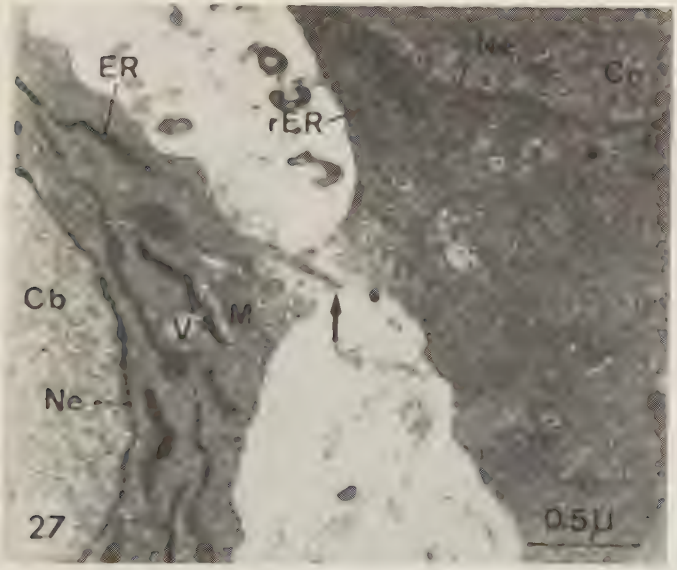
ER
rER
Ne
Cb
Cb
V
M
Ne
27
0.5μ

Fig. 28: Chondrocyte in the center of the proximal chondrogenic core at stage 27. The chondrocyte shows advanced differentiation. It contains extended cisternae of rough ER and numerous vesicles, both filled with amorphous material. There is no enzyme activity.

N = nucleus
Nu = nucleolus
Ne = nuclear envelope
rER = rough endoplasmic reticulum
L = lipid droplet
M = mitochondria
V = vesicle
Fi = fibrillar material
Fl = floccular material

x 16404

Fig. 29: Cross section of the myotube. Chick wing bud stage 27. Myotube contains several nuclei and shows strong ChE activity in the entire cisternae of the nuclear envelope and the sarcoplasmic reticulum. Myoblast has no enzyme activity.

Mb = myoblast
Mt = myotube
Ne = nuclear envelope
M = mitochondria
Mf = myofilament
SR = sarcoplasmic reticulum

x 14000

Fl
Ne
Vu
N
rER
L
V
28
Fl
1µ

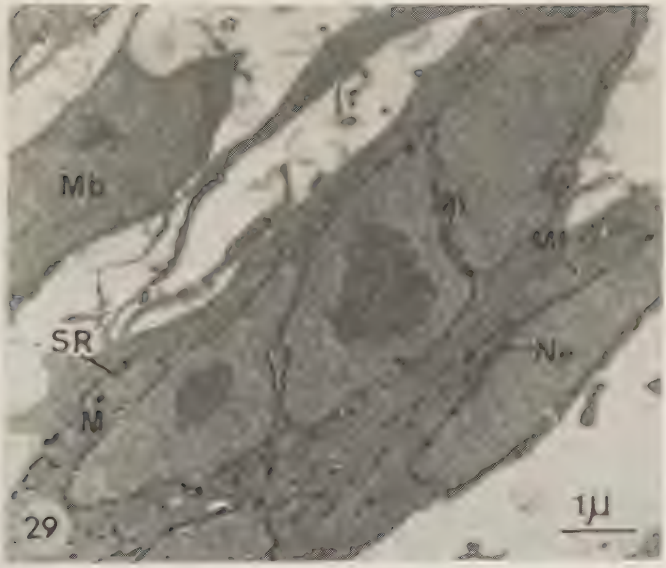
Mb
SR
M
N
29
1µ

Fig. 30: Myotubes at stage 27. The ChE positive myotubes with myofibrils are still surrounded by myoblasts with weak or no ChE activity. The ChE reaction is localized in the entire perinuclear cisternae and in the sarcoplasmic reticulum.

Mt = myotube
Mb = myoblast
MF = myofibril
Mf = myofilament
rER = rough endoplasmic reticulum
SR = sarcoplasmic reticulum
M = mitochondria
G = Golgi complexes

x 12768

Fig. 31: Higher magnification of the Figures 30 showing ChE positive myotube and ChE negative myoblast. In the myotube, the myofilaments are arranged into myofibrils which now are more developed than in younger stages. The Z-disc are also more well organized. The ChE positive tubules of the sarcoplasmic reticulum run parallel to the myofibrils.

Mt = myotube
Mb = myoblast
MF = myofibril
Mf = myofilament
rER = rough endoplasmic reticulum
SR = sarcoplasmic reticulum
M = mitochondria
G = Golgi complexes
Z = Z-disc

x 42040

Mb
M
rER
Mi
Z
MF
G
SR
Mt
31
0.5μ

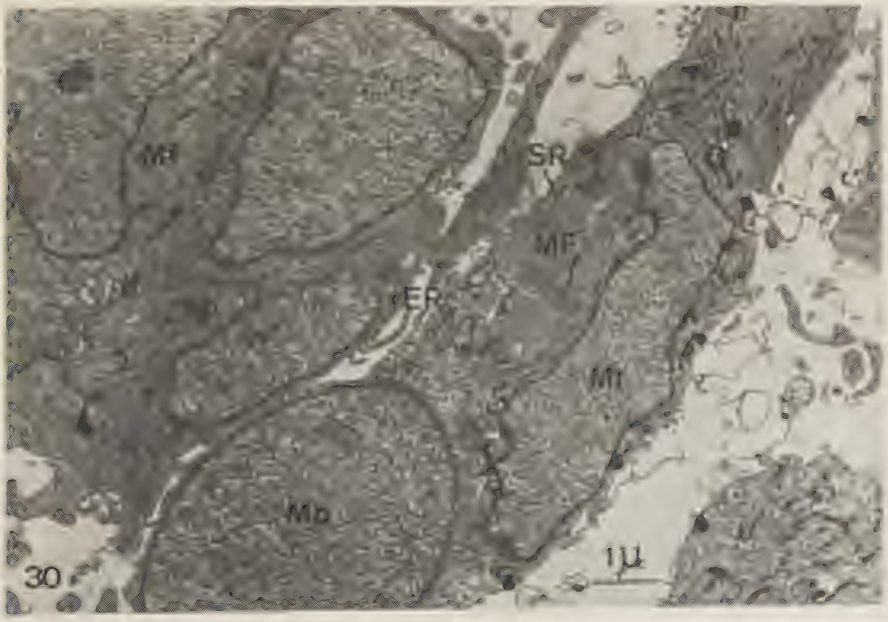
Mi
SR
MF
rER
Mt
Mb
30
1μ

Fig. 32: Lateral epithelium and cells in the sublateral epithelium at stage 27. Cells of the lateral epithelium and cells in the sublateral epithelium have no ChE activity.

LEC = lateral epithelial cells
SLE = sublateral epithelial cells
MC = mitotic cell

x 12000

Fig. 33: Fibroblasts in the soft tissue between the sublateral epithelium and the muscle at stage 27. Cells are elongated and contain abundant of rough endoplasmic reticulum and vesicles. The extended rER and vesicles are filled with amorphous material. Fibroblasts have no ChE activity.

C = centriole
rER = rough endoplasmic reticulum
M = mitochondria
V = vesicles

x 12768

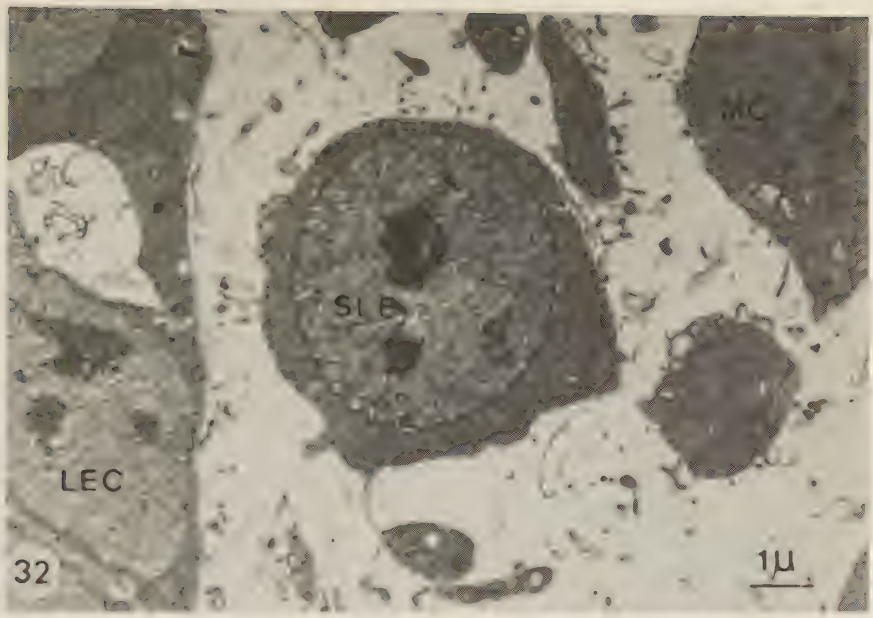
MC
SLB
LEC
32
1μ

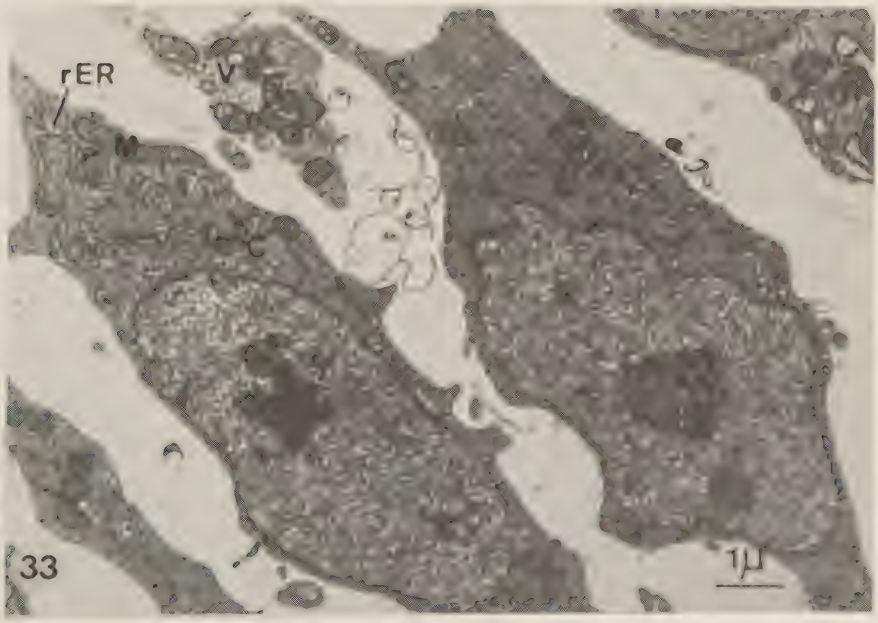
rER
V
33
1μ

Fig. 34: Sagittal cryostat section of mouse embryo at day 15 p.c. submitted to Karnovsky and Roots' reaction for cholinesterase. The mesenchyme caudal to the junction of the genital ducts and the urogenital sinus shows ChE activity (arrow). In addition ChE is seen in nerve fibres, muscular layers of bladder and intestine, muscle of body wall, liver and corpus cavernosum.

B = bladder
BW = body wall
CC = corpus cavernosum
GD = genital duct
I = intestine
L = liver
M = muscle blastemata
NF = nerve fiber
P = phallus
R = rectum
T = tail
UGS = urogenital sinus

x 50

Fig. 35: Cryostat section through the junctional area of the genital ducts and the urogenital sinus. Mouse embryo at day 15 p.c.. The ChE positive mesenchymatous condensation is located at the dorsal side of the urogenital sinus. The paravesical ganglia show strong ChE activity. Compare to Fig. 37.

G = ganglion
MC = mesenchymatous condensation
UGS = urogenital sinus

x 200

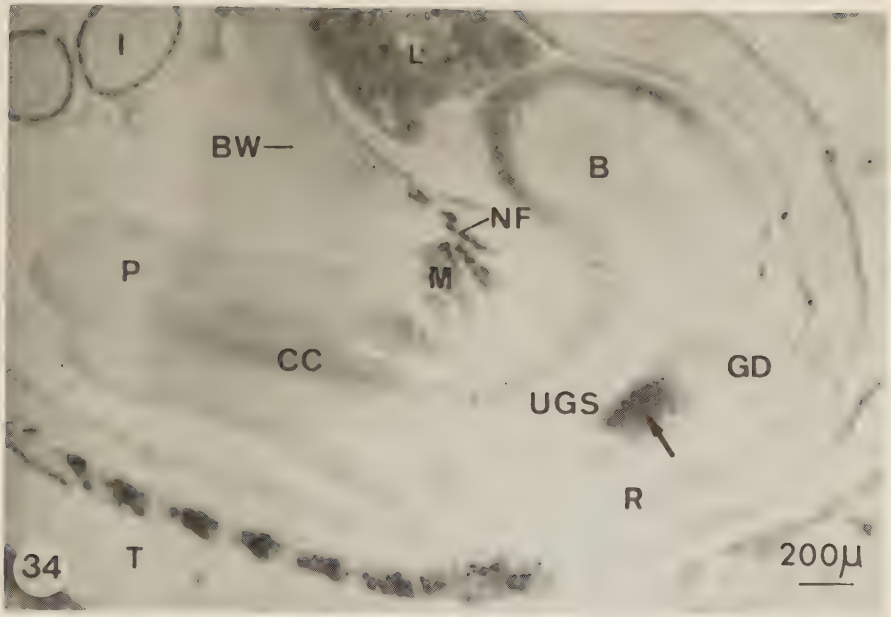
I
L
BW
B
NF
P
M
CC
GD
UGS
R
34
T
200μ

UGS
G
MC
35
100μ

Fig. 36: Schematic drawings of the genital tract of the mouse embryo in the indifferent stage.

A. Levels of areas sectioning

I. section cranial to the junctional area

II. section at the junctional area of the genital ducts and the urogenital sinus.

III. section caudal to the junctional area

B. Intensity of enzyme reaction (one plus to four plus for the positive reaction and none for the negative reaction) and location of E.M.-figures are indicated. Numbers refer to the E.M.-figures which are taken from the respective area.

Md = Müllerian duct

Wd = Wolffian duct

UGS = urogenital sinus

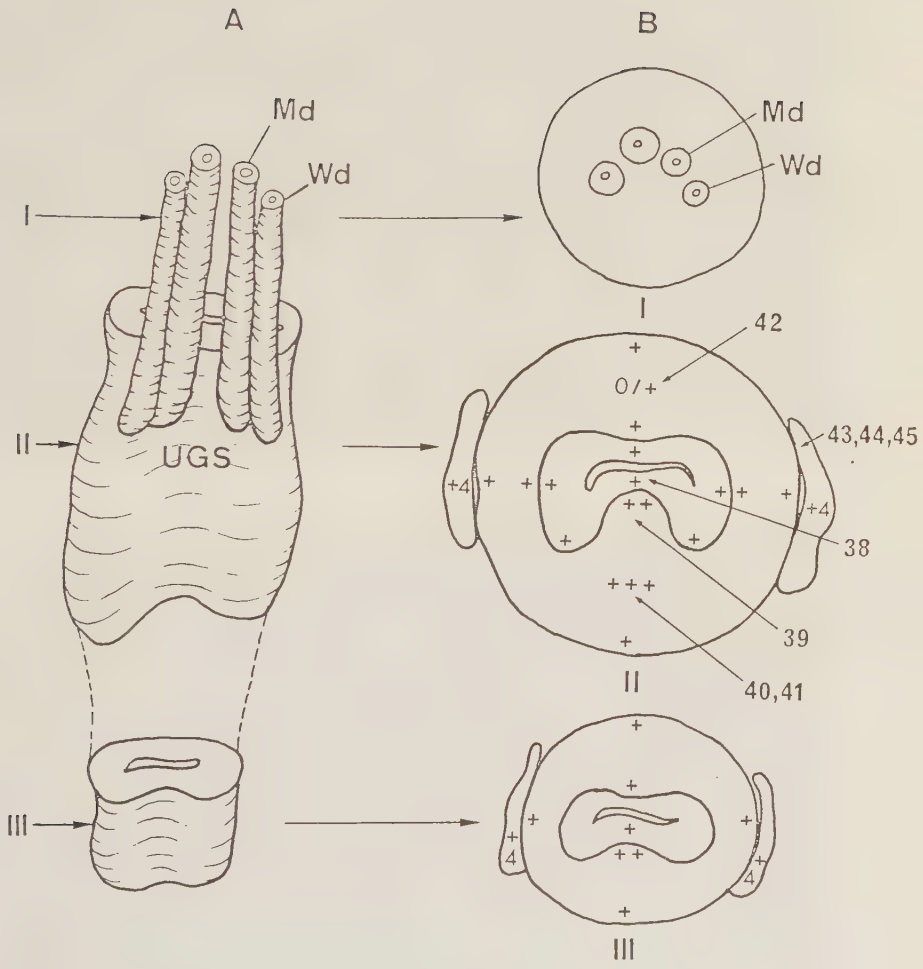


Fig. 36

Fig. 37: Semithin cross section near the junctional area where ChE reaction is strong. Azure II staining. Mouse embryo at day 15 p.c.. The urogenital sinus is lined by stratified cuboidal epithelium and surrounded by mesenchymal tissue. At the dorsal side of the urogenital sinus cells are densely packed into a whorl like mesenchymatous condensation.

SE = sinus epithelium
G = ganglia
MC = mesenchymatous condensation
UGS = urogenital sinus

x 315

Fig. 38: Epithelium of the urogenital sinus. Mouse embryo at day 15 p.c.. Cholinesterase staining with blocker, $2 \times 10^{-4}$ M ethopropazine (Lewis and Shute's method, 1969). Epithelial cells show ChE activity. The enzyme reaction is localized in the cisternae of the nuclear envelope and the ER. Distribution of the reaction product is not homogeneous throughout the cisternae.

N = nucleus
Ne = nuclear envelope
ER = endoplasmic reticulum
rER = rough endoplasmic reticulum
M = mitochondria
S = sinus

x 10032

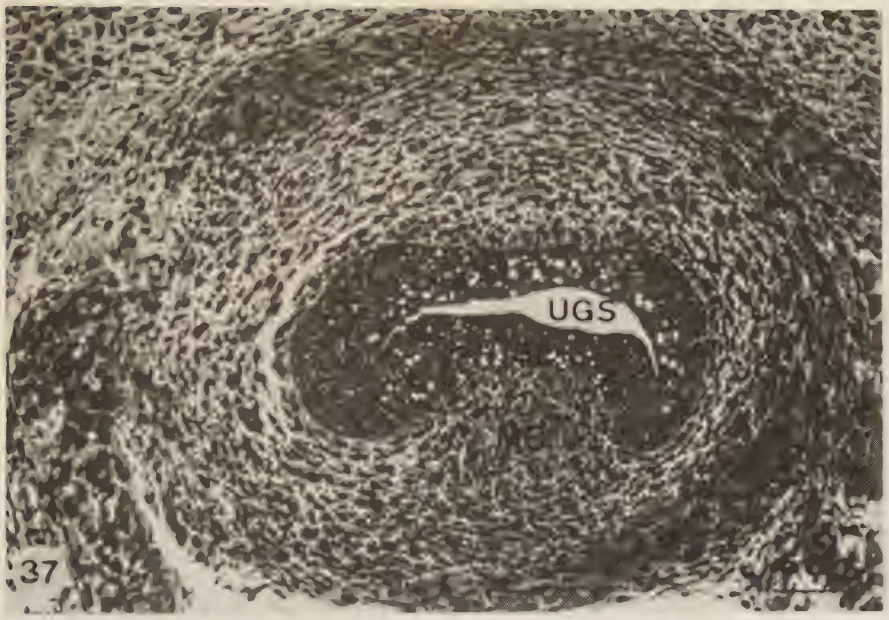
UGS
37

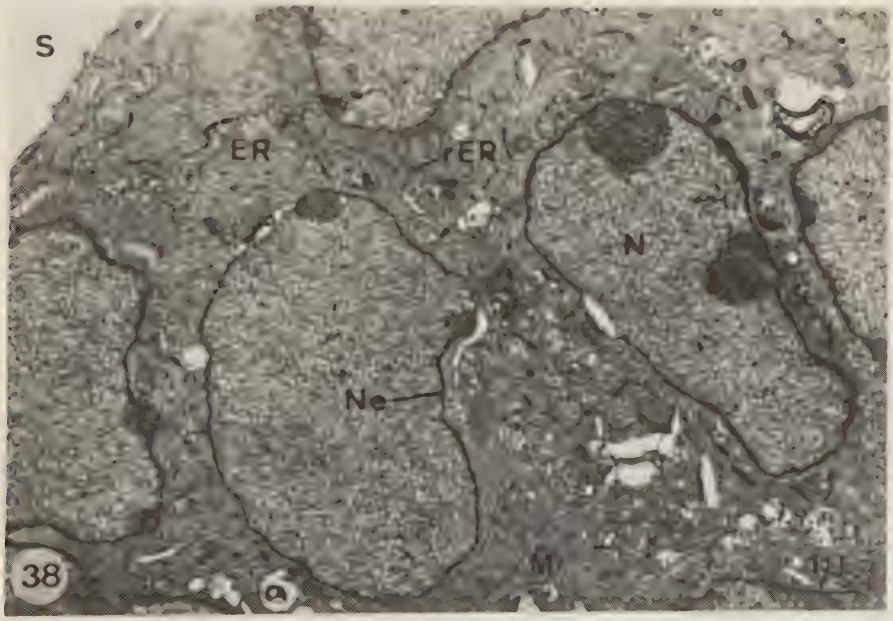
S
ER
ER
N
Ne
M
38
a

Fig. 39: Mesenchymal cells beneath the sinus epithelium. Mouse embryo at day 15 p.c.. Cholinesterase staining without ethopropazine. Patches of reaction product are localized in the perinuclear cisterna and in the profiles of the ER. Note activity in the basal part of epithelial cells (arrow).

BL = basal lamina
SP = sinus epithelium
N = nucleus
ER = endoplasmic reticulum
rER = rough endoplasmic reticulum
M = mitochondria

x 10032

Fig. 40: Mesenchymal cells in the whorl area. Mouse embryo at day 15 p.c.. Cholinesterase staining with ethopropazine. Cells are irregular in shape and connected to each other with small cytoplasmic processes. Cells show ChE activity in the perinuclear cisterna and the ER. Extracellular spaces contain procollagen microfibrils (arrows).

N = nucleus
ER = endoplasmic reticulum
rER = rough endoplasmic reticulum
M = mitochondria
L = lipid droplet

x 10032

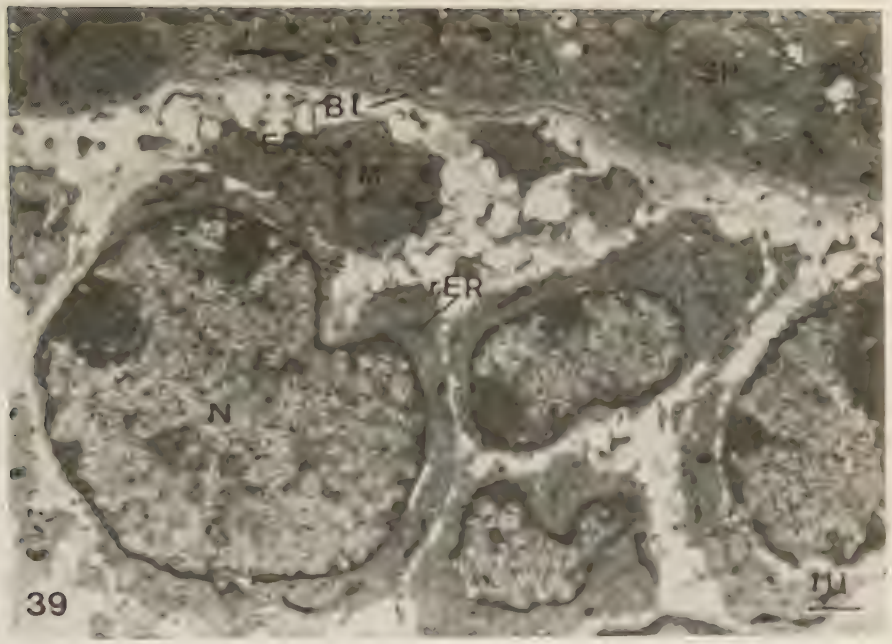
BL
M
ER
N
39

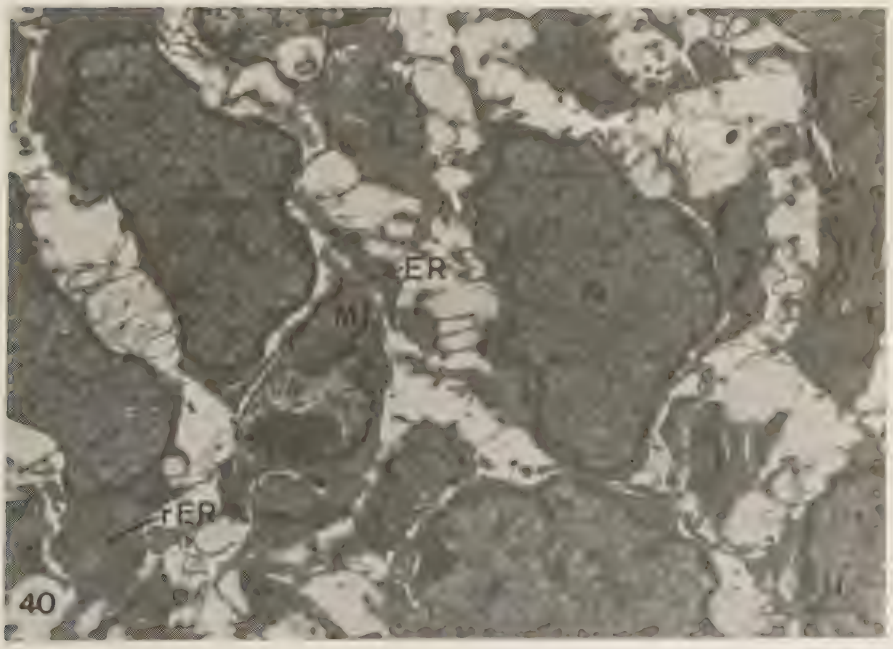
ER
M
ER
40

Fig. 41: Mesenchymal cells in the whorl area. Higher magnification than Fig. 40. Enzyme reaction is localized in the cisternae of the ER. In the rough ER, narrow areas of strong enzyme reaction alternate with areas with no reaction.

N = nucleus
ER = endoplasmic reticulum
M = mitochondria
L = lipid droplet

x 25536

Fig. 42: Cells in the middle layer of the mesenchyme at the ventral side of the urogenital sinus. Mouse embryo at day 15 p.c.. Cholinesterase staining with ethopropazine. Cells are elongated and loosely arranged. Cells have long cytoplasmic processes and contain rough endoplasmic reticulum, abundant mitochondria and Golgi complexes. Extracellular spaces contain bundles of fibrils (arrows). Cells show enzyme activity in short segments of the ER.

N = nucleus
ER = endoplasmic reticulum
rER = rough endoplasmic reticulum
G = Golgi complex
M = mitochondria

x 12768

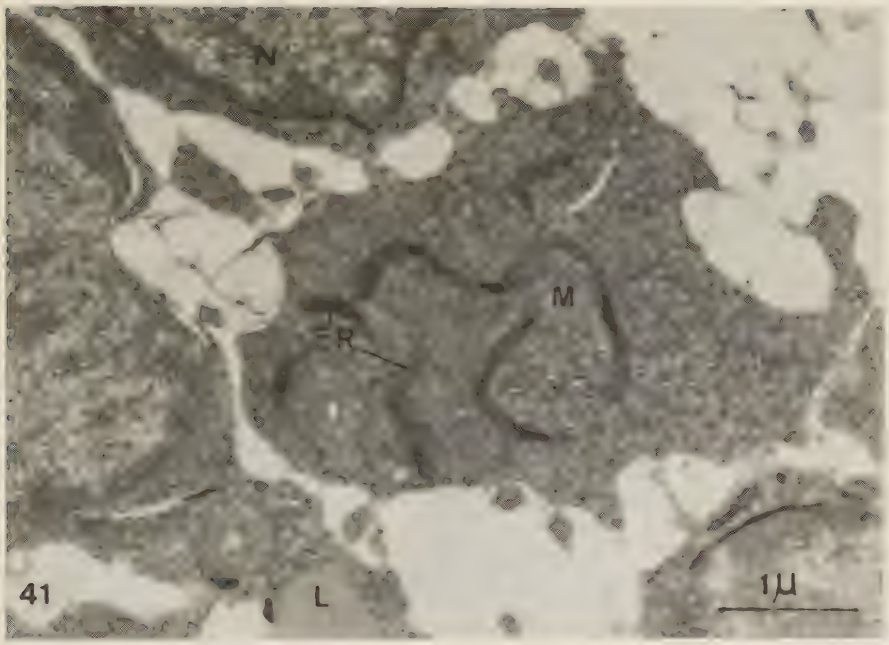
N
M
ER
41
L
1μ

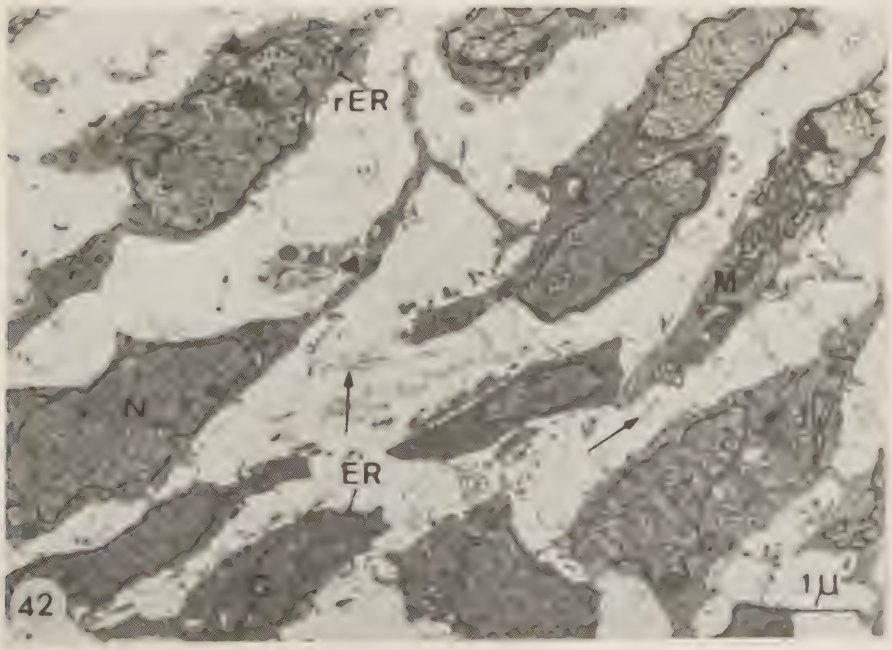
rER
M
N
ER
42
1μ

Fig. 45: Unmyelinated nerve fibers in the ganglion. Mouse embryo at day 15 p.c..Cholinesterase staining with ethopropazine. Reaction product is present in the interspaces between closely apposed axons.

A = axon
SC = satellite cell
rER = rough endoplasmic reticulum
G = Golgi complex
M = mitochondria

x 25536

45

Fig. 46: Sagittal cryostat section of male mouse embryo at day 17 p.c.. Cholinesterase staining after Karnovsky and Roots. ChE reaction is located in the mesenchyme caudally to the junction of the genital ducts with the urogenital sinus and in the mesenchyme directly above the outgrowth of the vesicular gland (arrows). Nerve fibers show very strong enzyme reaction. The enzyme activity is also present in the muscular layer of urethra, bladder and abdominal wall and in the corpus cavernosum.

AB = muscle of abdominal wall
B = bladder
CC = corpus cavernosum
DD = ductus deferens
E = epididymis
NF = nerve fibers
R = rectum
S = symphysis
T = testis
U = urethra
VG = vesicular gland
Wd = Wolffian duct

x 50

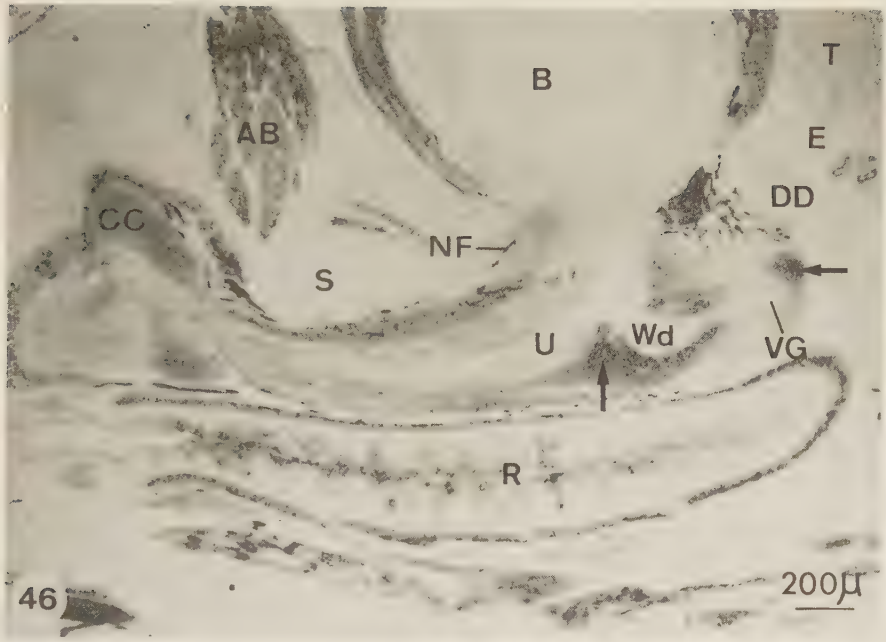
B
T
AB
E
DD
CC
NF
S
U
Wd
VG
R
46
200μ

Fig. 47: Schematic drawings of the male genital tract. Mouse embryo day 17 - 18 p.c..

A. Levels of cross sectioning (I, II and III) are shown

B. Intensity of enzyme reaction is indicated by 1 to 4 plus and the location of the following EM-figures is shown by their ordinal numbers.

U = urethra
VG = vesicular gland
Wd = Wolffian duct

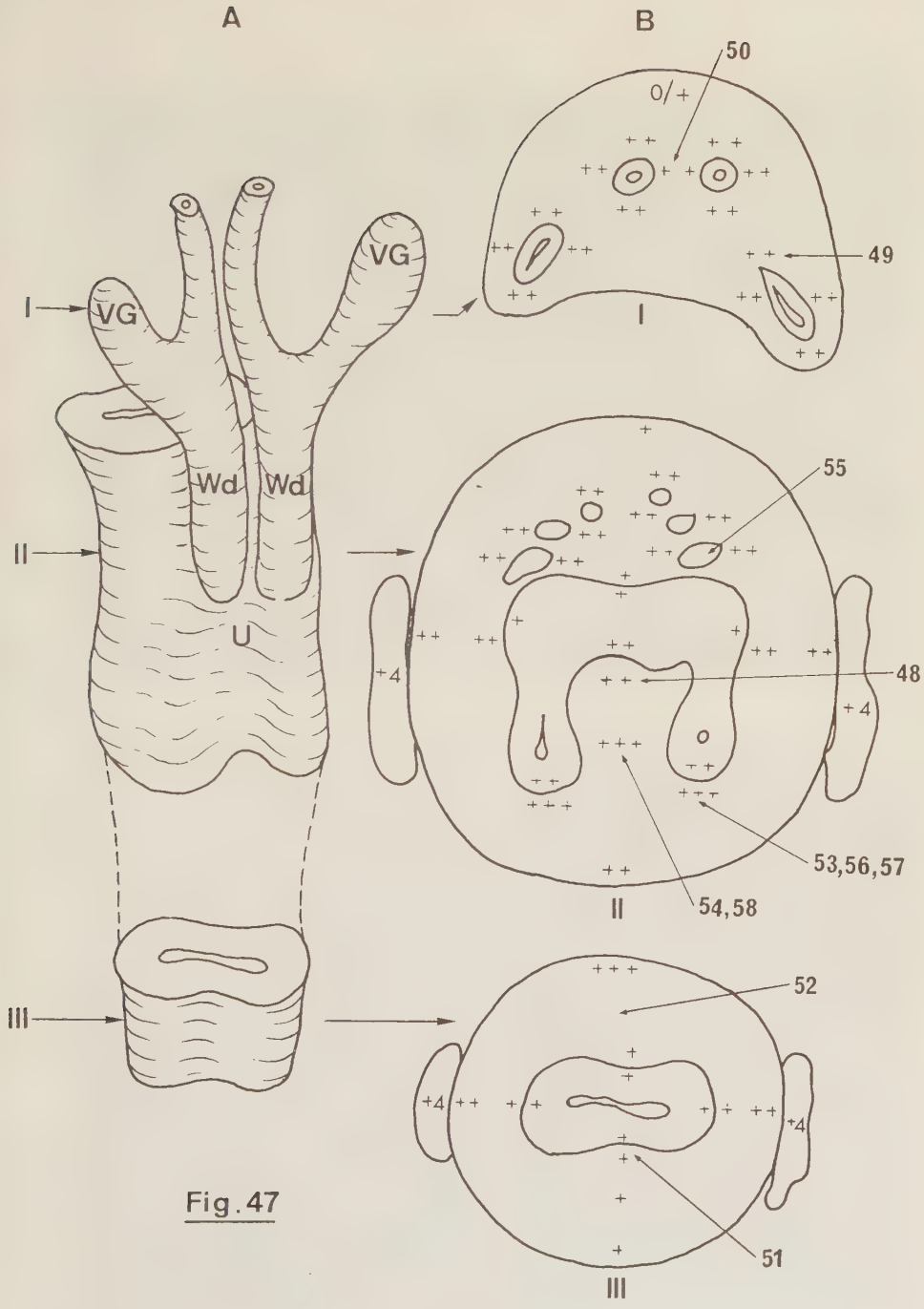


Fig. 47

Fig. 48: Mesenchymal cells at the dorsal side of the urogenital sinus. Male mouse embryo at day 17 p.c..Cholinesterase staining without ethopropazine. Cells show strong ChE activity in the cisterna of the nuclear envelope and the ER. Extracellular spaces contain more procollagen microfibrils when compared to the younger stages.

BL = basal lamina
ER = endoplasmic reticulum
M = mitochondria
N = nucleus
Ne = nuclear envelope
Np = nuclear pore
SE = sinus epithelium

x 5472

Fig. 49: From section cranial to the junctional area. Male mouse embryo at day 17 p.c.. Cholinesterase staining without ethopropazine. Mesenchymal cell surrounding the Wolffian duct shows ChE activity in the cisternae of the nuclear envelope and the ER, but negative in the Golgi areas. The profiles of the ER are commonly located close to mitochondria or extend to the plasma membrane (arrows). Note areas of strong enzyme reaction alternate with areas of weak reaction.

ER = endoplasmic reticulum
G = Golgi complex
M = mitochondria
N = nucleus
V = vesicle

x 31920

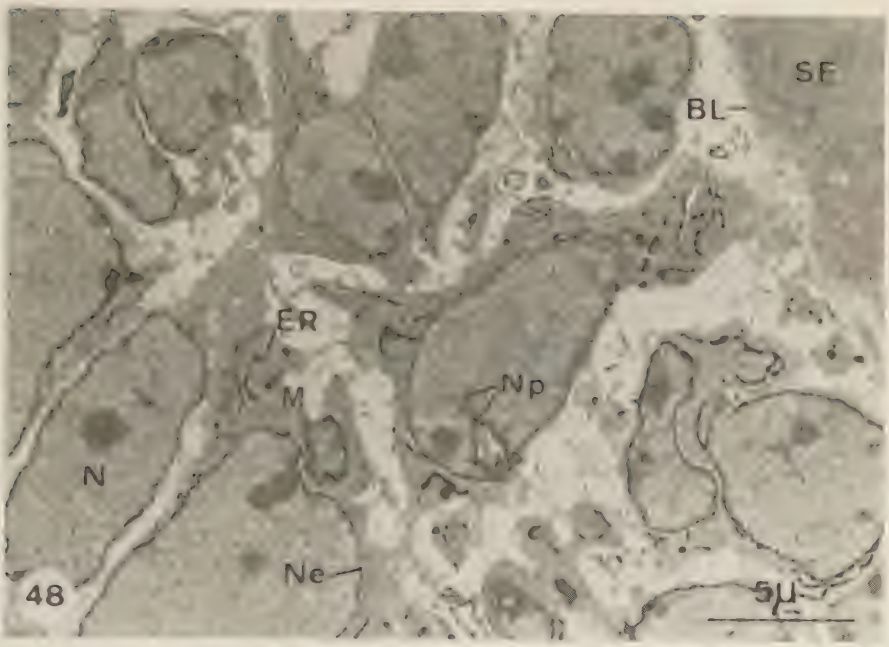
SF
BL
ER
M
Np
N
Ne
48
5μ

G
M
V
ER
N
49
1μ

Fig. 50: Mesenchymal cells from the same section as Fig. 49. Cells at the dorsal side show strong ChE activity.

ER = endoplasmic reticulum
rER = rough endoplasmic reticulum
G = Golgi complex
L = lipid droplet
M = mitochondria
N = nucleus

x 10032

Fig. 51: Section caudal to the junctional area. Male mouse embryo at day 17 p.c.. Cholinesterase staining without ethopropazine. Mesenchymal cells in the mesenchymatous condensation show less ChE activity than in the junctional area (compare to Fig. 48).

ER = endoplasmic reticulum
rER = rough endoplasmic reticulum
G = Golgi complex
L = lipid droplet
M = mitochondria
N = nucleus

x 10032

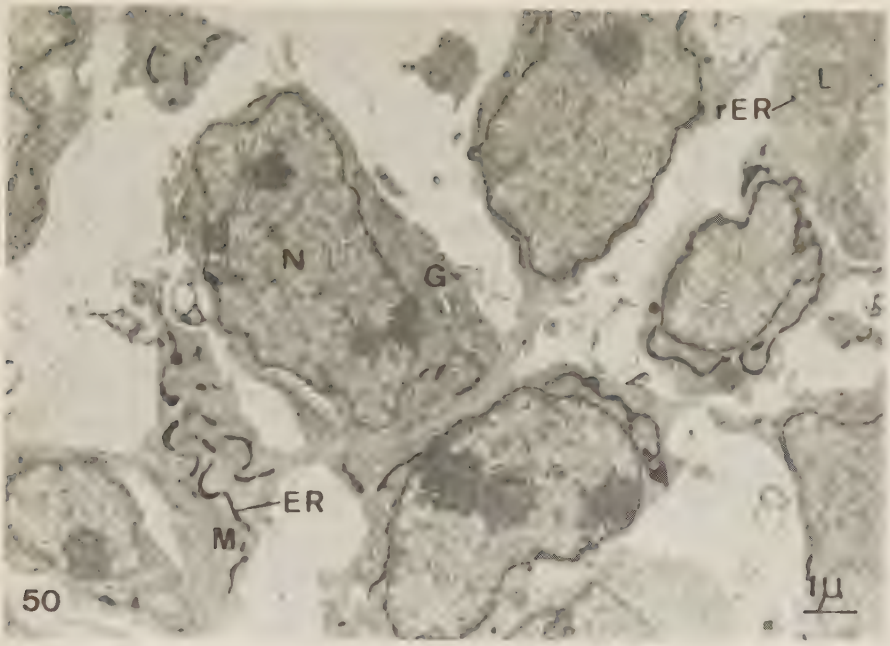
L
rER
N
G
ER
M
50
1μ

L
ER
rER
M
G
N
51
1μ

Fig. 52: Same section as Fig. 51. Cells in the loose mesenchymal layer at the ventral side show no or only weak reaction. They are more advanced in differentiation and contain abundant rough endoplasmic reticulum and polysomes. Extracellular spaces contain abundant collagen fibrils.

rER = rough endoplasmic reticulum
L = lipid droplet
M = mitochondria
N = nucleus
arrows = reaction product

x 10032

Fig. 53: Section from the junctional area. Male mouse embryo at day 18 p.c.. Cholinesterase staining without ethopropazine. Mesenchymal cells surrounding the epithelium of the urogenital sinus and the Wolffian duct show positive ChE reaction. Epithelial cells are negative.

UGS = epithelium of the urogenital sinus
Wd = epithelium of the Wolffian duct
BL = basal lamina
BV = blood vessel
ER = endoplasmic reticulum
rER = rough endoplasmic reticulum
L = lipid droplet
M = mitochondria
N = nucleus
RBC = red blood cell

x 5472

L
ER
G
N
M
52
1μ

UGS
M
BL
L
Wd
ER
N
ER
BV
RBC
53
5μ

Fig. 54: From the same section as Fig. 53. Cells of the mesenchymatous condensation show strong ChE activity in segment of the nuclear envelope and of the endoplasmic reticulum. Extracellular spaces are narrow and contain numerous collagen microfibrils.

C = centrioles
ER = endoplasmic reticulum
L = lipid droplet
M = mitochondria
N = nucleus
Np = nuclear pore

x 6476

Fig. 55: From the same section as Fig. 53. At the ventral side of the urogenital sinus, mesenchymal cells surrounding the bud of the prostate gland show positive ChE reaction. In the epithelial cells also some tiny spots with reaction product in typical location are visible.

PG = bud of the prostate gland
ER = endoplasmic reticulum
rER = rough endoplasmic reticulum
M = mitochondria
N = nucleus

x 3648

Np
N
ER
M
5μ
54

M
rER
N
ER
PG
6μ
55

Fig. 56: Section from the junctional area. Male mouse embryo at day 18 p.c.. Cholinesterase staining with ethopropazine. Cells of the mesenchymatous condensation at the dorsal side of the urogenital sinus show the same strong activity as without ethopropazine (compare to Fig. 53).

UGS = epithelium of the urogenital sinus
BL = basal lamina
ER = endoplasmic reticulum
rER = rough endoplasmic reticulum
L = lipid droplet
M = mitochondria
N = nucleus

x 6476

Fig. 57: Higher magnification of the section in Fig. 56. Stretches of strong AChE activity alternate with weak or no enzyme activity in the cisternae.

UGS = epithelium of the urogenital sinus
BL = basal lamina
ER = endoplasmic reticulum
rER = rough endoplasmic reticulum
L = lipid droplet
M = mitochondria
N = nucleus

x 16404

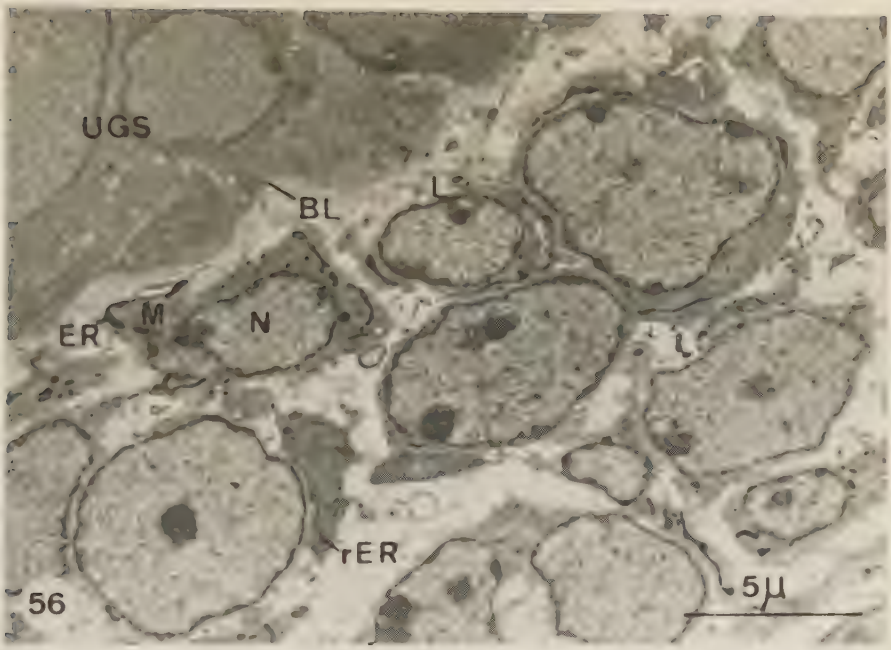
UGS
BL
L
ER
M
N
rER
56
5μ

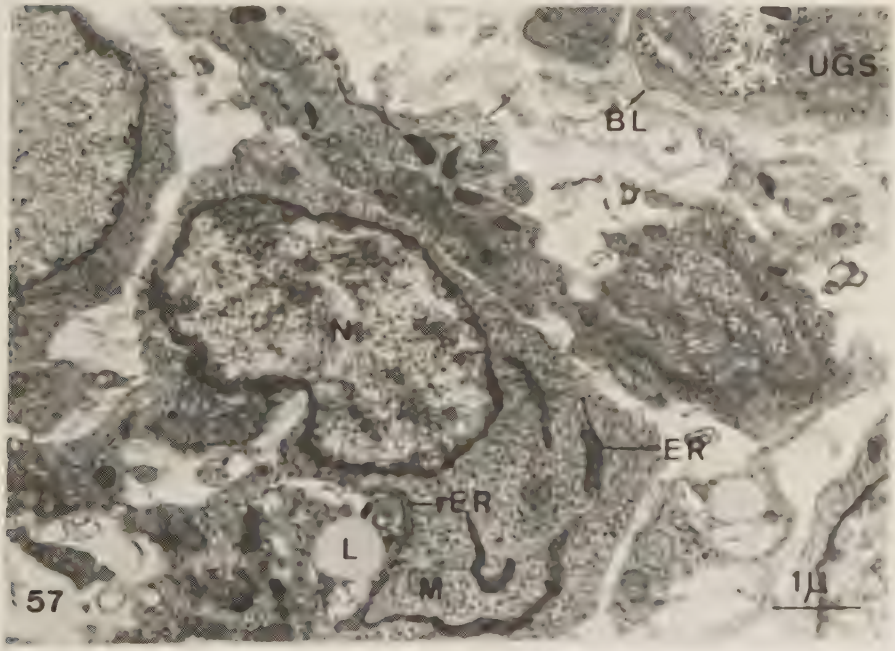
UGS
BL
M
ER
rER
L
M
57
1μ

Fig. 58: Mesenchymal cells from the same section as Fig. 56. AChE positive profiles of the endoplasmic reticulum are also located close to the plasma membrane forming special contact areas (arrow). Golgi complexes and centrioles have no enzyme reaction.

N = nucleus
ER = endoplasmic reticulum
M = mitochondria
C = centriole
G = Golgi complex

x 22064

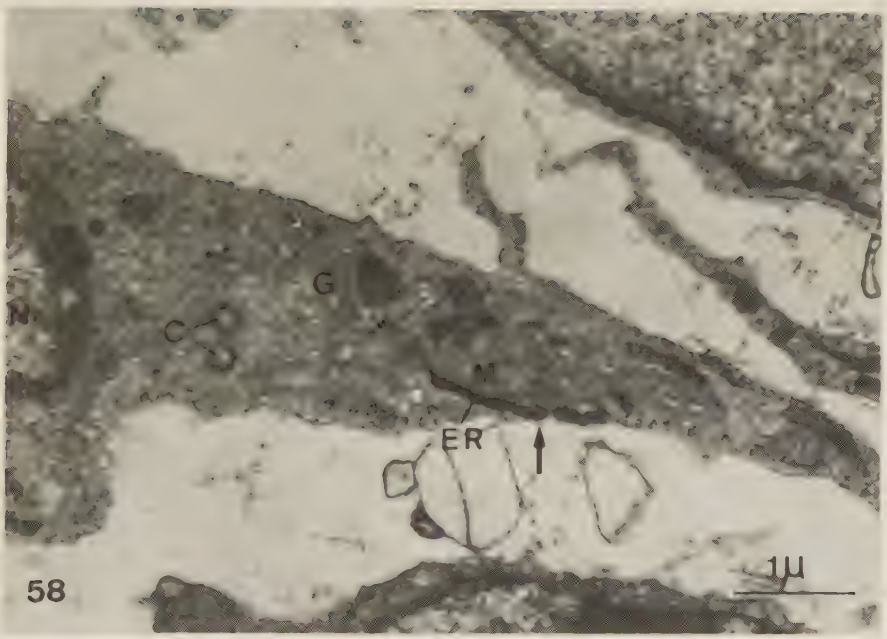


58

Fig. 59: Sagittal section of female mouse embryo at day 17 p.c.. Cholinesterase reaction after Karnovsky and Roots. ChE activity is strong in the mesenchyme located dorsally of the junction of the vagina with the urogenital sinus (arrow). The enzyme reaction is also present in the mesenchyme between vagina and the urethra, the ventral epithelium of the urethra. In addition, corpus cavernosum, the muscular layer of urethra, rectum and bladder and nerve fibers show ChE activity.

B = bladder
CC = corpus cavernosum
I = intestine
NF = nerve fibers
P = phallus
R = rectum
S = symphysis
U = urethra
V = vagina

x 50

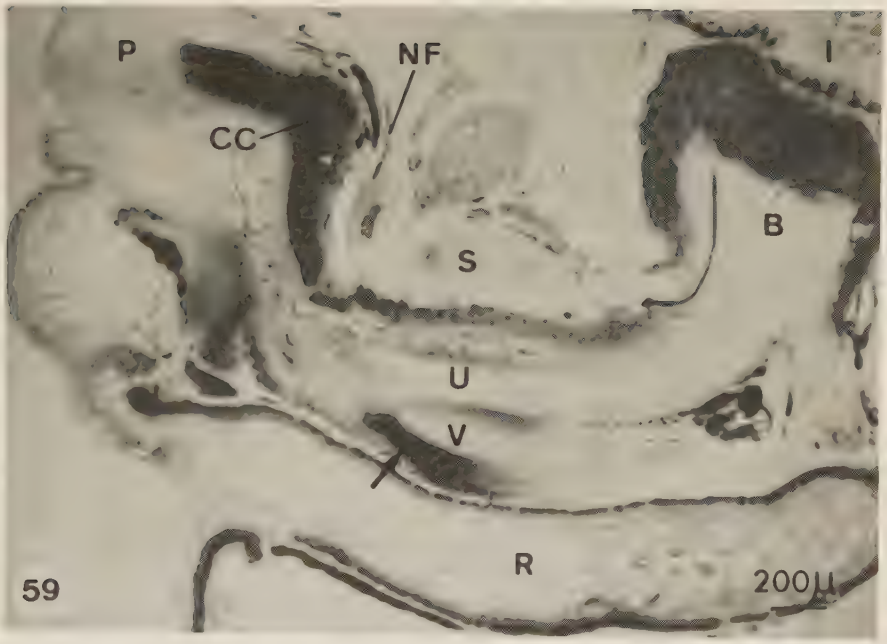
P
NF
I
CC
B
S
U
V
R
59
200μ

Fig. 60: Schematic drawings of the female genital tract of the mouse embryo at day 17 - 18 p.c.. The levels of cross sectioning (A), the intensity of enzyme reaction (B) and the ordinal numbers of EM-figures (B) are shown.

U = urethra
V = vagina
Wd = Wolffian duct

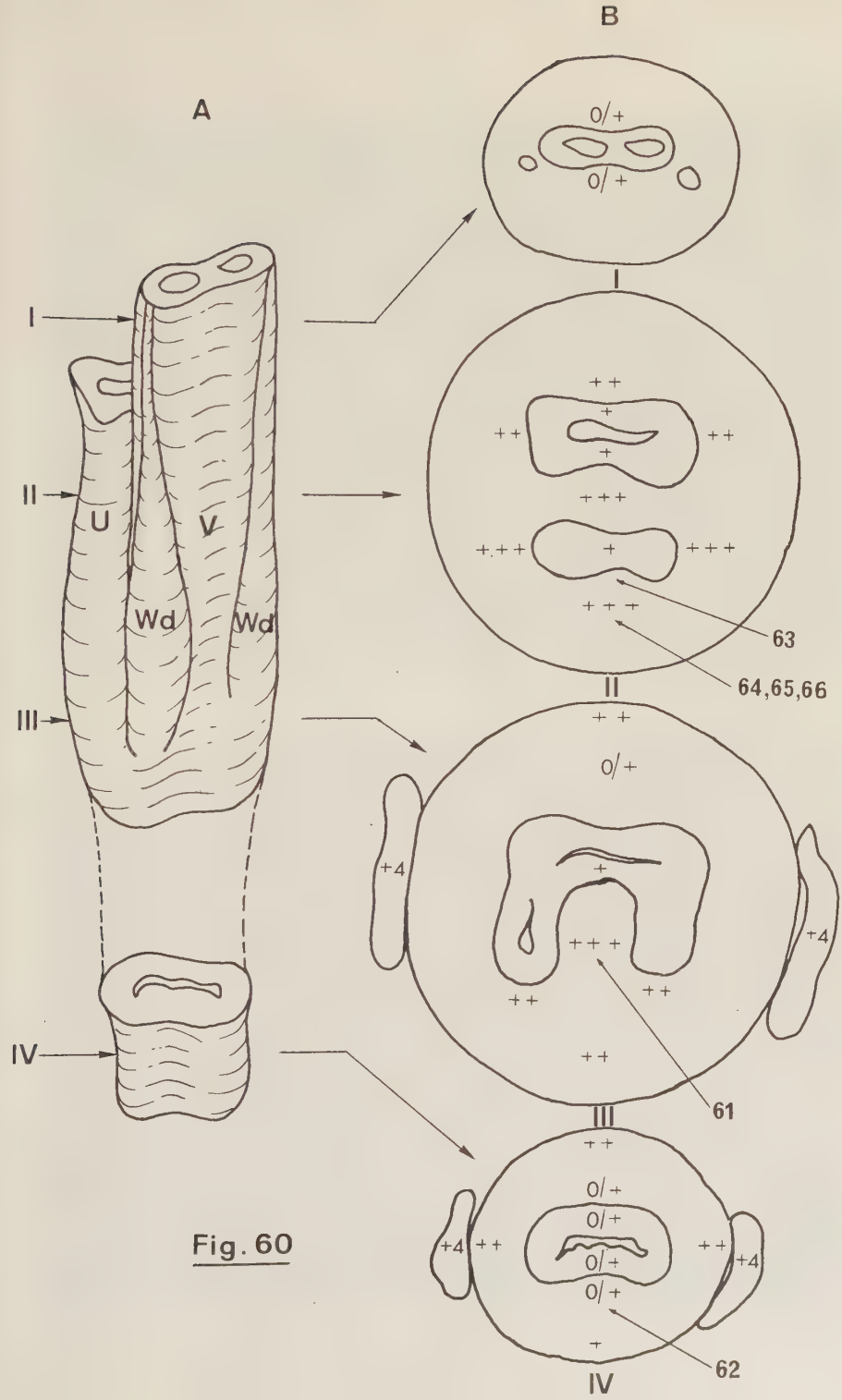


Fig. 60

Fig. 61: Section from the junctional area of the vagina with the urogenital sinus. Female mouse embryo at day 17 p.c.. Cholinesterase staining without ethopropazine. Cells of the dorsal mesenchymatous condensation show strong ChE activity.

ER = endoplasmic reticulum
G = Golgi complex
L = lipid droplet
M = mitochondria
N = nucleus

x 16404

Fig. 62: Section between the junctional area. Female mouse embryo at day 17.5 p.c.. Cholinesterase staining with ethopropazine. Epithelial cells and cells surrounding the urogenital sinus are ChE negative. The epithelial cells contain abundant glycogen.

SE = sinus epithelium
BL = basal lamina
g = glycogen
rER = rough endoplasmic reticulum
M = mitochondria
N = nucleus

x 16404

ER
G
N
61
1μ

g
SE
rER
BL
M
N
62
1μ

Fig. 63: Section above the junctional area where the sinus and the vagina still have a common mesenchymal layer. Female mouse embryo at day 17.5 p.c.. Cholinesterase staining without ethopropazine. Cells of the dense mesenchymal layer next to the epithelium of the vagina show strong ChE activity. Cells of the vaginal epithelium contain glycogen and exhibit very weak enzyme activity.

VE = vaginal epithelium
BL = basal lamina
ER = endoplasmic reticulum
rER = rough endoplasmic reticulum
g = glycogen
L = lipid droplet
M = mitochondria
N = nucleus

x 12768

Fig. 64: Same section as Fig. 63. Mesenchymal cells at the dorsal side of the vagina show strong ChE activity in the cisternae of the nuclear envelope and the endoplasmic reticulum.

ER = endoplasmic reticulum
rER = rough endoplasmic reticulum
G = Golgi complex
g = glycogen
M = mitochondria
N = nucleus

x 10032

BL
ER
rER
63
1μ

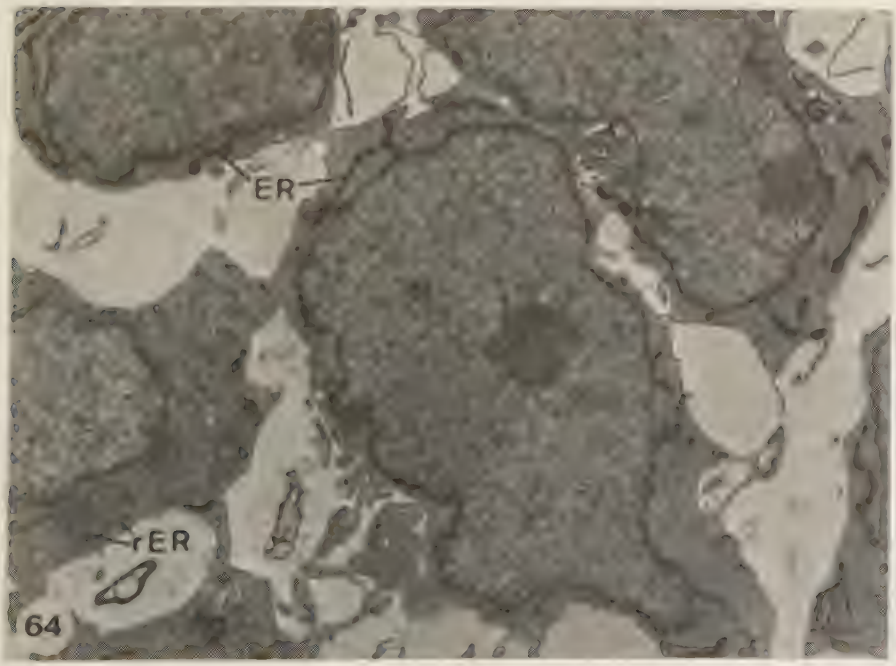
ER
rER
64

Fig. 65: From the same section as Fig. 63. ChE positive cisterna of the endoplasmic reticulum surrounds a mitochondrion.

ER = endoplasmic reticulum
M = mitochondria
N = nucleus

x 31920

Fig. 66: Same section as Fig. 63. Cells in the outer mesenchymal layer exhibit also positive reaction in the cisterna of the nuclear envelope and the endoplasmic reticulum. In the ER areas of strong reaction alternate with areas of weak reaction. The cisternae are extended and are lined by ribosomes. Extracellular spaces contain collagen fibers.

C = centriole
rER = rough endoplasmic reticulum
G = Golgi complex
M = mitochondria
N = nucleus

x 25536

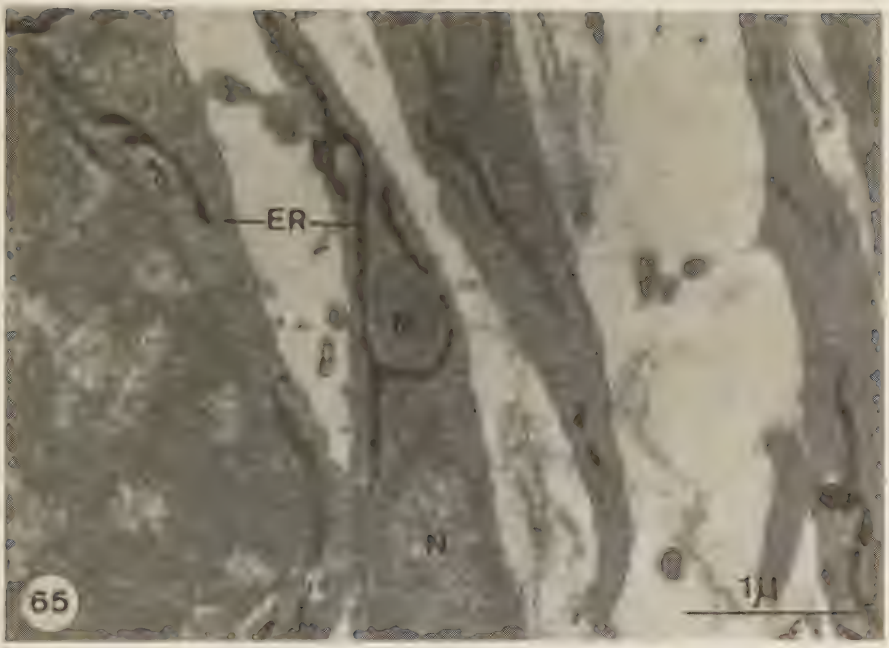
ER
N
65
1μ

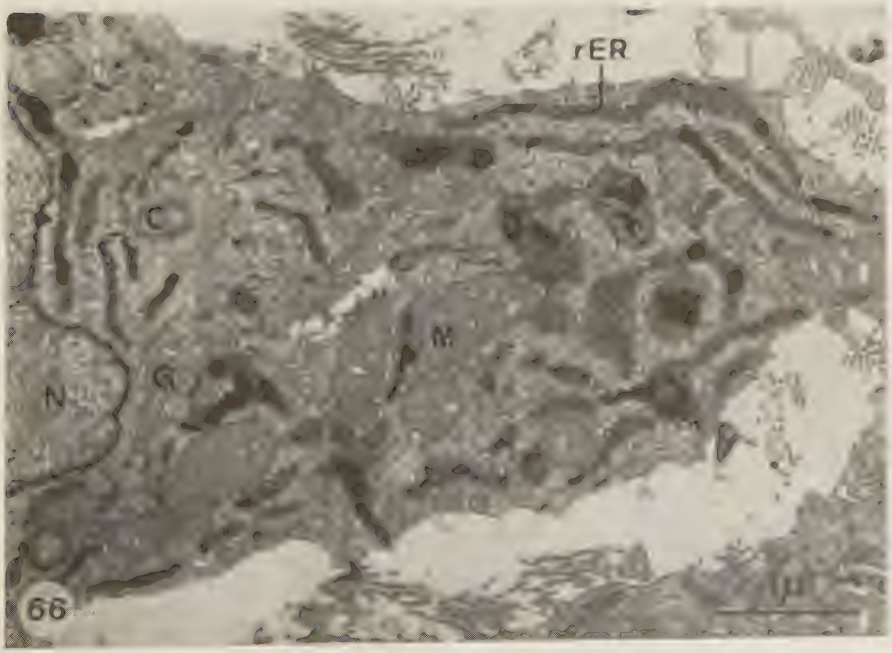
rER
C
N
M
66
μ

Fig. 67: Semithin cross sections of the urethra. Male mouse embryo at day 15, 17 and 20 p.c.. Azure II staining.

a) At day 15 p.c., the outer circular myogenic layer consists of densely packed mononucleated cells. Cells are spindle shaped and aligned in parallel.

b) At day 17 p.c., most of the mononucleated cells have elongated nuclei and cell bodies. Some of them show a light cytoplasm and possess nuclei. These light cells are the first differentiating myotubes.

c) At day 20 p.c., the myogenic layer is thicker than in the younger stages. It consists mainly of multinucleated cells. The multinucleated cells have large size, light cytoplasm and nuclei. The mononucleated dark myoblasts are aligned in parallel with the multinucleated cells.

ML = muscular layer
U = urethral epithelium

x 320

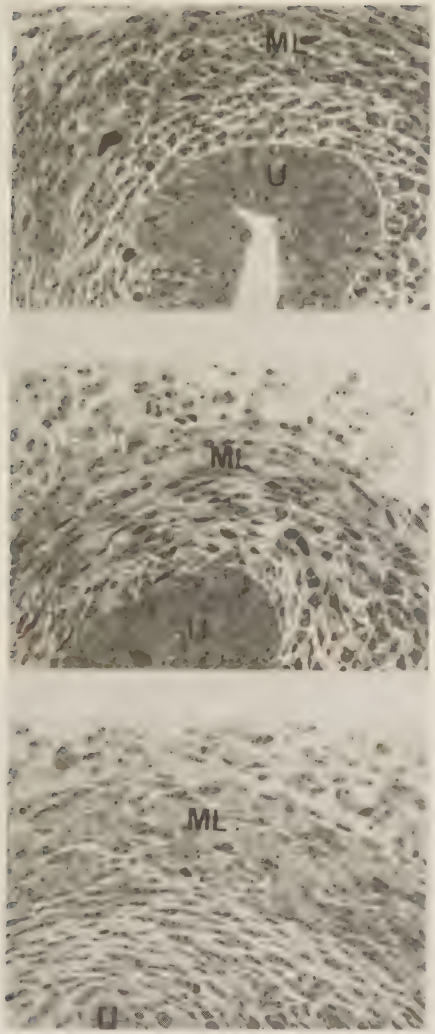


50μ

Fig. 67

Fig. 68: Urethral muscle of male mouse embryo at day 15 p.c.. Acetylcholinesterase staining (with ethopropazine). Myoblasts have euchromatic nuclei, one or two nucleoli and a small seam of electron dense cytoplasm. They show no AChE activity. Ganglial cells exhibit strong AChE activity.

GC = ganglial cell
Mb = myoblast

x 2554

Fig. 69: Muscular layer of female mouse embryo at day 15 p.c.. Cholinesterase staining without blocker, 2 x $10^{-4}$M ethopropazine. Myoblasts show strong ethopropazine sensitive ChE activity in the cisterna of the nuclear envelope and the endoplasmic reticulum.

C = centrioles
ER = endoplasmic reticulum
rER = rough endoplasmic reticulum
L = lipid droplet
M = mitochondria
N = nucleus

x 8408

GC
MD
68
10μ

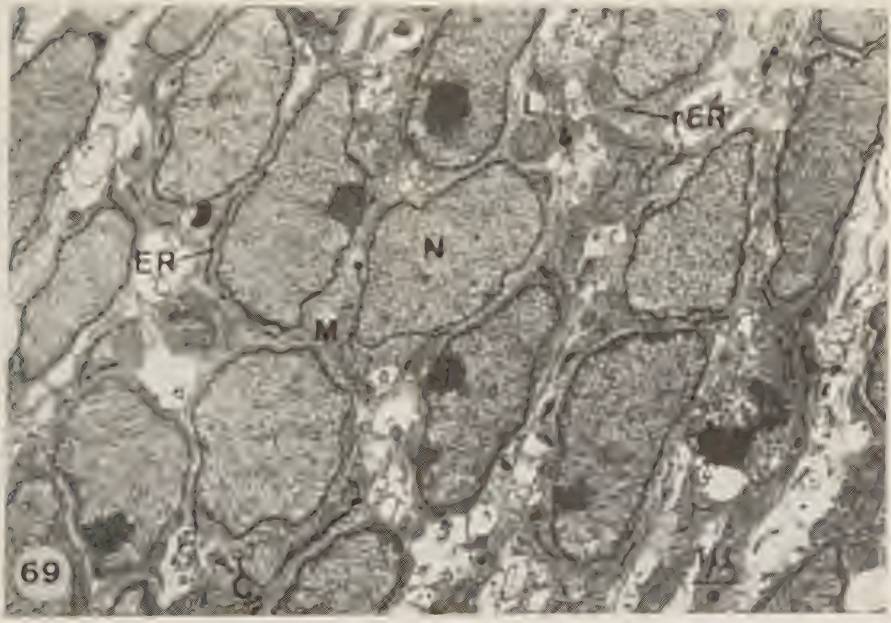
L
rER
ER
N
M
69

Fig. 70: Higher magnification of the section in Fig. 69. Enzyme activity of the myoblasts is not homogeneous. Areas of strong reaction alternate with areas of weak reaction.

ER = endoplasmic reticulum
rER = rough endoplasmic reticulum
L = lipid droplet
M = mitochondria
N = nucleus

x 22064

Fig. 71: Same section as Fig. 69. Some of the myoblasts contain thin filaments (arrows).

M = mitochondria
N = nucleus

x 41041

Fig. 72: Same section as Fig. 69. Myoblasts are closely apposed and form small maculae adherentes in the contact zones with the neighbouring cells (arrows).

ER = endoplasmic reticulum
M = mitochondria
N = nucleus

x 48336

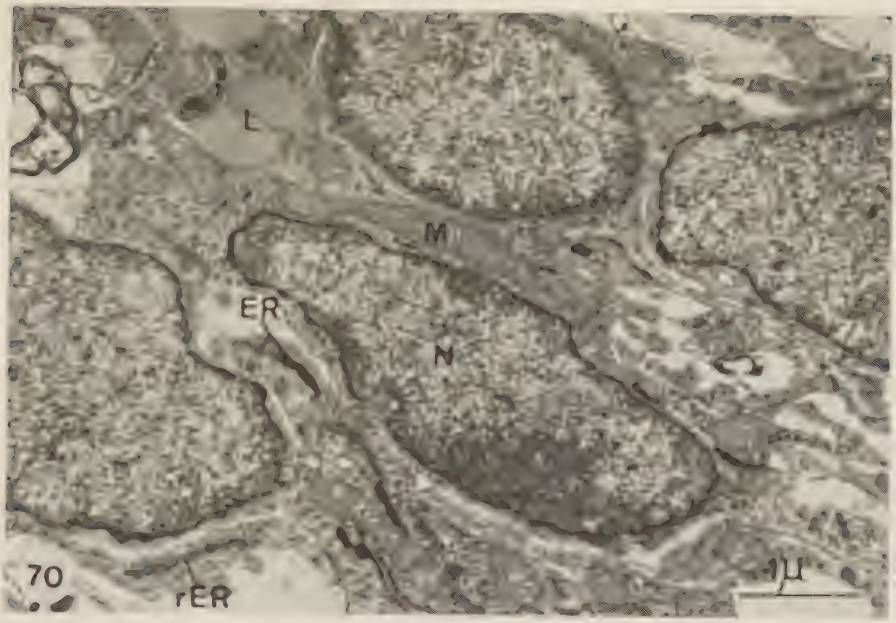
L
M
ER
N
70
rER
1μ

M
N
71
0.5μ

M
ER
N
N
72
0.5μ

Fig. 73: Myoblasts at day 16 p.c.. Female mouse embryo. Cholinesterase staining without ethopropazine. Cells contain large amounts of thin filaments (arrows). Enzyme reaction is localized in the cisternae of the endoplasmic reticulum and the nuclear envelope. In the endoplasmic reticulum, stretches of heavy activity alternate with areas of weak or no reaction.

ER = endoplasmic reticulum
rER = rough endoplasmic reticulum
M = mitochondria
N = nucleus

x 10032

Fig. 74: Same section as Fig. 73. Myoblasts are arranged in a cluster.

ER = endoplasmic reticulum
rER = rough endoplasmic reticulum
M = mitochondrium
N = nucleus

x 12612

rER
M
ER
N
73
1U

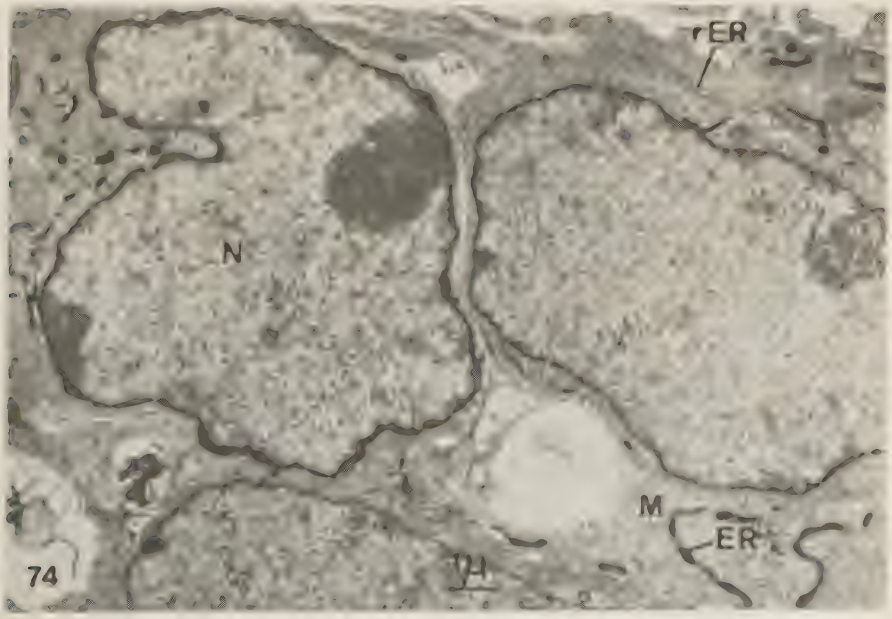
rER
N
M
ER
74
1U

Fig. 75: Myoblasts at day 17 p.c.. Male mouse embryo. Cholinesterase reaction without ethopropazine. Cells have now long cytoplasmic processes and contain numerous cisternae of endoplasmic reticulum and bundles of thin filaments. ChE positive cisternae of ER align around or apposed to the mitochondria.

BF = bundle of filaments
ER = endoplasmic reticulum
rER = rough endoplasmic reticulum
M = mitochondria
N = nucleus

x 8408

Fig. 76: Higher magnification of the section in Fig. 75. Flocculent material as precursor of a basal lamina covers the outside of the cell membrane (arrows).

BF = bundle of filaments
C = cilia
ER = endoplasmic reticulum
rER = rough endoplasmic reticulum
M = mitochondria
N = nucleus

x 16404

M
ER
ER
N
BF
1μ
75

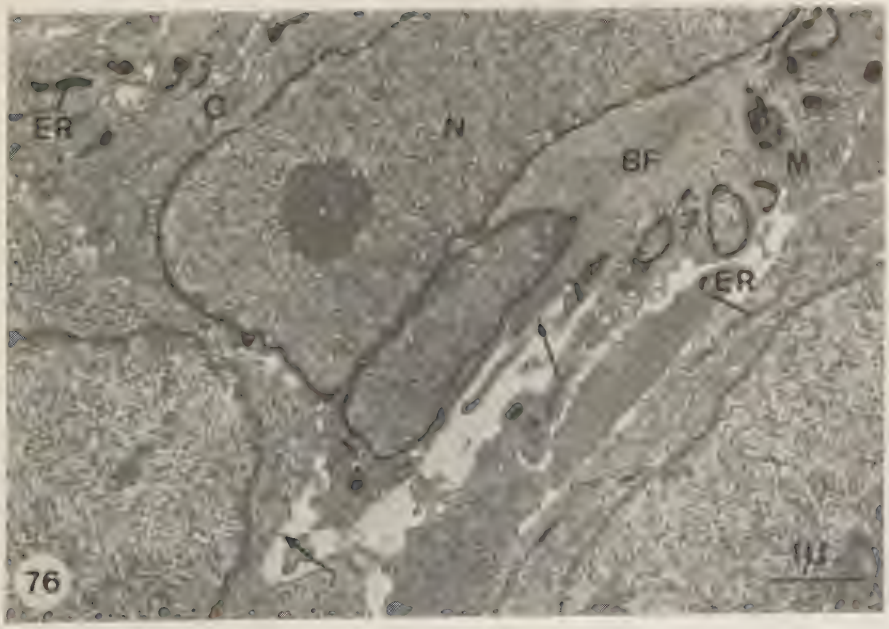
ER
C
N
BF
M
ER
1μ
76

Fig. 77: Section from female mouse embryo at day 17.5 p.c. Cholinesterase reaction without ethopropazine. Differentiating myotubes are clearly seen. They contain bundles of myofibrils. The myofibrils show Z-lines. Differentiating myotubes exhibit ethopropazine sensitive ChE activity in the perinuclear cisterna and the sarcoplasmic reticulum. ChE positive myoblasts with thick bundles of filaments are aligned in parallel to the differentiating myotubes.

Mb = myoblast
Mt = differentiating myotube
Z = developing Z-line

x 3648

Fig. 78: Higher magnification of Fig. 77. Differentiated myoblasts contain now an increased amount of endoplasmic reticulum, mitochondria, glycogen and bundles of filaments. They show strong ChE activity in the cisterna of the endoplasmic reticulum and the nuclear envelope. ChE positive cisternae of the ER are aligned around or are apposed to the mitochondria.

BF = bundles of filaments
ER = endoplasmic reticulum
G = glycogen
M = mitochondria
N = nucleus

x 16404

Mt
Mb
Mb
77
Mb
5μ

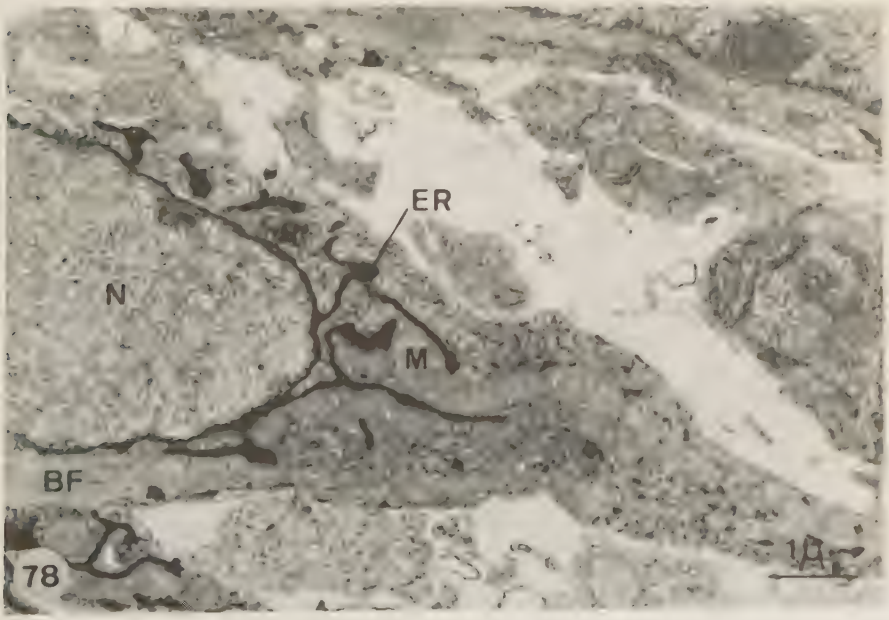
ER
N
M
BF
78
1μ

Fig. 79: Higher magnification of Fig. 77. Differentiating myotube contains thick and thin myofilaments which are aligned in order and arranged into myofibrils. There are irregular electron dense Z-lines in the bundles of myofibrils. Strong enzyme activity is localized in the tubules of the sarcoplasmic reticulum.

Mb = myoblast
Mt = differentiating myotube
M = mitochondria
MF = myofibril
Ne = nuclear envelope
SR = sarcoplasmic reticulum

x 25536

Fig. 80: Section from female mouse embryo at day 17.5 p.c. Acetylcholinesterase reaction with ethopropazine. Differentiating myotubes show strong AChE activity whereas myoblasts have no AChE activity.

Mb = myoblast
Mt = differentiating myotube
rER = rough endoplasmic reticulum
L = lipid droplet
M = mitochondria
MF = myofibril
SR = sarcoplasmic reticulum

x 8408

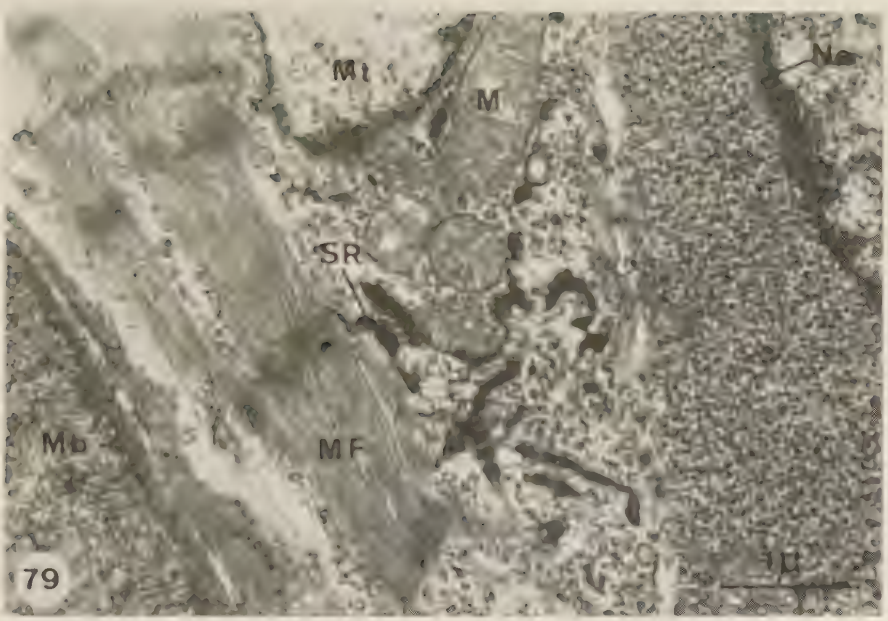
Mt
M
N
SR
Mb
MF
1μ
79

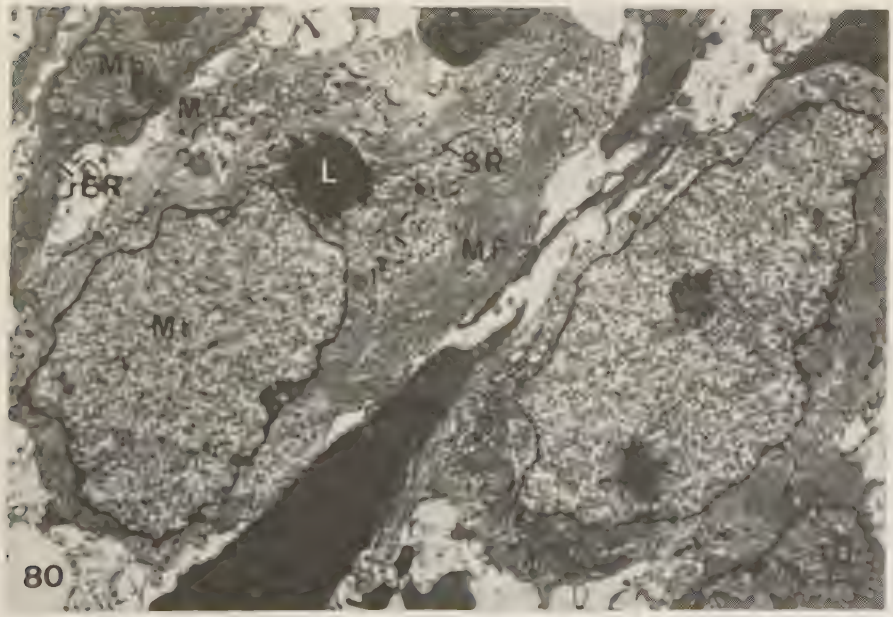
Mb
M
L
SR
SR
MF
Mt
80

Fig. 81: Higher magnification of Fig. 80. AChE activity is localized in the cisterna of the nuclear envelope and in the sarcoplasmic reticulum. AChE positive tubules of the sarcoplasmic reticulum run commonly parallel to the myofibrils or the plasma membrane.

Mb = myoblast
Mt = differentiating myotube
L = lipid droplet
M = mitochondria
MF = myofibril
N = nucleus
SR = sarcoplasmic reticulum

x 31920

Fig. 82: Semithin cross sections of the urethra. Male mouse embryo at day 18 p.c.. Azure II staining. Myogenic cell layer is thicker than in the younger stages especially at the ventrolateral side. Multinucleated cells are clustered in groups and are surrounded or mixed with myoblasts.

L = lumen of the urethra
Mes = mesenchymal cell layer
Myo = myogenic cell layer
UE = urethral epithelium

x 315

L
M
SR
N
МГ
81
1μ

Mes
L
LE
MYO
82
50μ

Fig. 83: Section from male mouse embryo at day 18 p.c.. Acetylcholinesterase with ethopropazine. Myotube shows more well arranged sarcomeres and contains AChE reaction in the tubules of the sarcoplasmic reticulum.

Mb = myoblast
Mt = myotube
BF = bundle of filaments
L = lipid droplet
M = mitochondria
MF = myofibril
rER = rough endoplasmic reticulum
SR = sarcoplasmic reticulum
V = vesicle
Z = Z-line

x 16404

Fig. 84: Myotube from the same section as Fig. 83. AChE positive cisternae of sarcoplasmic reticulum align parallel to the myofibrils or the plasma membrane.

N = nucleus
M = mitochondria
MF = myofibril
PM = plasma membrane
SR = sarcoplasmic reticulum
Z = Z-line

x 38612

Fig. 85: Myotube from the same section as Fig. 83. AChE positive cisterna of the sarcoplasmic reticulum forms the junction with plasma membrane. Note nuclear envelope contains AChE activity.

Ne = nuclear envelope
PM = plasma membrane
SR = sarcoplasmic reticulum

x 63840

MF
V
MF
I
MF
ER
M
Z
BF
SR
83

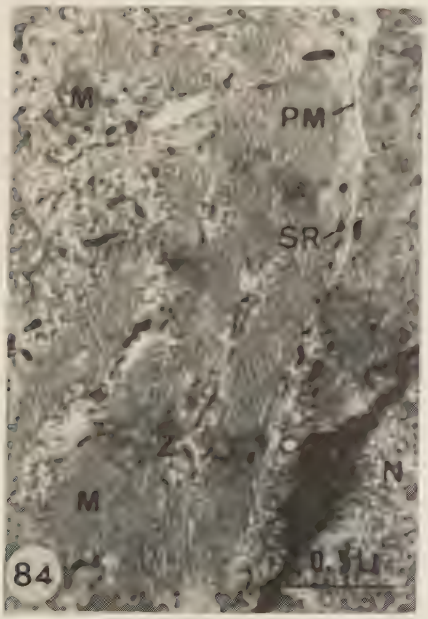
M
PM
SR
Z
N
M
84
0.5 μ

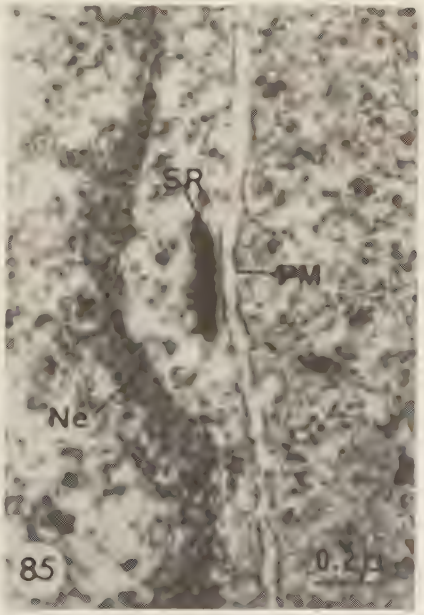
SR
PM
Ne
85
0.2 μ

Scientific publication

1. Vanittanakom, P., Koeplung, M. and Waiwattana, N.: Serum lipoprotein electrophoresis. Bull. Chiang Mai Med. Tech. 5 : 31 - 42, 1972.

2. Butthep, C., Vanittanakom, P. and Saeng-Udom, C.: Leukocyte alkaline phophatase activity in diseases. Bull. Chiang Mai Ass. Med. Sci. 10 : 9 - 16, 1977.

3. Vanittanakom, P.: Quality control in special histologic staining. Bull. Chiang Mai Ass. Med. Sci. 11 : 25 - 28, 1978.

4. Menakanit, W. and Vanittanakom, P.: Carcinoma of the penis in Northern Thailand (1966 - 1975). Modern Medicine of Asia 14 : 10 - 12, 1978.

5. Vanittanakom, P., Sahaphong, S., Boonpucknavig, V. and Bhamarapravati, N.: Hypervitaminosis A in rats. Modern Medicine of Asia 16 : 43 - 47, 1980.

6. Sinchaisri, T., Vanittanakom, P., Apinhasmit, K., Tantachamroon, T., Khansuwan, U., Winyar, B. and Suttajit, M.: The relationship between pathological changes and aflatoxin in the human liver diseases. Bull. Chiang Mai Ass. Med. Sci. 15 : 63 - 73, 1982. (This work was supported by China Medical Board of New York Inc. and the Faculty of Medicine, Chiang Mai University, Chiang Mai, Thailand, Grant No. 78 - 317.)

My academic teachers in Tübingen were:

D. Ammermann

D. Bunke

F. Dittmann

U. Drews

W. Engels

H.D. Frey

K.-S. Hermann

W. Schlote

B. Schwemmle

K.-U. Thiedemann

H. Wolburg

## Curriculum Vitae

| | |
|---|---|
| Name | : Pramote Vanittanakom |
| Date of Birth | : January 18, 1948 |
| Place of Birth | : Nakhonsawan province, Thailand |
| Nationality | : Thai |

### Education

| | |
|---|---|
| June, 1967-March, 1971 | Studied Medical Technology in the Faculty of Associated Medical Science, Chiang Mai University, Chiang Mai, Thailand. |
| March 18, 1971 | Received B.S. (Medical Technology). |
| June, 1972-April, 1974 | Post Graduate Studies in Pathobiology in the Faculty of Graduate Studies, Mahidol University, Bangkok, Thailand. |
| April 24, 1974 | Received M.S. (Pathobiology). |
| September, 1980-1984 | Studied for doctorate in Biology and did doctoral work in the Institute of Anatomy, Tübingen, Federal Republic of Germany. |

### Professional works

| | |
|---|---|
| April, 1971-May, 1972 | Scientist in the Department of Pathology, Faculty of Medicine, Ramathibodi Hospital, Mahidol University, Bangkok, Thailand. |
| May, 1974-March, 1975 | Instructor in the Department of Pathobiology, Faculty of Science, Mahidol University, Bangkok, Thailand. |
| April, 1975-February, 1979 | Lecturer in the Department of Pathology, Faculty of Medicine, Chiang Mai University, Chiang Mai, Thailand. |
| March, 1979-present | Assistant Professor in the same department. |

Offsetdruck Spengler
Lessingstraße 4 · 7401 Neustetten 1
Telefon (0 74 72) 2 21 45